

STRATIGRAPHY, ENVIRONMENTS OF DEPOSITION,  
PETROLOGY, AGE, AND PROVENANCE OF THE BASAL RED BEDS OF  
THE ARGANA VALLEY, WESTERN HIGH ATLAS MOUNTAINS, MOROCCO

by

Duke Forrest Jones

Submitted in Partial Fulfillment  
of the Requirements for the Degree of  
Master of Science in Geology

NEW MEXICO INSTITUTE OF MINING AND TECHNOLOGY

Socorro, New Mexico

July, 1975

## TABLE OF CONTENTS

	Page
ABSTRACT	
ACKNOWLEDGEMENTS	
LIST OF FIGURES	
LIST OF TABLES	
LIST OF PLATES	
CHAPTER I. INTRODUCTION	1
CHAPTER II. ENVIRONMENTS OF DEPOSITION	12
T <sub>1</sub> CONGLOMERATES	12
T <sub>2</sub> COARSE TO FINE CLASTICS	31
T <sub>3</sub> CONGLOMERATES	43
CHAPTER III. PETROLOGY	48
ANALYSIS OF PEBBLE AND POINT COUNT DATA	48
SUMMARY OF PETROGRAPHIC DATA	70
CHAPTER IV. PROVENANCE	95
INTRODUCTION	95
PROVENANCE FOR T <sub>1</sub> AND T <sub>2</sub> LITHOLOGIES	95
PROVENANCE FOR T <sub>3</sub> LITHOLOGIES	101
CHAPTER V. DEPOSITIONAL MODEL	104
LATERAL AND VERTICAL CHANGES IN ENVIRONMENTS OF DEPOSITON	104
DEPOSITIONAL MODEL FOR T <sub>1</sub> THROUGH T <sub>3</sub> DEPOSITION	107
CHAPTER VI. AGE OF T <sub>1</sub> , T <sub>2</sub> , AND T <sub>3</sub>	110
CHAPTER VII. SUMMARY AND CONCLUSIONS	113
ENVIRONMENTS OF DEPOSITION AND STRATIGRAPHIC MODEL FOR T <sub>1</sub> , T <sub>2</sub> , AND T <sub>3</sub>	113
AGE OF T <sub>1</sub> , T <sub>2</sub> , AND T <sub>3</sub>	115
APPENDICES	117
APPENDIX A. CLASSIFICATION SCHEMES	117
APPENDIX B. MEASURED STRATIGRAPHIC SECTIONS	122
APPENDIX C. COMPARISON OF T <sub>1</sub> , T <sub>2</sub> , AND T <sub>3</sub> OF THE ARGANA VALLEY WITH THE BASAL TRIASSIC SECTION AT TIZI N' TEST, MOROCCO	134

TABLE OF CONTENTS

	Page
APPENDIX D. COMPARISON OF T <sub>1</sub> , T <sub>2</sub> , AND T <sub>3</sub> OF THE ARGANA VALLEY WITH SIMILAR LITHOLOGIES IN THE NOVA SCOTIA, NEWARK-GETTYSBURG, AND CONNECTICUT BASINS IN NORTH AMERICA	138
REFERENCES	144

## ABSTRACT

Basal red beds cropping out on the eastern margin of the Argana Valley, western High Atlas Mountains, Morocco, contain a lower unfossiliferous unit of conglomerate and subordinate finer grained clastics, up to 1000 meters thick, interpreted as alluvial fan deposits built dominantly by braided streams. The conglomerates overlies with angular unconformity lower Paleozoic metamorphic rocks and locally, in the south, Stephanian (latest Carboniferous) nonmarine deposits both of which were the primary sources of detritus as indicated by petrographic and statistical analyses of conglomerates and sandstones. The conglomerates are gradationally overlain by up to 300 meters of coarse to fine clastics interpreted as meandering stream deposits. The coarse to fine clastics are firmly established in this study as Triassic in age on the basis of Rhynchosauroides. The coarse to fine clastics are overlain, with angular unconformity in the south, but conformably in the north, by a thin, 0 to 10 meters, conglomerate unit which is distinguished from other conglomerates by the occurrence of clasts of Hercynian volcanic and shallow intrusive rocks. This conglomerate is interpreted as a braided stream deposit, and is Triassic in age based on its stratigraphic position above and below rocks containing Triassic fossils. The contact relations of this conglomerate indicate that locally tectonism was synchronous with deposition.

These basal red beds of the Argana Valley are similar



in terms of environments of deposition, petrography, provenance, and fossils, to the basal Triassic red beds at Tizi n' Test, Morocco (Jones, 1975, Appendix C) and the Wolfville and Blomidon Formations of Maritime Canada (Klein, 1962). In terms of a paleotectonic setting the red beds represent the initial deposits in grabens or half-grabens that formed during the breakup of Pangaea as outlined by Kanes et al. (1973) and Dietz and Holden (1970).

## ACKNOWLEDGEMENTS

I wish to thank Dr. Ian Evans, University of Houston, for his help in assuring me a position with the University of South Carolina--National Science Foundation Moroccan Survey. I also wish to thank Dr. William H. Kaner, Director of the grant, for suggesting the problem and for his help in Morocco. Roy Brown and Dr. F. B. Van Houten gave me much assistance and offered many suggestions in the field. Harold Krueger provided age dating of igneous clasts. I am grateful to Drs. R. Flower, Christina Lochman-Balk and Donald Baird for their help in identifying fossils. I wish to thank the following friends who helped to prepare the manuscript and plates: Rosie Trujillo, Connie Faith, and Jim Cappa. I am also grateful to Martha Cinelli for typing the manuscript. Finally, I wish to thank my advisors Dr. John MacMillan, Dr. A. J. Budding, and Dr. Allan Gutjahr for their editorial comments.

## LIST OF FIGURES

Figure	Page
1. Index map of study area	2
2. External bedding in T <sub>1</sub> conglomerates	16
3. Interbedded conglomerates and pebbly mudstones in T <sub>1</sub>	17
4. Stratification in T <sub>1</sub> conglomerates seen at a distance	19
5. Nodular siltstone interbed in T <sub>1</sub> conglomerate	22
6. Bedding plane view of a T <sub>1</sub> pebbly mudstone bed	23
7. Tabular conglomerate bed in T <sub>1</sub>	25
8. Stratification in T <sub>2</sub> seen at a distance	34
9. Trough crossbedding, parallel bedding, and ripple cross lamination in a T <sub>2</sub> fine sandstone bed	37
10. Stratification in T <sub>2</sub> seen at a distance	38
11. Graph of the ratios of quartzite/phyllite versus sample areas	65
12. Graph of the ratios of quartz plus quartzite/phyllite plus clay matrix versus sample areas	66
13. Graph of the pooled ratios of quartzite/phyllite versus sample areas	67
14. Graph of the pooled ratios of quartz plus quartzite/phyllite plus clay matrix versus sample areas	68
15. Grain size distributions of five T <sub>1</sub> , T <sub>2</sub> , and T <sub>3</sub> sandstones	71
16. Photomicrograph of a typical T <sub>1</sub> Northern Sequence sandstone	87
17. Photomicrograph of a typical T <sub>1</sub> Southern Sequence sandstone	88
18. Photomicrograph of a typical T <sub>2</sub> sandstone	90
19. Photomicrograph of a typical T <sub>3</sub> sandstone	91
20. Geologic map of the Argana Valley and the inferred source areas	97
21. Permian fit of the continents	140

## LIST OF TABLES

Table	Page
I. Frequency data for pebble counts of conglomerates	50
Ia. Frequency data used in statistical testing of pebble counted conglomerates	51
II. Frequency data for point counted sandstones	52 & 53
IIa. Frequency data used in statistical testing of point counted sandstones	55
III. Results of pairwise chi-square tests for pebble counted conglomerates	59
IIIa. Results of pooled chi-square tests for pebble counted conglomerates	61
IV. Results of pairwise chi-square tests for point counted sandstones	62
IVa. Results of pooled chi-square tests for point counted sandstones	63
V. Comparison of $T_1$ and $T_2$ of the Argana Valley with some Triassic Basin fill deposits of North America	141 & 142

## LIST OF PLATES

Plate	Page
A. Geologic Map of the study area	in pocket
B. Lateral and vertical changes in environments of deposition	in pocket

## CHAPTER I. INTRODUCTION

### Brief Background

The Argana Valley is located 150 kilometers southwest of Marrakech in the western High Atlas Mountains, Morocco (Figure 1). The Valley is approximately 75 kilometers long from the village of Imi n' Tanoute in the north to Ameskhoud in the south, and has a maximum width of 25 kilometers near the village of Argana. A river, Oued Assif n' Ait Moussa, drains SSW into the Oued Souss and has eroded a Jurassic and Cretaceous cover and exposed in this area almost 2,500 square kilometers of Permo-Triassic red beds--one of the thickest exposed sections of Permo-Triassic rocks in Morocco.

These red beds in the Argana Valley overlie with angular unconformity lower Paleozoic metamorphic rocks and locally, in the south, Stephanian (latest Carboniferous) nonmarine deposits. The Paleozoic basement rocks are exposed in the mountains to the east of the valley. The Moroccan Geological Survey Marrakech Sheet (1:500,000) shows there the presence of: Cambrian schists and calcareous schists; Ordovician and Silurian schists and quartzites; undifferentiated Devonian rocks; and Hercynian basalts, andesites, and intrusives.

Major compression and magmatism occurred in this area during the Hercynian Orogeny 250 million years ago. The Stephanian deposits, now exposed locally along the south-



Figure 1. Index map of study area (from National Geographic Magazine, v. 139, 1971).

eastern border of the valley, have been interpreted as late Hercynian molasse (Van Houten, et al., 1974). The Stephanian deposits crop out on the tops of small horsts or "bouten-ierres" near Menizla and Tirkou (see Plate A and Figure 20), where they are angularly unconformable with lower Paleozoic metamorphic rocks below and with Permo-Triassic red beds above. The Stephanian deposits are distinguished from the younger red beds by their color (usually green or brown), bedding characteristics, and dominant clast lithology (see Chapter III, this thesis).

Extensional faulting in the Argana Valley produced horsts and adjacent grabens which received over 6,000 meters (Tixeront, 1971) of nonmarine Permo-Triassic sediments. Brown (1974) has shown through paleocurrent studies that active faulting affected sediment distribution. Tixeront (1971) believes the development of the Horst of Tirkou (Plate A) was synchronous with Permo-Triassic deposition. It is important to note that the eastern outcrop limit of Permo-Triassic rocks is the angular unconformity at the base of the section rather than a fault. Faults active during deposition were mostly transverse to the depositional strike of the red beds. The Permo-Triassic rocks are locally capped by basalt flows and cut by younger intrusions, but elsewhere interfinger with Lower Jurassic cyclic sabkha units (Brown 1974). The latter interfinger vertically with Middle Jurassic detrital red beds which are sharply but conformably overlain by Upper Jurassic and Cretaceous marine



carbonates.

During the Tertiary evolution of the High Atlas Mountains, erosion of this carbonate cover began. Alpine deformation is represented by east and northeast trending normal faults and open folds.

### Scope and Objective

Kanes et al. (1973) have interpreted Moroccan Mesozoic tensional faulting as resulting from a zone of spreading initiated beneath the continental crust of Pangaea. In the Argana Valley, the orientation of the faults has led to the conclusion that the tension was related to the opening of the Atlantic in accordance with the models proposed by numerous authors, notably Bullard et al. (1965), Dewey and Bird (1970), Dietz and Holden (1970), and Schenk (1971).

This study in conjunction with the study by Brown (1974) has the overall objective of developing a depositional model of the Argana Basin. If the Basin is a half-graben which formed during the initial rifting of Pangaea, its sediments should bear close resemblance to sediments that accumulated in other such half-grabens and grabens now exposed in North America as well as Africa.

No detailed descriptions of the basal Permo-Triassic units of the Argana Valley have been reported in the literature. It is an objective of this study to describe the lithology of the basal units of the Argana Valley and interpret their environment of deposition in order that they

may be compared in light of the aforementioned "Atlantic Rifting Model" with their stratigraphic equivalents elsewhere in Morocco, the eastern United States, and maritime Canada.

The basal units in the Argana Valley may be subdivided into a basal conglomerate unit, gradationally and conformably overlain by a middle unit of interbedded coarse to fine clastics, unconformably overlain by a thin upper conglomerate unit. This upper conglomerate is conformably overlain by fluvial deposits which grade into units interpreted as deltaic deposits by Brown (1974).

#### Statement of Specific Problems

The age of the red beds in the Argana Valley is not well established. The use of the hybrid term Permo-Triassic for the age of the units in the Argana Valley reflects a lack of index fossils and consequent uncertainty about the age of the deposits, rather than a well established Permian and Triassic age assignment. Vertebrate bone fragments found by Duffaud (1960) in the middle part of the sequence, approximately 900 meters above the basal units, are Upper Triassic in age. Duffaud et.al. (1966) emphasize the occurrence of an angular unconformity stratigraphically below the Upper Triassic fossils but within the basal red bed units, regard this unconformity as the boundary between the Permian and Triassic periods, and assign a Permian age to the basal red beds. In the basal part of the red bed

sequence near the village of Iferd (Plate A), the fossil Voltizia heterophylla has been found by de Koning (1957). Although this fossil has been attributed to the Triassic period by Mme. G. Termier (Tixeront, 1971), the genus actually ranges from Late Permian through Triassic (Scott, 1962). Thus the question of whether the basal units are, in part, Permian is unresolved.

Another problem is to determine the environment of deposition of each of the basal units briefly described above in order to construct a depositional model for the Argana Valley.

A third problem is to identify the source area(s) of the detritus in the lower Permo-Triassic rocks. It has not yet been established whether the detritus in the units was derived directly from lower Paleozoic metamorphic rocks or is second cycle detritus derived from Stephanian sediments now only locally exposed in the southeast portion of the valley. The original extent of these Stephanian deposits is problematical and an objective here is to make inferences about their original extent.

Sampling indicates there are two major sequences of conglomerate and sandstone, distinguished by clast composition, within the basal units of the Argana Valley. The two sequences are now juxtaposed along the Fault of Argana (Plate A) and it is uncertain whether they were contemporaneous and interfingering deposits, or whether their deposition was distinct in space and time. Establishment

of this relationship is fundamental to understanding the geometry of the surface on which the sediments were deposited, and to the correct determination of source area.

Tixeront (1971) has shown that the uppermost unit of concern in this study overlies with angular unconformity both of the two lower units as well as the lower Paleozoic basement. The cause and extent of the deformation represented by this unconformity are investigated because they bear significant consequences on solving all of the previously stated problems, namely the age, depositional setting and provenance of the Permo-Triassic rocks.

### Methods

Field work was conducted during the summers of 1973 and 1974. A new highway from Chichaoua southwest through the Argana Valley to Agadir was completed in the spring of 1973. In the Valley, accessibility to outcrops off the major highway, via dirt roads, was governed by terrain. In general, accessibility was good to the north of Argana and poor to the south. For this reason section work and sampling was concentrated in the north (see Plate A).

During section measurement particular attention was paid to the relative abundances of different lithologies, their external and internal bedding characteristics, and dominant clast lithology in the conglomerates in the basal units. Attention was also paid to the contacts between the three units themselves and between the units and the sub-

jacent lower Paleozoic and Stephanian rocks.

Environments of deposition of each of the units were determined by comparing their lithologic characteristics with the characteristics of modern and ancient deposits of known environments reported in the literature.

As noted previously, the present day outcrop limit of the basal units in the Argana Basin is an erosional limit. The units are not adjacent to faults that parallel their strike, they simply overlap an erosional surface cut into lower Paleozoic and, locally, Stephanian rocks. With this relationship, the distribution of detritus in the Permian-Triassic rocks could reflect directly the distribution of rock types within the lower Paleozoic and Stephanian deposits. A statistical sampling plan was employed in collecting pebble and point count data so that quantitative statements could be made about variation in pebble and grain composition within the units. Traverses across the lower Paleozoic and Stephanian rocks were conducted to determine if lithologic variations in these rocks could account for the observed variations in dominant clast and grain composition in the red beds, as indicated by statistical analysis of pebble and point count data.

Once two distinct conglomerate and sandstone sequences based on pebble and grain composition were recognized within the basal two units, sections were measured along the boundary between these sequences (see Plate A). During section measurement particular attention was paid to clast

lithology of individual beds and to the variability between beds in order to determine whether the two sequences are laterally gradational and interfingering or whether they are discrete deposits, possibly of different ages.

Thin sections were described in detail and point counted. Descriptions of lithic fragments in the sandstones are compared with petrographic descriptions of possible source rocks in order to determine the source area during deposition.

### Previous Work

The most detailed published work in the Argana Valley to date is that of Tixeront (1971). His map covers the entire valley on a scale of 1:100,000, and certain areas on larger scales. His maps were used in most aspects of the field work.

In a report on the cupriferous and uraniferous mineralization in the Argana Valley, Tixeront divided the Permian-Triassic sediments into 8 units labeled, from bottom to top, T<sub>1</sub> to T<sub>8</sub>. His nomenclature is used in this thesis and the three informal units discussed above correspond to T<sub>1</sub>, T<sub>2</sub>, and T<sub>3</sub>. Where data collected by the writer is in conflict with that presented by Tixeront explanations will be given.

Tixeront describes T<sub>1</sub> as a conglomerate sequence present in great thickness (up to 1800 meters) between the village of Timezgadouine in the north and Iferd in the

south and only locally present and much thinner elsewhere in the Valley (see Plate A). The conglomerates are violet to reddish-brown in color, poorly bedded and poorly sorted, with imbricated pebbles of quartzite, schist, sandstone, and minor amounts of vein quartz and limestone. Ambroggi (1963) notes also the presence of extrusive igneous rock fragments. The conglomerates have a sandy matrix. They are homogeneous in the lower part and become more regularly bedded and interbedded with sandstones in the upper part. The entire sequence fines upward. Tixeront determined the transport direction to be from east to west. He concludes that  $T_1$  resulted from fluvial deposition on a piedmont in the proximity of important relief. Ambroggi (1963) believes the conglomerates are formed in part by the process of sheetflow. Duffaud (1960) and de Koning (1957) emphasize the variable thickness of the conglomerates and attribute these variations in thickness to sedimentation on a surface with pre-existing relief.

Tixeront describes the second unit,  $T_2$ , as a brick red sandstone sequence also thickest in the central part of the basin and thin or absent north of Timezgadouine or south of Iferd. Tixeront does not describe the nature of the  $T_1$ - $T_2$  contact, but his cross sections imply a sharp contact. He describes  $T_2$  as composed of beds of brick red quartzitic sandstone that become thinner, finer grained, and more poorly consolidated up section. Tixeront notes the presence of intraformational conglomerate beds at the top of the

sequence. The sandstones are described as being composed mostly of angular quartz grains with rare feldspar and mica grains. Tixeront concludes that they, like the  $T_1$  conglomerates, accumulated in the proximity of important relief following brief transport.

Tixeront defines  $T_3$  as a thin but persistent and recognizable conglomerate unit that rests with angular unconformity on  $T_2$ ,  $T_1$ , or directly on the lower Paleozoic basement. He describes a poorly sorted conglomerate with pebbles of iron-stained, varicolored quartzite, vein quartz, and rare schist pebbles, cemented by calcite. Tixeront notes that  $T_3$  thins and becomes finer grained from east to west, and that the ratio of the number of vein quartz pebbles to the number of quartzite pebbles decreases in the same direction. The  $T_3$  unit is conformably overlain by  $T_4$ , a unit described as sandy mudstones with some reduced horizons interbedded with homogenous sandstones.



## CHAPTER II. ENVIRONMENTS OF DEPOSITION

T<sub>1</sub> CONGLOMERATESThickness and Geometry

Mapping by Tixeront (1971) shows T<sub>1</sub> conglomerates to be present in greatest thickness in the center of the Argana Valley between the villages of Iferd (in the south) and Timezgadouine (in the north). They are also present but thinner at Tirkou, and at sample locations 17 and 15 (see Plate A). The thickest section of T<sub>1</sub> measured in this study was 1000 meters in section I (see Appendix B), although Tixeront claims it is as thick as 1800 meters.

The three-dimensional geometry of T<sub>1</sub> is impossible to determine without subsurface data because it is overlain and covered by T<sub>2</sub>. However from mapping by Tixeront (1971) it is present in the subsurface at least as far west as sample area 16 (see Plate A) where it crops out in a small horst.

In two dimensions, T<sub>1</sub> is lenticular--existing as two major lenticular bodies between Iferd and Timezgadouine and three minor lenses at Tirkou, sample area 17, and sample area 15 (see Plate A). The two major lenticular bodies are as thick as 1000 meters and as thin as 100 meters and continuous laterally from 11 to 17 kilometers along strike. The minor bodies are from 30 to 50 meters thick at a maximum and pinch out over several hundred meters to several kilometers laterally.

As mentioned previously, the eastern outcrop limit of  $T_1$  is not a fault boundary but instead an onlap of angularly unconformable red bed conglomerates over Paleozoic rocks. Isolated patches of  $T_1$  to the east of the main outcrop limit (see Plate A), the great thickness of  $T_1$  just west of this limit, and the projection of its dip eastward suggest that  $T_1$  conglomerates once extended farther to the east of their present erosional limit. However large boulders (up to 90 cm in diameter) near the base of the unit near sample areas 19 and 4 (see Plate A), as well as its immature texture and, in part, poor rounding, suggest that  $T_1$  originally extended only several kilometers east of its present extent.

#### Dominant Lithology

The lithology of  $T_1$  is dominantly (about 80%) cobble (rarely boulder) to pebble conglomerates with a matrix ranging in grain size from coarse sand to silt or clay. The remaining 20 percent of the unit is composed of a complete range from coarse sandstones to mudstones.

Rather than discussing each lithology separately,  $T_1$  has been subdivided into lithologic associations, based on characteristic bedding types, contacts between lithologies, and sedimentary structures within each lithology. Moreover, these lithologic associations are believed to be indicative of specific depositional processes.

Association A

The dominant lithologic association, here referred to as Association A, comprises 90 to 95 percent of T<sub>1</sub>. It consists of about 90 percent conglomerate, 5 percent coarse sandstones, and 5 percent of a complete range from medium sandstones to mudstones.

The rocks of Association A are dominantly medium reddish-brown or violet in color. Tan, yellow, or buff zones are common in the lower 25 meters of Association A and less common elsewhere. The light colored zones often follow bedding suggesting they are genetically related to sedimentation units, but they also follow fractures and diverge along bedding planes suggesting a post-lithification phenomena. The cause and origin of the color are discussed in detail later. For the purpose of this section it is important only to note that the dominant reddish-brown color is due to iron oxide present as grain coatings.

Sorting in Association A ranges from very poor to very well and is usually moderate to poor. Well sorted rocks are usually fine sandstones or siltstones, although local concentrations of pebbles of a particular size grade are common in conglomerate beds. Sandstones show a wide range in textural maturity but are usually immature or submature following Folk's (1974) classification of textural maturity.

Roundness and sphericity of Association A conglomerate clasts are variable. Using the terminology of Klein (1962) Association A contains both roundstone and sharpstone

conglomerates, that is, locally clasts are well rounded and spherical to subspherical but elsewhere they are angular and have low sphericity. Roundness and sphericity of sandstone grains, and the geographic distribution of grain and clast roundness and sphericity values are discussed in detail later.

External bed forms. Bedding in Association A is usually ill-defined due to extremely rapid and irregular vertical and lateral changes in both grain size and grain orientation, but locally bedding is defineable on the basis of grain size and orientation.

Bedding in Association A is commonly  $1/3$  to 1 meter thick (medium to thickly bedded), but can be as thick as 3 meters. Following the classification scheme of Pettijohn and Potter (1964), beds are usually unequal in thickness, laterally variable in thickness, and discontinuous over a few meters. They are often crudely lenticular in shape (see Figure 2). Occasional irregular tabular or wedge shaped beds are present in minor abundance. Bedding is more laterally continuous in a dip direction than along strike.

The base of most Association A beds is a scour surface with variable relief up to about 1 meter and which commonly truncates other scour surfaces. Scour surfaces are irregular (see Figure 3) to concave upward and are usually overlain by coarse conglomerate. This type of bedding is termed cut and fill bedding by Bull (1972) and is



Figure 2. External bedding in T<sub>1</sub> conglomerates. The bed in the center of the picture is 1 meter thick. Note that the beds are unequal in thickness, variable in thickness laterally, discontinuous over a few meters, and crudely lenticular.



Figure 3. Interbedded conglomerates and pebbly mudstones in  $T_1$ . Note that conglomerate beds are crudely lenticular and overlie a scour surface. This type of cut and fill bedding is a characteristic feature of  $T_1$ . Note also the homogeneous internal character of the lower pebbly mudstone. Hammer in center of photo for scale is 30 centimeters long.

characteristic of external bedding in Association A.

Typically stratification is best observed from a distance (Figure 4), but strata observed at a distance usually contain several poorly defined sedimentation units.

Internal Bedding Characteristics. Beds of Association A display a dominantly oriented internal fabric as opposed to a disoriented one. The most common type of grain orientation is the alignment of elongate clasts with long axes parallel to bedding planes and perpendicular to the current direction determined by Tixeront to be east to west. The second most common internal fabric is pebble imbrication. Pebbles are imbricated throughout an entire bed or only locally around larger pebbles or boulders.

Crossbedding is a common internal structure in Association A. Crossbedding commonly occurs in the form of large and medium scale sets, from 10 to 50 centimeters thick, which are lenticular or wedge shaped (see Appendix A). Low angle planar or low to high angle trough shaped crossbeds are approximately equal in abundance. Crossbeds are defined by changes in grain size and/or grain orientation. Crossbedding is commonly better defined in lenses of coarse to medium sandstone where concentrations of small pebbles or granules define the cross-stratification.

Small scale crossbedding or ripple crossbedding is rare in Association A due to the general lack of rocks of fine grain size. However these types of crossbeds do occur in minor abundance in Association A near the upper





Figure 4. Stratification in  $T_1$  conglomerates seen at a distance. The conglomerates here are dipping to the west. Note that the stratification is more distinct in the hill in the center of the photo than in the hill in the foreground. The prominent ridge at the top of the hill in the right background is composed of Ordovician quartzite which underlies the  $T_1$  conglomerates with angular unconformity.



part of  $T_1$ , where finer grained beds are more numerous.

Also minor in abundance in Association A are parallel laminations defined by alternating laminae of differing grain sizes. In sandstones, small pebbles or granules often define thin beds or laminae which are parallel to external bedding.

This type of alternation of thin beds of different grain sizes is more abundant than graded bedding in Association A. In this alternation however, there is typically a decrease in the mean grain size of the individual thin beds or laminae from the base to the top of the bed, accompanied by an improvement in sorting. Graded bedding is present in minor abundance in Association A. Normal grading is more common, but reverse grading occurs. Grading is usually interrupted by a scour surface and beds that grade from conglomerate to fine sandstone or siltstone are extremely rare, but occur in Association A near the uppermost part of  $T_1$ .

Bedding Plane Features. Other than the abundant scour surfaces mentioned above, bedding plane features are rare in Association A. Ripple marks have heights up to 4 centimeters and are assymetric ripples with discontinuous and irregular crestlines. The coarse grain size of Association A precludes the development of casts of mud cracks, rain drop imprints, or organic tracks and trails. Finer units are commonly scoured deeply, decreasing the chances for preservation of bedding plane features.

Penecontemporaneous deformation features are also rare to absent. Some fine sandstones or siltstones which are typically parallel laminated acquire a nodular character associated with an increase in the amount of calcareous cement (see Figure 5). No casts of burrows were found associated with these nodular, concretionary horizons. These beds are gradational below with fine sandstone or siltstone and are scoured above by conglomerate. They are laterally impersistent due to truncation by scour surfaces.

#### Association B

Association B comprises 4 to 9 percent of  $T_1$  and consists of pebbly silt- or mudstone interbedded with homogeneous or nodular siltstones. This type of lithologic association is most common in the 800 to 900 meter interval in section I (see Appendix B). A few interbeds of Association A lithologies occur in this interval. Bedding is of medium thickness and crudely lenticular. The bases of most pebbly silt- or mudstone beds is a mild scour surface or a sharp but irregular non-erosive contact. Homogeneous or nodular siltstone interbeds commonly overlie sharply and are occasionally gradational below with pebbly silt- or mudstones. Pebbly silt- or mudstone beds are very poorly sorted compared with the conglomerate beds in Association A. Internally the pebbly silt- or mudstones typically have a disoriented or random fabric (see Figure 6). They are rarely crossbedded or graded. Intraformational clasts are

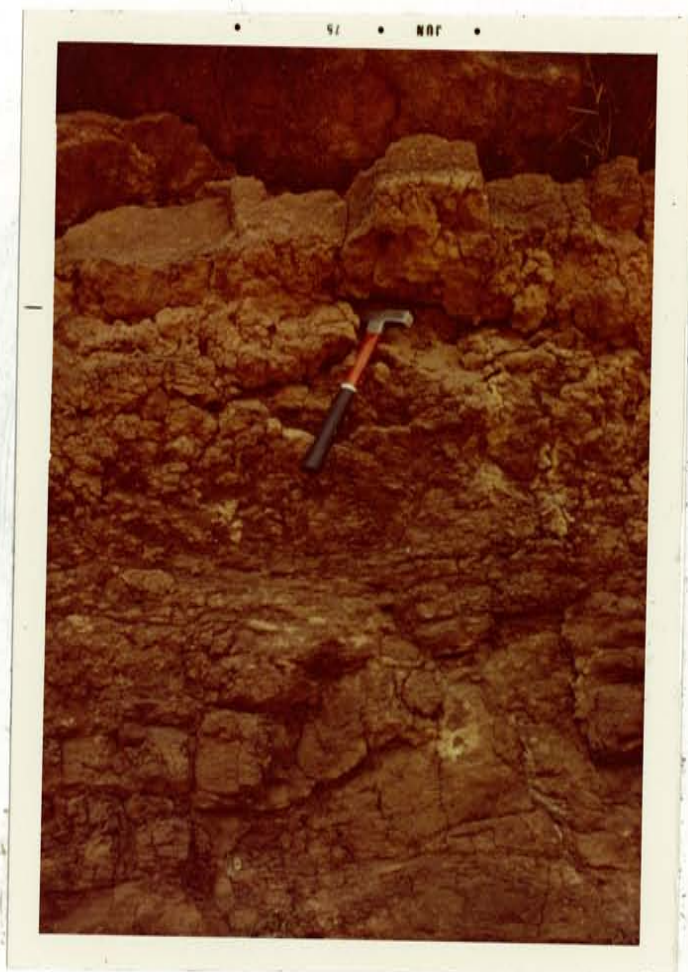


Figure 5. Nodular siltstone interbed in  $T_1$  conglomerate. The nodular character of the siltstone here is associated with an increase in the amount of calcareous cement, similar to the cornstone described by Steel (1974) and Bruck et al. (1967), and may be a fossil soil horizon. Hammer is 30 centimeters long.

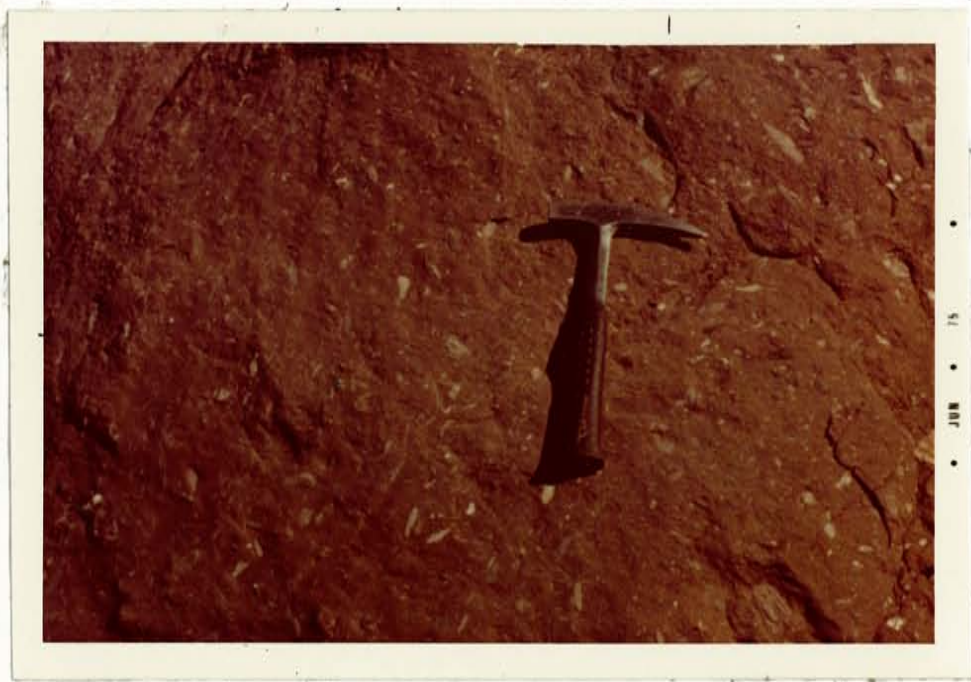


Figure 6. Bedding plane view of a  $T_1$  pebbly mudstone bed. Note the variety of pebble orientations, and how they "float" in a mudstone matrix. Hammer is 30 centimeters long.

absent or rare within the pebbly silt- or mudstones.

### Association C

The remaining 1 percent of  $T_1$  is composed of tabular conglomerate beds with sharp non-erosive basal contacts here referred to as Association C (see Figure 7). Beds of this nature, found only at sample area 17, are commonly of medium thickness composed of moderately sorted, well packed conglomerate, with only occasional parallel aligned elongate pebbles. These tabular beds are commonly scoured by conglomerate or coarse sandstone and their shape modified so they are laterally continuous along strike only up to about 20 meters and along dip up to 30 meters.

### Interpretation of $T_1$ Depositional Environment

The Association A units, principally irregularly cut and fill bedded conglomerates with a well defined, oriented internal fabric are similar to modern braided stream channel fills as described by Doeglas (1962) and Williams and Rust (1969) and ancient braided stream deposits described by Bluck (1967), Smith (1970), and Steel (1974). The channels of braided streams are shallow and thus shift often due to crevassing, infilling, or blockage by large boulders (Davis, 1938; Doeglas, 1962; Beatty, 1963). The shifting nature of shallow braided stream channels gives rise to the rapid lateral and vertical variations in grain size and the irregular bedding of braided stream deposits.





Figure 7. Tabular conglomerate bed in T<sub>1</sub>. Note the non-erosional, sharp basal contact with the underlying coarse sandstone. Also note the moderate sorting of the conglomerate and the decrease in the amount of matrix as compared with Figure 6. This bed is overlain by a coarse sandstone bed with a mild scour base. The pencil, for scale is 14 centimeters long.

These are characteristic features of Association A. Channel fills in Association A commonly show a decrease in median and largest grain size from the base to the top and slightly better sorting at the top similar to the channel fills observed by Williams and Rust (1969).

Williams and Rust (1969) indicate that the grain size in braided stream deposits in the Yukon ranges from boulders to clay sized grains with gravel greater than two millimeters in diameter most abundant. Rocks of Association A have similar grain sizes. Sorting in braided streams is generally poor with zones of better sorting occurring in channel floors (Doeglas, 1962). Sorting in Association A is moderate to poor with localized zones of better sorting often above the lowest part of a scour surface.

Two of the most common internal bedding structures in modern braided stream deposits are pebble imbrications and parallel alignment of elongate pebbles (Doeglas, 1962; Williams and Rust, 1969). These features are ubiquitous in Association A conglomerates and coarse pebbly sandstones.

Another prominent feature of braided stream deposits is crossbedding. Williams and Rust found two dominant types of cross-stratification in the Donjek River; medium to large scale planar cross strata in conglomerates to fine sands, and small scale cross laminae in medium to fine silt. In braided streams in France, Doeglas (1962) notes that beds with a scour surface at the base are typically trough crossbedded or cross laminated. Steel

(1974) notes the abundance of cut and fill bedding and large scale trough cross-stratification in conglomerates and sandstones of the New Red Sandstone in Scotland. Most abundant in Association A are large to medium scale, low angle planar or low to high angle, trough cross strata. Trough cross strata probably developed during channel filling as outlined by Doeglas (1962, Figure 22) and low angle planar cross strata probably developed on longitudinal bars, a feature noted by the writer in the Rio Salado of central New Mexico, a braided tributary to the Rio Grande. Bluck (1967) also notes the abundance of planar cross strata in alluvial fan stream deposits (his Conglomerate B), and trough cross strata in braided stream deposits (his Conglomerate C) from the Upper Old Red Sandstone in Scotland.

The less abundant parallel bedded or laminated units in Association A, usually sandstones and siltstones, either represent deposits on longitudinal bars during waning flood stages as observed by Doeglas (1962), or are overbank deposits. However, individual thin beds of pebbles within some of these fine-grained parallel bedded units indicate high flow regime conditions and in this case the parallel beds are probably the result of deposition on flat channel floors during flooding.

Doeglas notes a dominance of alternating thin beds of different grain sizes rather than graded bedding in braided rivers in France. As noted by Smith (1970) in the Shawangunk conglomerate (Silurian) of Pennsylvania, some



beds record an increase in flow regime vertically by reverse grading, but others show a decrease in flow regime by normal graded bedding. More often however, alternating thin beds of different grain sizes decrease in thickness and average grain size vertically as opposed to single beds showing internal grading. Similar relations are noted in Association A.

The relative scarcity of ripple bedding, bedding plane features and penecontemporaneous deformation features in Association A can be explained by the relative scarcity of sediments finer than conglomerates. Abundant scour surfaces cut into fine units attest to the low preservation potential of the above features. Although Williams and Rust (1969) and Doeglas (1962) describe abundant ripple marks and plentiful vegetation in modern braided rivers, Steel (1974) notes a scarcity of these characteristics in the lower Mesozoic New Red Sandstone of Scotland. Steel notes that the scarcity may be due to erosion after deposition and a similar interpretation is suggested for Association A.

High angle planar foreset crossbeds are rare in Association A indicating the scarcity of transverse bars. This may reflect rapid deposition during flood periods of short duration so that dunes, whose downstream migration produce this sedimentary structure, did not form (Smith, 1970), or it may be because Association A channels were too narrow and shallow, and shifted too often for transverse bars to form.

The origin of the concretionary calcareous siltstones noted in a few places in Association A is problematical. Their occurrence at the top of horizontally laminated siltstones and beneath conglomerate beds is similar to the occurrence of cornstone beds described by Steel (1974) and the carbonate horizons described by Bruck et al. (1967). These writers have interpreted such beds as ancient caliche or soil horizons, but such an interpretation here in the absence of detailed petrographic data is tentative. These units are minor in abundance in Association A.

Thus, Association A is interpreted as braided stream deposits, and includes the deposits produced during stream flooding as well as the deposits produced during waning flood stages or during normal period of flow. No distinction has been made between these types of deposits produced during different stages of flow, as Steel (1974) has made for the New Red Sandstone in Scotland. All types of deposits as distinguished by Steel are present and interbedded and interfingering in Association A.

The Association B pebbly silt- or mudstone beds are interbedded with the previously described Association A braided stream deposits. Association B beds are interpreted as mudflow deposits on the basis of their very poor sorting, homogeneous internal fabric of disoriented pebbles in a mud- or siltstone matrix, non-erosional basal contacts, and lack of other sedimentary structures. The lenticular bed shape is not characteristic of the laterally

extensive mudflows described by Steel (1974) and Bluck (1967) but more like the mudflows described by Sharp and Nobles (1953) which tend to follow pre-existing stream channels. Thicknesses of individual flows correspond to those given by Sharp and Nobles (1953), usually from one to three feet. Rarely, pebbly silt- or mudstones grade upward into silt- or mudstones lacking pebbles. These units are interpreted as less viscous flows which were density stratified during deposition. Like the mudflows described by Steel (1974), Association B mudflows are closely associated with fine sandstones, siltstones and interbedded conglomerates of, in this case, Association A.

Association C conglomerate beds with non-erosive but sharp bases are interpreted as sheetflood deposits. The few beds of this type observed in  $T_1$  are moderately sorted, typical of sheetflood deposits described by Bull (1964). Davis (1938) indicates that sheetfloods have a transporting and depositing nature rather than an eroding nature and consequently their deposits have an abrupt non-erosive basal contact. Like the tabular beds in Association C, Davis (1938) describes sheetflood deposits as being sheet-like in cross section, usually one to three feet thick and composed of coarse sand or gravel with a smaller amount of matrix than mudflows (compare Figures 6 and 7).

In summary,  $T_1$  is interpreted as a unit composed dominantly of braided stream deposits with minor interbedded mudflow and sheetflood deposits. This association

of lithologies is characteristic of alluvial fan deposits (Bull, 1968, 1972; Blissenbach, 1965). The criteria for the recognition of alluvial fan deposits described by Bull (1972) are: 1) oxidized deposits; 2) scarcity of preserved organic matter; 3) interbedded and interfingered braided stream deposits, mudflow deposits, and sheetflood (or debris flow) deposits; 4) high length to width ratio of beds; 5) cut and fill structure; 6) variable hydraulic conditions of transport and deposition resulting in variable sorting, particle size, and thickness of beds; 7) a decrease in clast size away from the source; 8) characteristic C-M plots of sediments; 9) interfingering with talus slope and playa lake deposits; and 10) radial flow directions away from the source.

Of these ten criteria, the first seven are characteristic of  $T_1$ . Due to cementation and possible diagenetic alternation of grain size, extensive grain size analyses were not attempted and therefore C-M plots were not carried out. Talus slope or landslide deposits, if present, were probably to the east of the present erosional limit of  $T_1$ . Playa lake deposits are not characteristically associated with all alluvial fans, particularly not those in temperate or humid climates. Detailed paleocurrent measurements were not made due to lack of time.

## $T_2$ COARSE TO FINE CLASTICS

Tixeront (1971) describes  $T_2$  as coarse sandstone beds

overlain by interbedded coarse sandstone and fine sandstone overlain by fine sandstone covered by a sandy drain. This brief description is inadequate to precisely define the environment of deposition of  $T_2$ . The following descriptions of the unit Tixeront has mapped as  $T_2$  come from sections I, II, V, VI, VII, and VIII (see Appendix B), and bedding descriptions at other localities.

### Thickness and Geometry

As mapped by Tixeront (1971),  $T_2$ , like  $T_1$ , is a lenticular body thickest in the center of the Argana Valley between Iferd and Timezgadouine, and thin to absent elsewhere to the north and south. Tixeront reports a maximum thickness of 1800 meters, but the thickest section measured in this study is slightly more than 200 meters thick (see section I, Appendix B).

### Bed Lithologies and Geometries

The unit  $T_2$  has a wider variety in the abundances of rocks of different grain sizes than  $T_1$ . Overall, medium, fine, and very fine grained sandstones occur in equal abundance and are dominant in  $T_2$ . Coarse sandstone and siltstones are second in abundance followed by conglomerates, coarse pebbly sandstones, and shales which are minor in abundance.

Bed thickness in  $T_2$  ranges from several meters down to several centimeters. Beds are either tabular, wedge, or

lenticular in shape and are laterally continuous from 10 to several hundred meters. Bed shape and lateral continuity are a function of grain size. Conglomerate beds or coarse pebbly sandstone beds are commonly highly lenticular in shape and rarely continuous laterally for more than 10 meters. They range in thickness from several to 30 centimeters. These coarse beds usually grade upward into, or are scoured above by, coarse to medium grained sandstone beds also lenticular in shape but often continuous laterally up to 30 meters. Coarse to medium grained sandstone beds range in thickness from several up to 100 centimeters. These beds usually grade vertically and laterally into medium to fine grained sandstones which are of comparable thicknesses but laterally continuous up to 100 meters, and usually wedge or lenticular in shape. These medium to fine sandstone beds in turn grade vertically and/or laterally into very fine sandstone to siltstone beds which are laterally continuous up to about 300 meters. The shape of these very fine sandstone to siltstone beds is usually tabular. They may be several meters thick, but are commonly one to two meters thick.

Thus,  $T_2$  consists of thin to medium bedded lenticular or wedge shaped bodies of coarse grained lithologies which are offset laterally and vertically from each other and are separated by tabular beds of very fine sandstones or siltstone (see Figure 8). The coarser lenticular or wedge shaped units are more continuous along dip than along

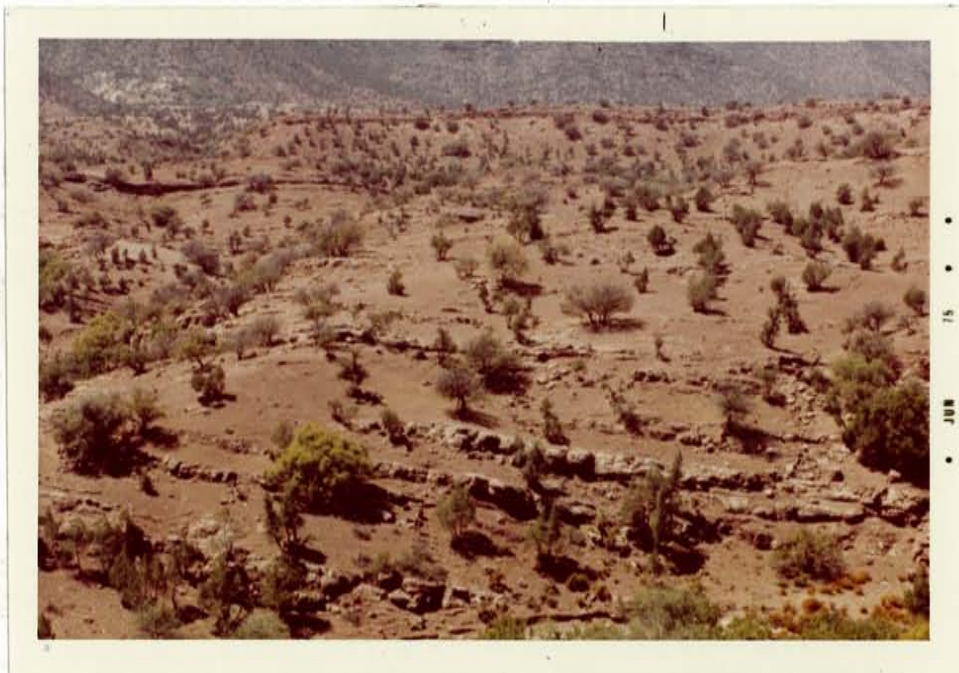


Figure 8. Stratification in  $T_2$  seen at a distance. Note how the lenticular or wedge shaped, resistant, coarser grained units are offset vertically and laterally by tabular, slope forming finer grained units. Note also how the coarser units decrease in abundance and thickness upward. The nearly flat lying persistent unit in the background is  $T_3$  which overlies  $T_2$  with angular unconformity.

strike, but not to the same degree as units in  $T_1$ .

The decrease in average grain size vertically in  $T_2$ , suggested by Tixeront, is accomplished by a vertical decrease in the abundance and thickness of the coarser units and an increase in abundance and thickness of tabular very fine sandstone and siltstone units (see Figure 8).

### Primary Sedimentary Structures

The kinds and relative abundances of sedimentary structures in  $T_2$  are related to grain size, so that lithologies which display similar structures are grouped together in the discussion below.

Beds of conglomerate and coarse pebbly sandstones have an oriented internal fabric defined by parallel alignment of elongate clasts and pebble imbrications. Red sandstone or siltstone clasts are common. Large to medium scale, low to high angle trough crossbedding or low angle planar crossbedding is abundant. Graded bedding is common and is usually normal grading although locally reversals do occur. The beds grade from conglomerate or coarse pebbly sandstone to medium sandstone and occasionally fine sandstone.

Coarse to medium grained  $T_2$  sandstones commonly are trough crossbedded or crosslaminated. The crossbeds or laminae are defined by changes in grain size or by alignment of elongate grains. The crossbedding is usually of medium scale with the thickness of the crossbed sets generally decreasing upward within a bed. Pebbles are commonly



localized at the base of trough shaped sets of cross laminae. Other sedimentary structures noted in minor amounts are parallel laminations, individual pebble laminae, and ripple crosslamination, or the coarse to medium grained sandstones can be internally homogeneous. Ripples have typically highly irregular crest geometries, are assymmetric, and vary in height up to 3 centimeters. Beds of coarse to medium sandstone have either a scour base or are gradational with underlying conglomerates and/or pebbly coarse sandstones. They commonly grade upward and/or laterally into fine sandstone beds.

Fine sandstone beds are medium to thinly bedded or laminated. They may be homogeneous or parallel laminated but are often ripple crosslaminated or trough crossbedded (see Figure 9). Thin laminae of siltstone or mudstone are commonly interbedded with the fine sandstone. Possible disturbed bedding or convolute laminations occur in some fine sandstone beds but are not common. Bedding planes within parallel bedded fine sandstone exhibit parting lineation. Accretion bedding occurs but is not common (see Figure 10). The beds have either mild scour bases or are gradational with coarser rocks below. They are almost always gradational above with overlying very fine sandstones and/or siltstones.

Interbedded very fine sandstones and siltstones show a wide variety of sedimentary structures. Internally the two lithologies are thin bedded or laminated (see Figure 10),



Figure 9. Trough crossbedding, parallel bedding, and ripple crosslamination in a  $T_2$  fine sandstone bed. Note the mild scour base into siltstone below. Divisions on the rod are 50 centimeters.



Figure 10. Stratification in  $T_2$  seen at a distance. Note the parallel bedding in very fine sandstones and siltstones just to the left of the man in the lower right corner. These are scoured above by a laterally discontinuous coarse sandstone bed which internally is low angle planar and trough crossbedded, and possibly epsilon cross-stratified. These coarse units are gradational with finer grained rocks above. Note also how a vertical section through these units would result in a cyclic variation in grain size from coarse to fine to coarse again.

bioturbated, homogeneous, or ripple crosslaminated. Commonly they exhibit nodular or concretionary bedding associated with an increase in calcareous cement. Bedding plane features are abundant. They include casts of horizontal and vertical burrows, root casts, reptile track molds and possible casts of raindrop imprints. Mudcrack casts occur but are rare. Occasionally these very fine sandstone and siltstone beds grade upward into shales or mudstones with the same types of sedimentary structures.

#### Other T<sub>2</sub> Lithologies

Comprising less than 1 percent of T<sub>2</sub> but requiring description are thin beds of silty limestone or micritic limestone. These units always overlie very fine sandstones, siltstones, or mudstones. They have a sharp non-erosive basal contact and are scoured above by conglomerates or sandstones or are overlain sharply by more very fine sandstone or siltstone beds. Several of the beds of carbonate are laterally continuous up to 200 meters and change very little in thickness laterally. Internally these beds are homogeneous except in the lower few centimeters where there are irregular wavy thin beds or laminae discontinuous over 10 centimeters. Carbonate horizons such as these were found in sections I and VI only, although calcareous fine sandstone to siltstones are common throughout T<sub>2</sub>.

## Cyclic Vertical Sequences in T<sub>2</sub>

The cyclicity in T<sub>2</sub> occurs as repeated variations in grain size and associated sedimentary structures. Cycles are observed to vary in thickness and are commonly incomplete.

Typically each T<sub>2</sub> cycle is several meters thick with an average of 3 cycles every 10 meters (see Appendix B, sections V, VII, and VIII). Cycles begin with a scour surface at the base cut into very fine sandstone, siltstone, or rarely mudstone. Overlying the scour surface are either conglomerates, coarse pebbly sandstones, or coarse to fine sandstones. The coarser units are gradationally overlain by very fine sandstones, siltstones or mudstones. Another scour surface begins the next cycle.

## Interpretation of T<sub>2</sub> Depositional Environment

The deposits of unit T<sub>2</sub> resemble the channel and flood plain sediments of modern meandering streams as summarized by Pettijohn et al. (1973) and Matthews (1974). They also resemble the deposits of certain ancient alluvial deposits, notably the Devonian Lower Old Red Sandstone described by Allen (1964), the Devonian Wood Bay Formation of Spitsbergen described by Moody-Stuart (1966), the Blomidon Formation of the Triassic of Nova Scotia described by Klein (1962), and the Permo-Triassic flood plain sediments of the New Red Sandstone described by Steel (1974, his group II) and Bruck et al. (1967).

Beginning at the base of a typical cycle, conglomerate and coarse pebbly sandstones are interpreted as channel lag deposits which formed in the deepest part of meandering river channels (see Pettijohn et al., 1973, Figure 11-11; Matthews, 1974, Figure 10.24; and Allen, 1964, Figure 10). These lag gravels in  $T_2$  are intermediate between the types  $D_1$  and  $D_2$  described by Steel (1974) in that they are thin (less than 1 meter thick) like his  $D_1$  coarse members but laterally impersistent like his  $D_2$  coarse members. The trough shaped lower erosional surfaces of  $T_2$  conglomerates and coarse sandstones correspond in shape to the channel beds of low-sinuosity rivers as described by Moody-Stuart (1966) where erosion takes place on both sides of the channel.

Coarse to medium grained sandstones exhibiting trough crossbedding are also interpreted as channel deposits, but here the crossbedding implies these units formed by the downstream migration of dunes in a shallower portion of the river channel. An upward decrease in the thickness of sets of trough crossbeds implies a decrease in flow regime. Pebbles localized at the base of trough sets probably are lag concentrates (see Allen, 1964, Figure 5). Parallel pebble laminae indicate upper flow regime deposition and bed-load transport over relatively flat channel banks (see Allen, 1964, Figure 10). The fact that these coarse to medium sandstones in  $T_2$  are rarely cut deeply by fine sandstone beds makes them analogous to the stream bed deposits of low-sinuosity rivers defined by Moody-Stuart (1966).

The trough or wedge shape of these beds further constrasts with the tabular bed shapes characteristic of his high sinuosity stream model.

Fine sandstones which gradationally overlie coarse to medium sandstones or which overlie a scour surface cut into very fine sandstones or siltstones are also interpreted as channel fills deposited under lower flow regime conditions. The lack of abundant accretion bedding or epsilon cross-bedding suggests streams of low-sinuosity (Moody-Stuart, 1966). Trough crossbedded, fine sandstones result from the downstream migration of dune bed forms. Parallel bedded and low angle planar crossbedded fine sandstones result from deposition over relatively flat channel beds. Ripple cross-laminated fine sandstones result from the downstream migration of ripple bed forms. Occasional convolute laminae probably indicate rapid dune migration resulting in unstable foreset angles and slumping prior to lithification (Allen, 1964).

Very fine sandstones and siltstones are interpreted as overbank deposits on the basis of evidence of vegetation, burrowers, reptile tracks, parallel laminae of alternating very fine sandstone and siltstone, and occasional ripple crosslamination. Allen interprets concretionary nodules high in calcium carbonate as an indication of ground water movement through the sediment before lithification. They are common in T<sub>2</sub> overbank flood plain deposits and their presence along with the relative scarcity of mudcrack casts

indicates the flood plain areas were probably inundated with water both at the surface and at shallow depths by ground water. Overbank deposits of  $T_2$  generally overlie the entire upper surface of the channel fill deposits. This is another criteria presented by Moody-Stuart for low-sinuosity rivers.

In summary it would appear that  $T_2$  exhibits most of the characteristics set forth by Moody-Stuart (1966) as indicative of low-sinuosity streams. However, as Figures 8 and 10 show, there is no dominance of channel deposits over overbank deposits and perhaps  $T_2$  would best fit a model in between low-sinuosity and high sinuosity as described by Moody-Stuart. This is supported by the presence of some accretion bedding in channel sandstones and the increased variability in lateral continuity of channel deposits along dip as compared with  $T_1$  braided stream deposits which consistently are more laterally continuous in the direction of transport.

The origin of the silty limestone or micritic limestone beds present in minor abundance in  $T_2$  is deferred until their petrographic description is presented.

### $T_3$ CONGLOMERATES

#### Thickness and Geometry

Tixeront (1971) describes  $T_3$  as a thin but continuous conglomerate unit that overlies with angular unconformity  $T_1$ ,  $T_2$ , or the lower Paleozoic basement. As mapped by him (see Plate A),  $T_3$  usually overlies  $T_2$ , but overlies  $T_1$  only



at sample area 16, and overlies the lower Paleozoic basement at a locality 2 kilometers southwest of Timezgadouine.

Tixeront has mapped  $T_3$  south of Iferd as far as Tamagoust.

In this study, however,  $T_3$  is redefined as containing clasts of volcanic rock fragments because this is the only criteria which can be used to distinguish  $T_3$  conglomerates from conglomerates in  $T_1$ ,  $T_2$  or  $T_4$ . Following this definition,  $T_3$  does not occur south of sample area 5, where Tixeront has apparently mapped basal  $T_4$  conglomerates, which contain no volcanic rock fragments, as  $T_3$ . Moreover, following this definition  $T_3$  does not overlie lower Paleozoic rocks 2 kilometers southeast of Timezgadouine, but overlies  $T_2$  there.

Section measurement indicates  $T_3$  is thickest in the south at sample area 5 where it is a maximum of 3 meters thick. The unit becomes finer grained and thins gradually northward to 1 meter thick at sample area 2 and pinches out several hundred meters north of there. The two-dimensional geometry of  $T_3$  parallel to strike is that of a wedge thickest in the south and continuous for 21 kilometers to the north before pinching out. Because  $T_3$  is overlain by  $T_4$  its three-dimensional geometry is not known.

### $T_3$ Lithologies

The unit  $T_3$  is composed of dominantly (greater than 80%) cobble, or rarely boulder, to pebble conglomerates with minor interbedded sandstones and siltstones. The

remaining part of the unit (less than 20%) is composed of pebbly coarse sandstones to medium sandstones with interbedded fine sandstones and siltstones.

The conglomerates are reddish-brown in color and have a sandy matrix. Sorting is moderate to poor comparable to sorting in  $T_1$  conglomerates. Clasts show a wide variability in shape and roundness but are generally subequant in shape (following Zingg's, 1935, classification) and subangular to subround (following Power's, 1953, classification). Further details of clast and matrix composition are discussed later.

Sandstones of  $T_3$  are reddish-brown in color, moderately to poorly sorted and usually texturally submature.

#### External Bed Form and Thickness

Conglomerate beds of  $T_3$  are up to 1.5 meters thick (medium to very thickly bedded). Cut and fill bedding is most common; beds are crudely lenticular and laterally continuous up to 10 meters. Scour surfaces have a maximum relief of 1 meter.

Coarse pebbly sandstone to medium sandstone beds are 25 to 50 centimeters thick. They, like the conglomerate beds, are lenticular but are laterally continuous up to 15 meters. Cut and fill bedding is most common but some beds are wedge shaped. Accretion bedding does not occur.

Fine sandstones to siltstones are laminated or thinly bedded, very irregular in thickness and discontinuous

laterally over a few meters due to truncation by scour surfaces.

### Primary Sedimentary Structures

Conglomerates of  $T_3$  display a less well defined internal oriented fabric than  $T_1$  conglomerates, due to the presence of fewer bladed or tabular clasts, however, the clasts are usually aligned with long axes in the plane of bedding or are imbricated. Thin beds or laminae of sandstone or siltstone are often present within conglomerate beds. These are usually parallel laminated and occasionally pebbles or granules define single laminae. Less often  $T_3$  conglomerates are internally homogeneous.

Commonly the upper parts and lateral edges of  $T_3$  conglomerates are gradational with coarse pebbly to medium sandstone beds, but less commonly the coarse pebbly to medium sandstones have mild scour bases.

Coarse pebbly to medium grained sandstones are internally medium to large scale trough crossbedded, or parallel thin bedded, or low angle planar crossbedded. Bedding is commonly defined by changes in grain size, rarely by changes in grain orientation. Alternating beds of differing grain sizes usually become thinner and finer grained upward and laterally. Normal graded bedding (to medium or fine grained sandstone) occurs in minor abundance. Thin, discontinuous interbeds of fine sandstone or siltstone are common, and become more abundant upward.

Fine sandstones and/or siltstones are ripple cross-laminated, parallel laminated or homogeneous internally. Burrow casts or other bedding plane features besides ripple marks are rare.

The unit  $T_3$  is conformably overlain by  $T_4$ . In terms of grain size the contact between the units is gradational. Because  $T_3$  is defined on the basis of the presence of clasts of volcanic rock fragments, the boundary between the two units is picked above the uppermost occurrence of beds containing clasts of volcanic rock fragments.

#### Interpretation of Depositional Environment of $T_3$

The unit  $T_3$  is interpreted as a braided stream deposit on the basis of its coarse grain size, cut and fill bedding, trough crossbedding, and lateral discontinuity of bedding. Thin interbeds of sandstone and siltstone were probably deposited during the waning stages of flooding as noted by Doeglas (1962).

## CHAPTER III. PETROLOGY

## ANALYSIS OF PEBBLE AND POINT COUNT DATA

Field and petrographic work shows that there are two  $T_1$ - $T_2$  sequences based on pebble and grain composition. The two sequences are now juxtaposed at the Fault of Argana (see Plate A) and for simplicity the sequence to the north of the fault will be called the Northern Sequence and the sequence to the south the Southern Sequence (see Plate A).

The Northern Sequence is characterized by subangular, bladed or tabular clasts which consist of subequal amounts of quartzite and phyllite rock fragments. Quartz in the quartzite rock fragments is fine grained. Igneous and terrigenous sedimentary rock fragments occur in minor abundance in Northern Sequence conglomerates and sandstones. The Southern Sequence is characterized by subrounded, sub-equant to oblate clasts which consist dominantly of quartzite and limestone rock fragments. Quartz in the quartzite rock fragments is fine to coarse grained. Igneous, terrigenous sedimentary, and phyllite rock fragments occur in minor abundance in the Southern Sequence.

The associations of lithologies and sedimentary structures and textures described in this and the preceding chapter indicate a nearby source area for  $T_1$ ,  $T_2$ , and  $T_3$  deposits. Therefore, mineralogic changes in conglomerates and sandstones should reflect similar changes in the source area(s) supplying the detritus.

In order to quantitatively describe the observed variability in clast composition and its relationship to source area(s), pebble count data for the conglomerates and point count data for the sandstones was gathered using statistical sampling plans.

### Sampling Methods

Pebble count data from each station shown on Plate A is summarized in Table I. At each locality an orthogonal grid is constructed whose spacing is equal to the diameter of the largest pebble or boulder in the outcrop to ensure that no clasts are counted twice. Grid spacing varies from 8 centimeters in  $T_2$  conglomerates up to 30 centimeters in  $T_1$  conglomerates. The total number of counts varies with the size of the outcrop from 109 to 275. In this study, the minimum longest clast diameter for accurate distinction between the different types of rock fragments in the field is one centimeter. Therefore, clasts whose longest diameters are smaller than one centimeter are classified as matrix along with the sandstone, siltstone, or mudstone matrix of the conglomerates. Because the amount of matrix in conglomerates is related to depositional environment, as well as source area, the amount of matrix is not included in the statistical analysis, and the data in Table Ia is used instead.

Point count data is summarized in Table II. Seventeen sandstones from  $T_1$ ,  $T_2$ , and  $T_3$  lithologies were point

Table I. Frequency data for pebble counts of conglomerates.

Lithology	Northern Sequence			Southern Sequence													
	T <sub>1</sub>	T <sub>2</sub>		T <sub>1</sub>	T <sub>2</sub>	T <sub>1</sub>	T <sub>2</sub>	T <sub>3</sub>									
Sample No. Clast Composition	19	1	4	12	3	13	11a	11	21	6	10	7	8	5	9	18	20
quartzite	70	32	20	46	11	14	113	127	99	96	85	62	104	67	53	25	24
phyllite	52	28	24	38	17	61	3	4	1	2	0	0	1	3	0	0	1
matrix	83	61	65	149	90	155	54	92	65	95	100	153	161	103	109	167	96
vein quartz	2	0	1	1	0	0	2	1	5	7	1	1	5	3	1	7	7
limestone	0	0	0	0	0	0	29	0	31	15	32	9	4	15	29	2	14
terrigenous rock fragment	0	0	0	0	0	0	2	0	2	0	1	0	0	10	6	0	0
igneous rock fragment	0	1	0	0	0	0	0	0	0	1	0	0	0	0	11	41	52
sample size (n)	207	122	110	234	118	230	205	224	203	216	219	225	275	201	209	242	194
grid spacing (cm)	30	15	15	20	8	8	18	20	15	15	15	18	8	20	no	10	25
															data		

Table Ia. Frequency data used in statistical testing of pebble counted conglomerates

Lithology	Northern Sequence		Southern Sequence		
	T <sub>1</sub>	T <sub>2</sub>	T <sub>1</sub>	T <sub>2</sub>	T <sub>3</sub>
Sample No. Composition	19 1 4 12 3 13	11a 11 21 6 10 7 8	5 9 18 20		
quartzite	70 32 20 46	11 14	113 127 99 96 85 62 104	67 53 25 24	
phyllite	52 28 24 38	17 61	3 4 1 2 0 0 1	3 0 0 1	
vein quartz	2 0 1 1	0 0	2 1 5 7 1 1 5	3 1 7 7	
igneous rock fragments	0 1 0 0	0 0	0 0 0 1 0 0 0	0 11 41 52	
limestone	0 0 0 0	0 0	29 0 31 15 32 9 4	15 29 2 14	
terrigenous rock fragments	0 0 0 0	0 0	2 0 2 0 1 0 0	10 6 0 0	
sample size (n)	124 61 45 85	28 75	149 132 138 121 119 72 114	98 100 75 98	
grid spacing (cm)	30 15 15 20	8 8	18 20 15 15 15 18 8	20 no data 10 25	
ratio of quartzite/ phyllite	1.35 1.14 0.83 1.21	0.65 0.23	37.67 31.75 99.0 48.0	104.0 22.33	24.0
standard deviation	0.20 0.25 0.22 0.22	0.23 0.06	4.73 3.99 13.49 6.77	13.74 3.50	5.58
95% confidence interval	0.95 to 1.75	0.64 to 1.64	23.77 to 39.73	76.52 to 131.48	15.33 to 29.33



Table II. Frequency data for point counted sandstones

Lithology	Northern Sequence						Southern Sequence											
	T <sub>1</sub>			T <sub>2</sub>			T <sub>1</sub>			T <sub>2</sub>			T <sub>3</sub>					
sample No.	D	E	C	F	I	12	19	13	25	11	7-IV	10-IV	21-A	1-V	9	22-B	18	
Composition																		
quartz	11	17	20	30	43	20	56	22	43	89	40	35	73	33	19	27	23	
quartzite	20	12	22	5	28	8	5	3	29	0	30	17	13	18	15	12	18	
phyllite	26	25	11	2	17	33	0	22	1	0	7	3	0	8	4	4	1	
chlorite & muscovite mtx.	0	0	0	0	0	3	24	0	0	2	0	0	12	0	3	0	0	
chert	2	0	1	0	7	34	0	5	1	0	5	1	0	0	15	4	15	
feldspar	0	0	0	0	0	0	0	0	0	0	0	0	2	5	3	7	2	
igneous rock fragments	0	1	0	0	0	6	0	0	0	0	1	0	0	1	6	5	14	
sedimentary rock fragments	0	0	0	0	12	8	0	2	0	0	13	6	0	1	0	1	1	
opaques	0	2	1	0	2	3	0	6	0	0	2	0	8	1	1	0	3	

Continued on next page

Table II. Frequency data for point counted sandstones (continued)

Lithology	Northern Sequence					Southern Sequence												
	T <sub>1</sub>					T <sub>2</sub>	T <sub>1</sub>		T <sub>2</sub>	T <sub>3</sub>								
Sample No.	D	E	C	F	I	12	19	13	25	11	7-IV	10-IV	21-A	1-V	9	22-B	18	
Composition	0	0	0	0	0	1	0	0	0	0	0	0	0	0	0	0	0	0
heavy minerals	0	0	0	0	0	1	0	0	0	0	0	0	0	0	0	0	0	0
mica	0	0	0	1	0	0	0	0	0	0	0	0	0	0	0	0	0	0
iron oxide matrix	21	36	35	50	41	25	10	16	10	7	26	52	36	6	5	12	0	0
calcite cement	0	1	1	5	0	52	0	12	35	0	20	26	6	10	28	15	16	0
silica cement	0	0	0	0	0	0	0	0	0	2	0	0	0	0	0	0	0	0
questionable grains	6	5	7	7	0	2	0	12	16	0	6	10	0	9	0	10	6	0
pore	14	1	2	0	0	5	5	0	15	0	0	0	0	8	1	3	1	0
sample size (n)	100	100	100	100	150	200	300	100	150	100	150	150	150	100	100	100	100	100

counted using a mechanical stage. A variety of constituent minerals, matrix, and cements occurs, however, not all the constituents occur in each sample nor do they all occur in significant proportions in each sample. Because the amount of matrix, cement, and pore space are affected by depositional environment and diagenetic alternation, as well as changes in the source area, they are not included in the statistical analysis of mineralogic variability. Also, some difficulty is encountered in distinguishing quartz grains from fragments of quartzite, fragments of phyllite from chlorite plus muscovite matrix, and chert grains from devitrified volcanic rock fragments. Therefore these mineralogic categories are combined, respectively, in Table IIa which presents the frequency data used in the statistical analysis of mineralogic variability in the sandstones. Note also that minor constituents are combined to reduce the number of zero entries.

An initial inspection of the data in Tables Ia and IIa leads to several questions. Are the apparent compositional differences between the three sample groups--Northern Sequence, Southern Sequence, and T<sub>3</sub> samples--statistically significant? If so, on the basis of which mineralogic categories can the the groups be compared or contrasted? In order to answer these questions, statistical analyses are used.

Table IIa. Frequency data used in statistical testing of point counted sandstones

Lithology	Northern Sequence				Southern Sequence												
	T <sub>1</sub>		T <sub>2</sub>		T <sub>1</sub>		T <sub>2</sub>		T <sub>3</sub>								
Sample No.	D	E	C	F	19	1	12	13	25	11	7-IV	10-IV	21-A	1-V	9	22-B	18
Grain Composition	31	29	42	35	61	71	28	26	82	89	70	52	85	57	34	43	43
quartz + quartzite	26	25	11	2	24	17	33	27	0	2	7	3	13	8	7	4	1
phyllite + chlorite & muscovite matrix	2	1	1	0	0	7	43	5	1	0	6	1	1	5	24	19	32
chert + feldspar + igneous rock fragments	0	0	0	0	0	12	8	2	0	0	13	6	0	1	0	1	1
sedimentary rock fragments	0	2	1	1	0	2	4	6	0	0	2	0	7	1	1	0	3
opaques + mica + heavy minerals	59	57	55	38	85	109	116	66	83	91	98	62	106	72	66	67	80
sample size (n)	1.19	1.16	3.82	17.50	2.54	4.18	0.85	0.96		44.5	10.0	17.33	6.54	7.12	4.86	10.75	43.0
ratio of quartz + quartzite/ phyllite + clay matrix	0.26	0.26	1.16	4.07	0.43	0.64	0.18	0.22		6.63	1.57	3.29	1.31	1.26	1.03	2.09	8.46
standard deviation	0.67	0.64	1.50	9.36	1.68	2.90	0.49	0.52		31.24	6.86	10.75	3.92	4.60	2.80	6.57	26.08
95% confidence interval	to	to	to	to	to	to	to	to		to	to	to	to	to	to	to	to
	1.71	1.68	6.14	25.64	3.40	5.46	1.21	1.40		57.76	13.14	23.91	9.16	9.64	8.92	14.93	59.92

Methods of Statistical Analysis

To test the validity of the groupings in Tables Ia and IIa, a form of the Chi-Square Goodness of Fit Test is used. For this test, a chi-square distributed variable is calculated for pairs and groups of samples. This calculated variable is then compared with the tabulated chi-square variable with  $k-1$  degrees of freedom where  $k$  is the total number of compositional categories compared (see Carver, 1971, p. 411). Testing is applied with a 0.05 level of significance. If the calculated chi-square variable is smaller than the tabulated variable, then the null hypothesis that the compared samples come from populations with similar distributions of pebble or grain compositions is accepted. If the calculated value is larger than the tabled value then the null hypothesis is rejected at the 0.05 level.

The following formula is used in calculations:

$$\chi^2 = \sum_{i=1}^m \sum_{j=1}^k \left[ \frac{N_{ij} - \frac{n_i \sum_{i=1}^m N_{ij}}{\sum_{i=1}^m n_i}}{\frac{\sum_{i=1}^m N_{ij}}{m} \frac{n_i}{\sum_{i=1}^m n_i}} \right]^2$$

where

$\chi^2$  = the calculated chi-square value

$n_i$  = the total number of observations in sample  $i$

$N_{ij}$  = the number of observations in category  $j$  in sample  $i$

m = the total number of samples being compared

k = the total number of categories used in the calculations

This formula is used when pairs of samples are compared (in which case m equals 2) or when groups of samples, or pooled samples, are compared (in which case m equals the number of samples being grouped or pooled). Results of the chi-square tests are summarized below.

In order to make quantitative assessments of where the compositional variability lies, ratios between certain compositional categories are calculated. Of particular interest are the ratio of quartzite to phyllite in the conglomerates and the ratio of quartz plus quartzite to phyllite plus chlorite and muscovite matrix in the sandstones. In order to place confidence intervals on these ratios, a variance for each ratio is calculated using the following formula from Chayes (1971):

$$\text{Variance } (X_1/X_2) = \frac{1}{(nP_2)^4} \left[ (nP_2)^2 nP_1(1-P_1) + (nP_1)^2 nP_2(1-P_2) + 2n^2 P_1 P_2 nP_1 P_2 \right]$$

where

n = the total number of observations in the sample or group of samples

$P_1$  = the proportion of the total number of grains or pebbles in category  $x_1$  (quartzite or quartz plus quartzite)

$P_2$  = the proportion of the total number of grains or pebbles in category  $x_2$  (phyllite or phyllite plus chlorite and muscovite matrix)

Using these calculated variances, 95 percent confidence

intervals are placed on each ratio by taking plus and minus twice the standard deviation of the ratio. The results of these calculations are discussed below.

### Results of Chi-Square Goodness of Fit Testing

Pebble Count Data. For the pebble count data, chi-square variables are first calculated between pairs of samples; the results are shown in Table III. In this table, the A in the upper left means that samples 1 and 19 come from populations with the same distributions of pebble compositions. The blank entry below the A indicates that the null hypothesis is rejected when samples 4 and 19 are tested. The table shows that  $T_1$  conglomerates of the Northern Sequence can be considered to be from a population with the same distribution of pebble compositions, but that this population is different from the underlying populations of  $T_1$  and  $T_2$  conglomerates of the Southern Sequence. No sample pairs between the three major groups, that is, Northern Sequence, Southern Sequence and  $T_3$ , can be considered to be from the same population. However, within the Southern Sequence some  $T_1$  conglomerates are from a population with the same distribution of pebble compositions as some  $T_2$  conglomerates. Samples 3, 13, 11, 5, and 9 come from populations with distributions of pebble compositions distinct from each other and any other sample. These results suggest that the three major groupings of samples in Table Ia are valid, and to further test this hypothesis, samples are pooled and compared.





Results of the pooled chi-square tests are given in Table IIIa. The table indicates that the distinction, based on clast composition, between three major sample groups--Northern Sequence, Southern Sequence, and  $T_3$  samples--is statistically significant. Furthermore, the distinction between  $T_1$  and  $T_2$  within the Northern Sequence and within the Southern Sequence is also statistically significant.

Point Count Data. The results of the pairwise chi-square test for point counted sandstones are given in Table IV. Note that the null hypothesis is accepted between several  $T_1$  and  $T_2$  samples from both the Northern and Southern Sequences. Note also that the null hypothesis is accepted between several samples from the Northern Sequence and the Southern Sequence unlike the conglomerates, where no samples compared between the major groups come from populations with the same distributions of pebble compositions.

These data suggest that the distinction between the two groups--Northern and Southern Sequences--is perhaps not statistically significant based on grain composition, and so to test this, samples were pooled and compared. Results of the pooled chi-square tests for sandstone samples are given in Table IVa. Pooling of samples indicates that the distinction between the three major sample groups is statistically significant based on grain composition. Within the Northern Sequence, the distinction between  $T_1$  and  $T_2$  is also statistically significant, but this is not the case for the Southern Sequence.



Table IV. Results of Pairwise Chi-Square Tests for Point Counted Sandstones

Northern Sequence	Northern Sequence						Southern Sequence						Explanation			
	T <sub>1</sub>			T <sub>2</sub>			T <sub>1</sub>			T <sub>2</sub>						
	D	E	C	F	19	1	12	13	25	11	IV	7-10-21	IV	Al-V	9	22-B
E	A															
C	A	A														
F			A													
19				A												
1																
12																
13	A	A														
25									A							
11										A						
7-IV											A					
10-IV												A				
21-A													A			
1-V														A	A	A
9																
22-B																A
18																A

A means accept the null hypothesis that the samples come from populations with the same distributions of grain compositions

no entry means reject the null hypothesis at the 0.05 level of significance

Table IVa. Results of Pooled Chi-Square Tests for Point Counted Sandstones

		Northern Sequence				Southern Sequence				Explanation
		all T <sub>1</sub> & T <sub>2</sub>	all T <sub>1</sub>	all T <sub>2</sub>	all T <sub>1</sub> & T <sub>2</sub>	all T <sub>1</sub>	all T <sub>2</sub>	all T <sub>1</sub> & T <sub>2</sub>		
Northern Sequence	all T <sub>1</sub>	reject							accept means accept the null hypothesis that the samples come from populations with the same distributions of grain compositions	
	all T <sub>2</sub>	reject	reject							
Southern Sequence	all T <sub>1</sub> & T <sub>2</sub>	reject	reject	reject					reject means reject the null hypothesis at the 0.05 level	
	all T <sub>1</sub>	reject	reject	reject	reject					
	all T <sub>2</sub>	reject	reject	reject	reject	accept				
	all T <sub>3</sub>	reject	reject	reject	reject	accept	accept	reject		

## Results of Ratio and Ratio Variance Calculations

Ratios of the frequency of quartzite to phyllite clasts in the conglomerate samples and quartz plus quartzite to phyllite plus chlorite and muscovite matrix in the sandstone samples are given in Tables Ia and IIa. Note that samples with a zero entry in the ratio are omitted. These ratios are useful in distinguishing samples from the Northern Sequence from samples of the Southern Sequence. Initial inspection of the data indicates that Northern Sequence samples have low values of the ratios compared with Southern Sequence samples. Figures 11 and 12 are plots of the ratios and their 95 percent confidence intervals versus location and stratigraphic position. Figure 11 indicates that indeed conglomerates from the Northern Sequence can be distinguished from Southern Sequence conglomerates on the basis of this ratio, but that  $T_3$  conglomerates cannot be distinguished from Southern Sequence samples on this basis. Figure 12 indicates that sandstone samples from the Northern Sequence overlap in some cases with Southern Sequence and  $T_3$  samples. Figures 13 and 14 are plots of the pooled ratios versus sample location. Figure 13 indicates that pooled Northern Sequence samples can be distinguished from pooled Southern Sequence and  $T_3$  samples on the basis of the quartzite to phyllite ratio in the conglomerates. The figure also indicates that within the Northern Sequence,  $T_1$  conglomerates cannot be distinguished from  $T_2$  conglomerates. However, within the Southern Sequence,  $T_1$  conglomerates can be distinguished from  $T_2$

Figure 11. Graph of the Ratios of quartzite/phyllite versus Sample Areas (lines with bars are the 95% confidence intervals for each ratio)

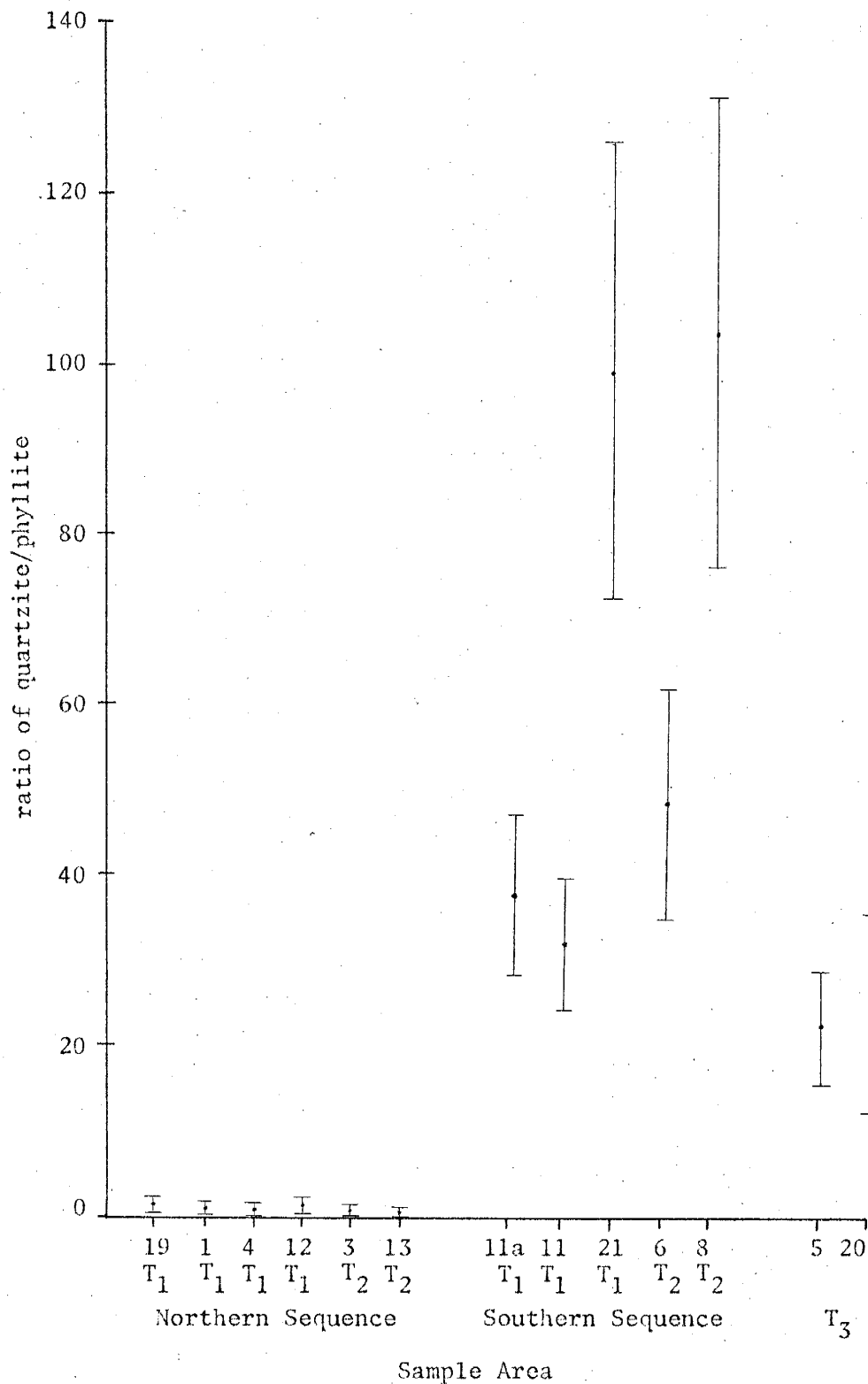


Figure 12. Graph of the Ratios of quartz + quartzite/phyllite + clay matrix versus Sample Areas (lines with bars are the 95% confidence intervals on each ratio)

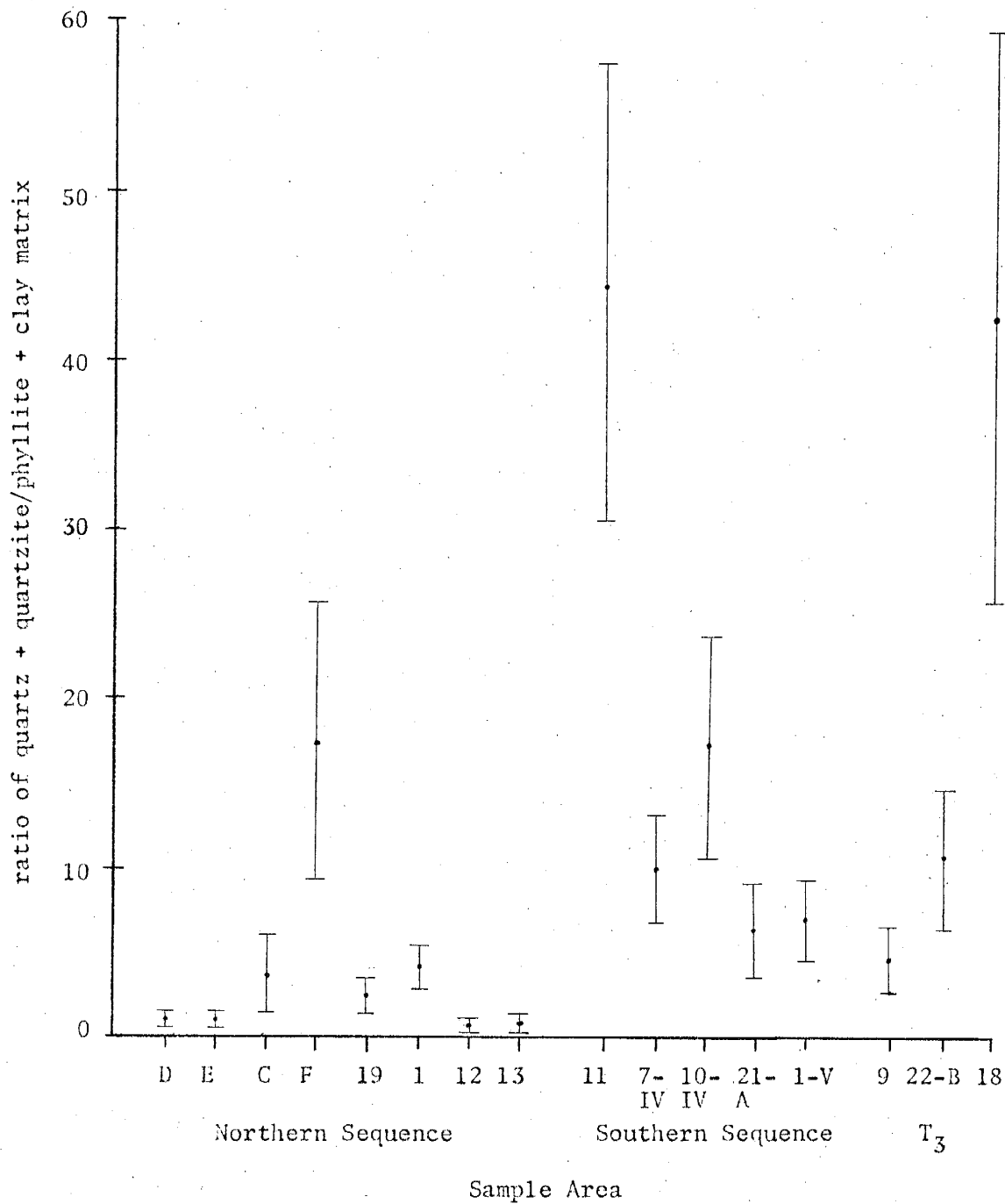


Figure 13. Graph of the Pooled Ratios of quartzite/phyllite versus Sample Areas (lines with bars are the 95% confidence intervals for each ratio)

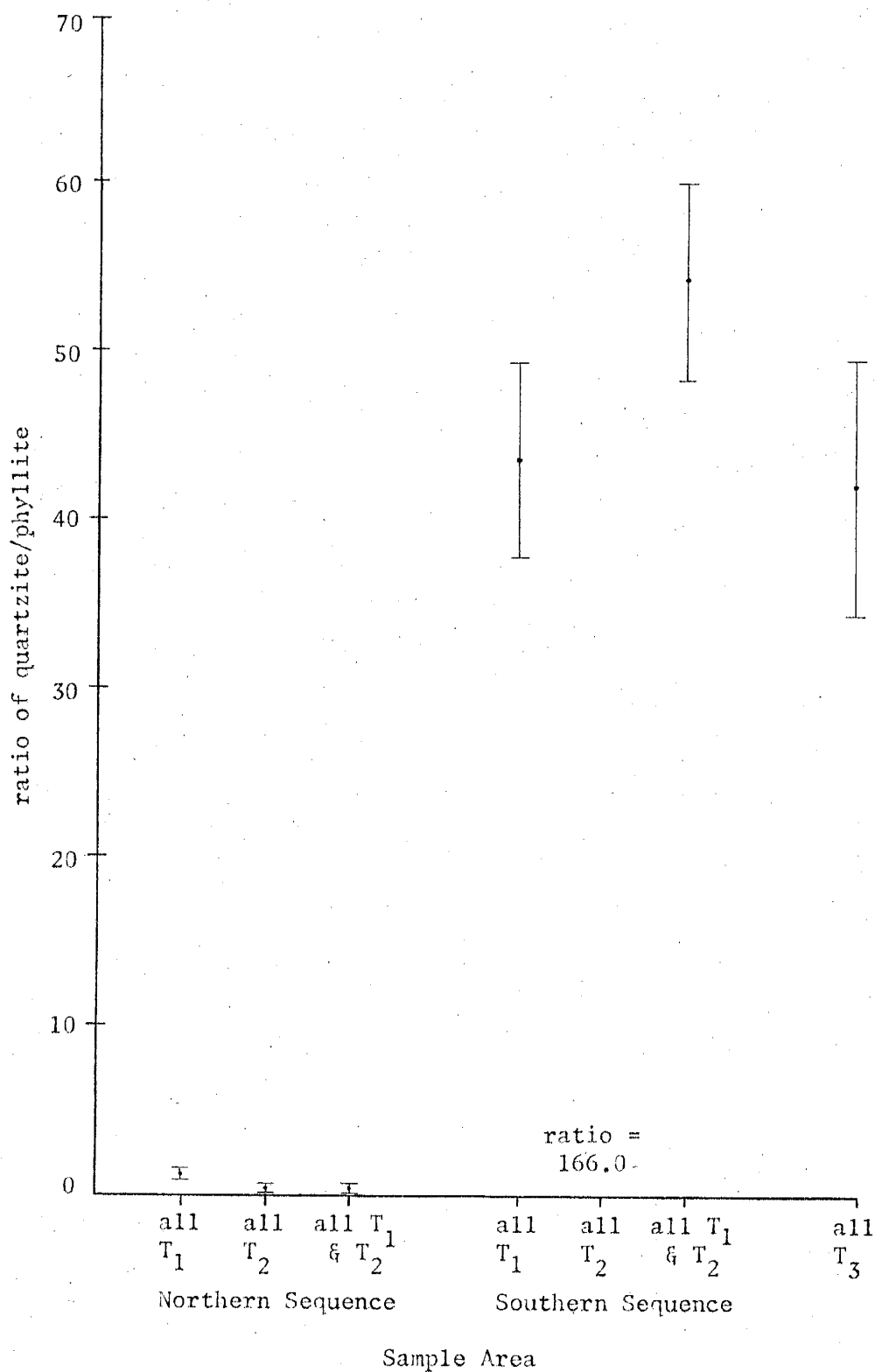
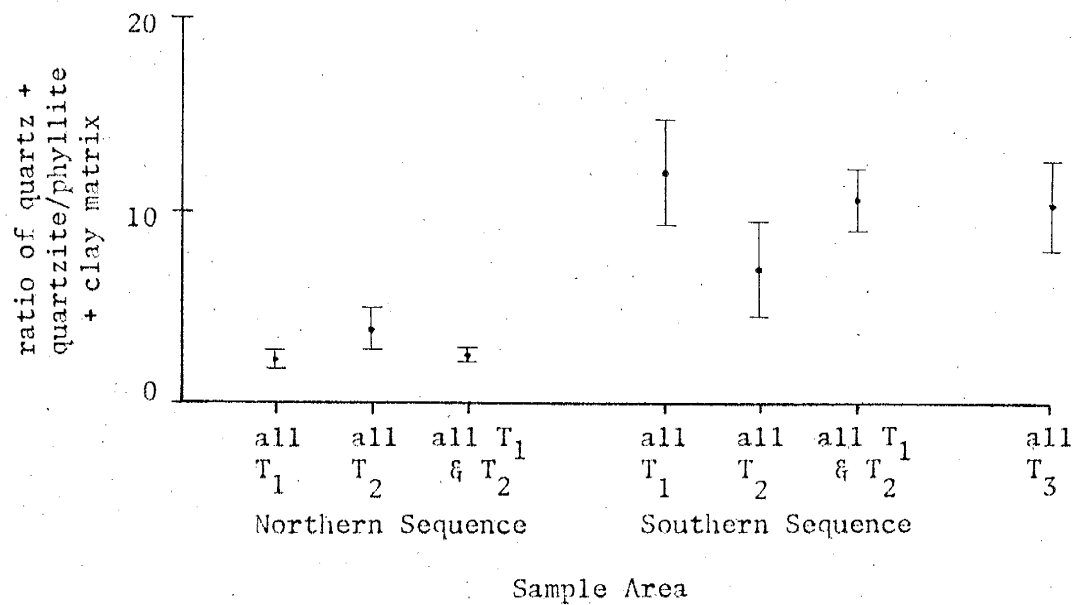




Figure 14. Graph of the Pooled Ratios of quartz + quartzite/phyllite + clay matrix versus Sample Areas (lines with bars are the 95% confidence intervals for each ratio).



conglomerates by a lower value of the ratio in the  $T_1$  samples. Figure 14 indicates that sandstone samples from the Northern Sequence can be distinguished from Southern Sequence and  $T_3$  sandstones on the basis of the quartzite plus quartz to phyllite plus chlorite and muscovite matrix ratios. Figure 14 also indicates that  $T_2$  sandstones from the Northern Sequence cannot be distinguished from  $T_2$  sandstones of the Southern Sequence on the basis of this ratio, but that  $T_1$  sandstones from the Northern Sequence can be distinguished from  $T_1$  sandstones of the Southern Sequence.

#### Summary

It appears that pebble composition of the conglomerates is more useful in distinguishing  $T_1$  from  $T_2$  from  $T_3$  samples than grain composition of the sandstones. The marked change in pebble compositions of  $T_1$  and  $T_2$  lithologies across the Fault of Argana (see Plate A) suggests that the Northern Sequence was derived from a different source than the Southern Sequence. Stratigraphic work near the fault indicates that there is no interbedding of  $T_1$  between the Northern and Southern Sequences. However, in  $T_2$  in section II (see Plate A and Appendix B) in the southernmost part of the Northern Sequence, there are numerous conglomerate beds with rounded quartzite and limestone clasts characteristic of  $T_1$  and  $T_2$  of the Southern Sequence. These data suggest that  $T_2$  of the Northern Sequence is interfingering with either  $T_1$  or  $T_2$  of the Southern Sequence. The problem of the juxtaposition of

the Northern and Southern Sequences along the Fault of Argana and their source area(s) is discussed in more detail in Chapters IV and V.

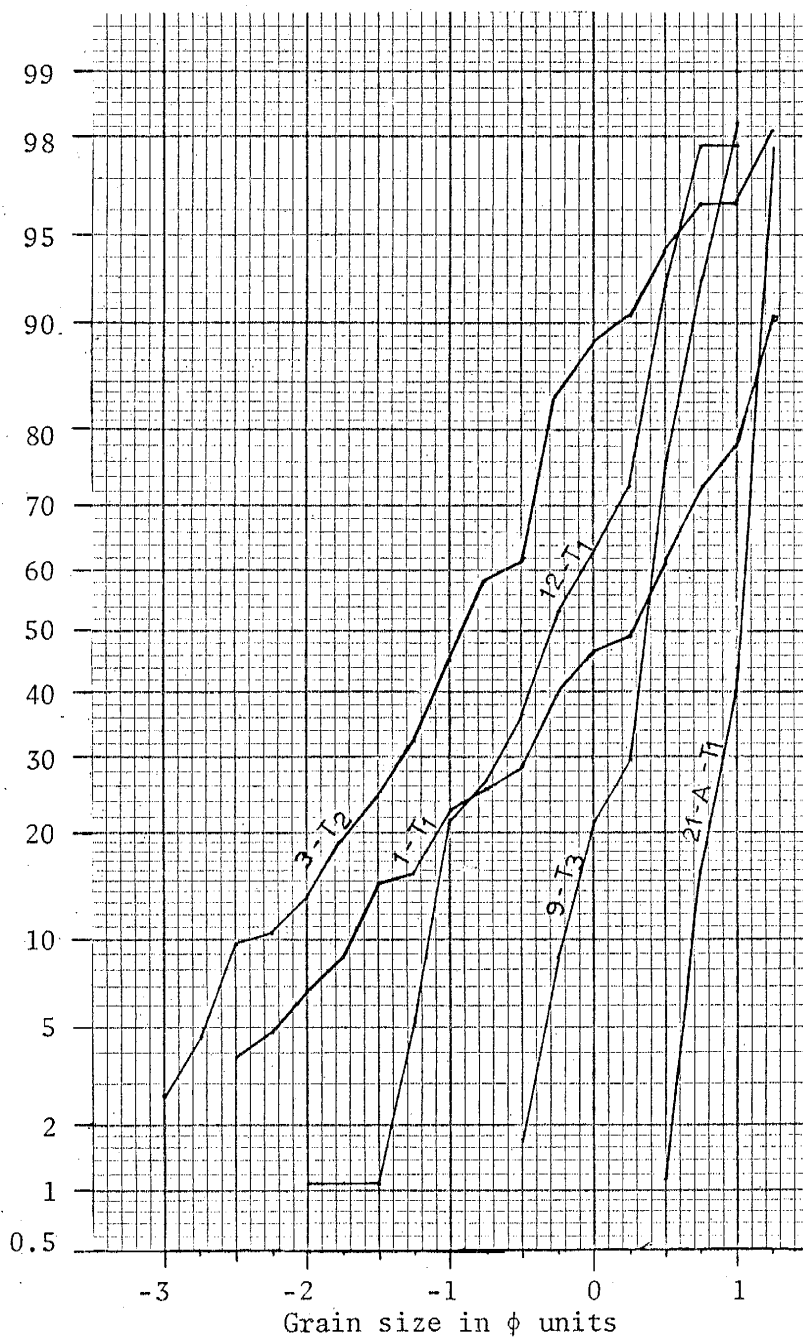
#### SUMMARY OF PETROGRAPHIC DATA

No detailed petrologic data for sandstones of  $T_1$ ,  $T_2$ , and  $T_3$  lithologies has previously been published. The following descriptions of the mineralogy, texture, and grain size distributions is based on petrographic analysis of thin sections of these sandstones. These descriptions are used to interpret the source area of the sandstones and how this source area changed through time.

Despite the geographic and stratigraphic variability in the percentages of sandstone components, the types of components are similar for most of the sandstones studied. Therefore mineralogic and textural data is summarized for all the sandstones regardless of location or lithology. Following this summary is a section discussing pertinent distinctions between samples from different locations or lithologic units.

#### Grain Size

Sandstones varied from fine grained to pebbly coarse grained. Thin section diameters were converted to sieve diameters as outlined by Friedman (1958) for samples 1, 12, 21-A, 3, and 9. Cumulative frequency distributions for these samples are given in figure 15. From the distributions,

Figure 15. Grain size distributions of five  $T_1$ ,  $T_2$ , and  $T_3$  sandstones.

Folk and Ward (1957) statistical parameters	1-T <sub>1</sub>	Sample Number 12-T <sub>1</sub>	and 21-A-T <sub>1</sub>	Lithology 3-T <sub>2</sub>	9-T <sub>3</sub>
median ( $Md_\phi$ )	0.3 $\phi$	-0.3 $\phi$	1.05 $\phi$	-0.95 $\phi$	0.35 $\phi$
mean ( $Mz$ )	0.05 $\phi$	-0.33 $\phi$	0.98 $\phi$	-1.02 $\phi$	0.28 $\phi$
sorting ( $\sigma_I$ )	1.2	0.65	0.2	0.95	0.4
skewness ( $Sk_I$ )	-0.03	-0.03	-0.3	0.85	-0.2

sample statistics after Folk and Ward (1957) were computed and are given in the figure.

Sorting values for the sandstones studied ranged from 0.2 to 1.2 or from very well sorted to poorly sorted.

### Grain Shape

Idiomorphism, sphericity, and roundness vary with grain mineralogy. Therefore these characteristics are discussed below for each mineral and rock fragment type. Roundness and sphericity values were obtained by visual comparison with the charts by Krumbein and Sloss (1963, p. 111) and Powers (1953, p. 117-119).

### Textural Maturity

The textural maturity, as defined by Folk (1974), of these sandstones is immature due to the presence of greater than 5 percent matrix, defined in this study as grains smaller than fine silt sized. Sample 18, the only sample which has less than 5 percent matrix, is texturally sub-mature due to poor sorting.

### Grain to Grain Contacts

A randomly selected sample of 598 grains from the sandstones studied, indicates the average number of grain to grain contacts per grain is 3.2. No systematic correlation between sample lithology and the number of contacts per grain or the types of grain contacts occurs. Point contacts

and straight-line contacts are most abundant and subequal. Straight-line contacts result from the parallel alignment of elongate grains. Concavo-convex contacts are second in abundance and appear to be the result of more competent grains such as quartz, quartzite, or chert indenting less competent ones such as phyllite, or sedimentary rock fragment, rather than the result of pressure solution between grains.

### Mineralogy

Each of the 15 compositional categories in Table II are discussed separately. The types of minerals and rock fragments from each lithology are mostly similar and so the data is summarized regardless of lithology first, and then distinctions between lithologies based on detailed petrographic criteria are discussed.

Quartz Varieties. Quartz ranges from 11 to 89 percent of the samples studied. Grains have sphericity values ranging from 0.1 to 0.9 with average sphericities of 0.5 to 0.7. Roundness of quartz grains varies between 0.1 and 0.7 and averages 0.2 to 0.3 or angular to subangular. The most abundant type of quartz has slightly to strongly undulose extinction, and is composed of semi-composite or composite grains (as defined by Folk 1974, p. 74, his types A4, 5, and 6). Commonly this type of quartz has lower sphericity values and is more angular than other quartz types. Boehm lamellae are common in this quartz type. Scattered gas and fluid-

filled vacuoles are present and are often arranged in lines or planes. Regular and irregular mineral inclusions (as defined by Mackie, 1899) are rare; identifiable inclusions are of hornblende, mica, and opaque grains.

In terms of a genetic classification, this quartz type most closely resembles Folk's (1974, p. 70) schistose metamorphic and stretched metamorphic types. The similarity between this type of quartz and quartzite rock fragments makes their distinction in some cases impossible. Thus, a separate category of questionable grains is established in Table II.

Other quartz varieties are observed in minor abundances. Fairly common are subequant, subrounded single grains with straight to slightly undulose extinction, scattered vacuoles, and rare microlites of zircon, plagioclase, or biotite. These grains are similar to Folk's (1974, p. 74) types A1 and 2 which he classifies as common (plutonic) quartz (p. 70). Less common are quartz grains with abundant vacuoles giving a milky appearance. These resemble Folk's vein quartz type. Least common are well rounded equant quartz grains with silica overgrowths in optical continuity. These grains are indicative of a preexisting sedimentary source (Folk, 1974, p. 73; Pettijohn, 1957, p. 514; and Pettijohn, Potter and Siever, 1972, p. 32).

Quartz grains are generally unetched, but are ubiquitously coated with iron oxide. Occasional grains are fractured and the fractures filled with iron oxide or sparry

calcite. Quartz grains commonly indent less competent metamorphic or sedimentary rock fragments. Elongate grains have a preferred orientation of their long axes parallel to the plane of bedding.

Chert Varieties. Chert is a minor constituent of the samples studied, ranging from 0 to 21 percent and averaging 3.4 percent (see Table II). It shows a narrower range in sphericity and roundness than quartz and is usually subequant and subangular to subrounded.

Few chert grains are 100 percent chert. Instead, veinlets of quartz, and inclusions of silt to sand sized quartz grains, opaques, and unidentifiable lath-like crystals commonly occur. Chert grains are usually reddish-brown or grey in plane light due to iron oxide coating, specular hematite coating, and less often iron oxide disseminated within the grains. The association of igneous rock fragments with samples with high percentages of chert, and the internal characteristics of the chert described above suggests that most chert grains could be fragments of devitrified and silicified, fine grained, porphyritic volcanic rock fragments and not of sedimentary origin. Suttner (1969) has noted that some of the chert in sandstones from the Morrison and Kootenai Formations in Montana may be of volcanic origin, although he found only one chert grain with a feldspar microlite. In this study, any chert clasts with feldspar microlites or phenocrysts are classified as igneous rock fragments.



One chert grain found in sample 1-V has concentric banding defined by crystal size of the silica. This rounded grain is strikingly similar to the silicified oolites of the Mines Formation (Cambrian) of Pennsylvania (see Pettijohn, 1957, p. 431) and a similar origin is proposed for this grain.

Chert grains have undergone more replacement than quartz grains or metamorphic rock fragments. Sparry calcite is the common replacement mineral. Note in Table II that most samples with high percentages of chert have high percentages of calcite cement. Most chert grains are coated with iron oxide, but some grains are replaced as much as 75 percent by sparry calcite, and the original grain boundary is distinguishable by a concentration of iron oxide within the sparry calcite.

Feldspar. Feldspar is also a minor constituent of the samples studied ranging from 0 to 7 percent and averaging 1.1 percent (see Table II). Most of the feldspar grains exhibit twinning; the types of twinning in order of abundance are Albite, Carlsbad-Albite, or rarely Albite-Pericline twinning. Virtually all of the observed feldspars are of the plagioclase group although one or two grains of microcline are present. Commonly the feldspars are partly replaced by sparry calcite. Sericitized feldspars are less common, and completely fresh grains are rare. A few feldspar grains are untwinned, have a poikilitic texture with quartz inclusions, and have the optical properties of orthoclase. Almost all feldspars are coated with iron oxide.

Igneous Rock Fragments. These rock fragments are a minor constituent of the samples studied except in T<sub>3</sub> samples where they constitute an average of 8.3 percent (see Table II). The common variety of igneous rock fragments consists of granule or coarse to medium sand sized grains of dominantly chert, with embayed, hexagonal-bipyramidal, or anhedral quartz, and/or sub- to euhedral twinned plagioclase crystals up to 1.5 millimeters in diameter, and opaque grains up to 0.5 millimeters in diameter.

Field observations indicate that plutonic as well as extrusive igneous pebbles or boulders occur in T<sub>1</sub>, T<sub>2</sub>, and T<sub>3</sub> sandstones. Granitic pebbles and boulders (up to 30 centimeters across) are found in T<sub>1</sub> conglomerates in the vicinity of sample areas 4 and 12 in minor abundance. Thin section analysis of one of these pebbles indicates a composition dominantly of quartz with minor altered potassium and plagioclase feldspar, biotite, and opaques. Chert and sparry calcite combined comprise at least 20 percent of the thin section as replacement minerals, and the pebble is coated with iron oxide.

Fine grained igneous rock fragments commonly occur in uppermost T<sub>2</sub> conglomerates or in T<sub>3</sub> conglomerates. One amygdaloidal basalt pebble occurs in a T<sub>1</sub> conglomerate bed near sample area 11, but fine grained igneous rock fragments are absent elsewhere in T<sub>1</sub> conglomerates.

One clast of a fine grained igneous rock from a T<sub>3</sub> conglomerate bed is highly altered and consists of about

50 percent chert, 25 percent calcite, and 25 percent opaque to translucent iron oxide concentrated along fractures.

A pebble of a coarse grained igneous rock from a T<sub>3</sub> conglomerate bed consists dominantly of graphically intergrown quartz and kaolinized potassium feldspar with minor Albite twinned and Carlsbad-Albite twinned plagioclase phenocrysts, altered (to iron oxide) biotite, chlorite, and opaque minerals.

Metamorphic Rock Fragments. These are the dominant types of rock fragments of most of the samples studied. They average about 21 percent of each sample and range from 0 to 46 percent (see Table II). The metamorphic rock fragments are composed of dominantly quartz and sericite with minor opaques, plagioclase, heavy minerals, chert, and calcite. A relationship exists between sphericity, and internal grain size and mineralogy of the metamorphic rock fragments. This relationship is described below.

For this study, quartzite rock fragments are defined as metamorphic rock fragments having a quartz to sericite ratio greater than one. Opaque grains comprise up to 20 percent of some quartzite fragments. Quartzite grains have sphericity values averaging from 0.5 to 0.6 and are commonly subangular. Grain size of the quartz in the rock fragments varies from coarse to very fine sand. Grain size occasionally varies within a rock fragment. Finer grained quartzites tend to have more sericite and lower sphericity values. Sutured and concavo-convex grain boundaries indicative of precipitation and pressure solution are most common between

quartz grains. Most quartz grains are elongate parallel to the long dimension of the rock fragment. The quartz has slightly to strongly undulose extinction as defined by Folk (1974), vacuoles arranged in lines and planes, and Boehm lamellae. Microlites of hornblende, zircon, garnet, and biotite are rare. Quartzite fragments are ubiquitously coated with iron oxide and are occasionally indented by quartz grains.

Phyllite rock fragments are herein defined as metamorphic rock fragments with a quartz to sericite ratio less than one. Opaque grains usually comprise less than 10 percent of the fragments. Phyllite fragments have lower sphericities (average sphericity value about 0.4) than quartzite rock fragments, but they are also subangular. Phyllite grains often have irregular or ill-defined boundaries due to post-depositional compaction (to be discussed in detail below). Quartz in phyllite fragments is silt to very fine sand sized and has similar characteristics to the quartz in quartzite fragments. Some phyllite rock fragments display mineralogic banding with laminae of dominantly quartz plus opaque grains alternating with laminae of sericite. Sericite in all phyllite fragments defines a schistose fabric which gives a silky sheen to the phyllite pebbles in hand specimen. Iron oxide coats the phyllite grains in thin section. Many phyllite grains are indented by quartz, quartzite, or chert grains.

Metamorphic rock fragments with roughly equal percent-

ages of quartz and sericite are classified as questionable grains in Table II.

Sedimentary Rock Fragments Excluding Chert. A wide variety of sedimentary rock fragments occur in T<sub>1</sub>, T<sub>2</sub>, and T<sub>3</sub> sandstones, in minor quantities (see Table II). Both terrigenous and carbonate rock fragments are found. Sphericity values are commonly 0.4 and the grains are subrounded to rounded. Irregular grain boundaries are common due to post-depositional effects (discussed below).

Terrigenous sedimentary rock fragments are commonly fine grained sandstones to silty mudstones. Less commonly medium grained sandstones occur. Angular quartz grains and iron oxide matrix are the major constituents of the terrigenous rock fragments, and opaque grains, chlorite and muscovite, and hornblende are minor constituents. The rock types are commonly quartzarenites, quartzwackes, or silty quartz mudstones (see Appendix A, classification system). Higher percentages (up to 30%) of sericite in a few quartzwackes makes these fragments difficult to distinguish from metamorphic rock fragments. The category for questionable grains was used for these fragments.

A wide variety of carbonate rock fragments occur. Most of these grains have undergone recrystallization and/or replacement. Common recognizable rock types according to Folk's classification of limestones are micrites, biosparites, biosparrudites, and biolithites. Recognizable fossil fragments are of coral, bryzoans, algae, trilobites,

crinoids, and pelecypods. One biolithite pebble was thin sectioned and sent to W. A. Oliver, Jr. of the U.S. National Museum for identification. According to him the specimen is a coral of the Phillipsastrea (Pachyphyllum) species, comparable to similar specimens found previously in Mauritania and Algeria. The range of this species is Late Middle to Early Late Devonian. A trilobite fragment in a biosparrodite pebble was identified by Christina Lochman-Balk (personal communication, 1974) as Cornuproetus species, similar to trilobites found in Lower Middle Devonian crinoidal limestones in southern Morocco.

Opagues. Opaque grains are minor constituents of the sandstones ranging from 0 to 6 percent and averaging 1.4 percent of the samples (see Table II). Grains are commonly subequant but are surrounded by concentrations of opaque to translucent iron oxide, so that original grain boundaries and roundness values are difficult to determine. In reflected light, most of the grains are reddish-brown. A few grains however, are sparkly metallic grey in reflected light. These optical characteristics suggest that magnetite is probably the dominant opaque mineral, and specular hematite a minor opaque mineral.

Heavy Minerals and Mica. Detrital heavy mineral grains are rare in the sandstones (see Table II). Euhedral zircon and sub- to anhedral hornblende are the two minerals which commonly occur. A few grains of epidote and biotite occur. Two detrital muscovite grains were counted in sample F and

although 1 or 2 grains were noted in most samples, the percentage of mica is commonly much less than 1.

Matrix. For the purpose of this study, matrix is defined as grains finer than fine silt sized. Two types of matrix are present in the sandstones. Hematite plus clay minerals matrix comprises an average of 19 percent of the samples and chlorite plus muscovite matrix averages a little more than 2 percent per sample (see Table II).

Hematite plus clay minerals matrix refers to aggregates of clay sized grains which can be opaque with a reddish-brown reflection, or translucent with a dark reddish-brown color. An oriented mount of this matrix was analyzed by X-ray diffraction. Component clay minerals are illite, kaolinite, and possible illite-smectite mixed layer clays. Hematite is also found in the clay fraction. No quantitative X-ray analyses were undertaken.

Hematite plus clay minerals matrix tends to be concentrated around opaque grains, hornblende, and biotite grains, igneous rock fragments, and sedimentary rock fragments with a wacke texture. In several samples, hematite plus clay minerals matrix is mixed with calcite cement. In samples 7-IV and 10-IV the matrix defines relic grain boundaries and relic internal fossil structures of what were once carbonate rock fragments that are now replaced by coarsely crystalline sparry calcite cement.

The presence of concentrations of hematite around iron bearing minerals and rock fragments suggests that some of

the hematite is derived by post-depositional oxidation of the iron bearing grains. However, considering the relative scarcity of the iron bearing minerals and rock fragments, some of the iron oxide must be derived elsewhere. Its presence as a grain coating, and in older rocks to the east of the erosional limit of  $T_1$ ,  $T_2$ , and  $T_3$  sandstones suggest that much of the iron oxide was deposited at the same time as sand size debris.

Chlorite and muscovite matrix is often difficult to distinguish from fine grained phyllite rock fragments. Some of this type of matrix is probably derived from these rock fragments since many fine grained metamorphic rock fragments containing chlorite and muscovite have undergone squeezing and bending during post-depositional compaction, and now have irregular and sometimes indefinite boundaries surrounded by chlorite and muscovite matrix. The high percentages of chlorite and muscovite matrix in samples 19 and 21-A are difficult to account for unless the matrix was deposited along with the grains since these samples contain no recognizable phyllite rock fragments. The uniform distributions of the matrix in these samples support this conclusion.

Cements. The most common cement in the sandstones is calcite which averages about 10 percent (see Table II). The most common form of calcite is coarsely crystalline sparry calcite which occurs as a blocky mosaic. Another form of cement is medium crystalline sparite mixed with hematite plus clay minerals matrix. The calcite cement is present



largely as a pore filler and is rarely present at grain to grain contacts as is iron oxide.

Silica cement is absent in all samples except sample 11 where it is only a very minor constituent (see Table II).

### Sedimentary and Tectonic Structures

The most common sedimentary structures in the sandstones are the parallel alignment of elongate grains, grain imbrications, and bedding defined by alternating laminae of differing grain sizes. Occasional normal grading was observed on a small scale over a few millimeters.

Tectonic structures consist of fractures at an angle to bedding and parting along bedding planes. Spaces produced by parting and fracturing are filled by cements.

### Diagenesis

Both chemical and structural diagenetic changes have occurred in the sandstones. Common chemical changes include cementation, oxidation of opaque grains, and selective mineral replacement. Structural changes are manifest by deformation of grains and rock fragments due to post-depositional compaction.

Deformed grains are commonly fine grained metamorphic and sedimentary rock fragments. They are locally bent around grains of quartz, quartzite, or chert or are simply indented by these more competent grains. The substantial number of concavo-convex contacts is mostly due to more

competent grains indenting less competent ones. This is indicated by the realignment of micas in the fine grained rock fragments parallel to the boundary of the indenting grains.

Rarely, pressure has caused more competent grains to not only indent less competent ones, but to fracture them as well. Straight-line contacts are the result of contacts between parallel aligned elongate grains, rather than the result of post-depositional precipitation. Data indicate that samples with more straight-line than point or concavo-convex contacts tend to have less matrix than samples with more point or concavo-convex contacts.

Chemical diagenetic changes in the sandstones are numerous and complex. In this study, only a general diagenetic sequence based on commonly observed petrographic criteria is proposed. (1) Following compaction and some expulsion of water, one of the first diagenetic reactions is the oxidation of ferrous iron to ferric iron. This is evidenced in the sandstones by concentrations of hematite around opaque and heavy minerals, and igneous rock fragments. Devitrification of the ground mass in fine grained igneous rock fragments and silicification of detrital grains of feldspars may have occurred at, if not prior to, this time. (2) The next diagenetic changes in the sandstones are: the precipitation of calcite cement in pore spaces and voids within the hematite plus clay mineral matrix; the replacement of chert, quartz, and feldspars in the igneous rock

fragments by calcite; and the replacement of iron oxide coated micrite or microsparite rock fragments by sparry calcite, resulting in microstylolitic contacts between the iron oxide and the sparry calcite.

#### Distinction Between T<sub>1</sub>, T<sub>2</sub>, and T<sub>3</sub> Based on Detailed Petrographic Criteria

These lithologies, particularly T<sub>1</sub> and T<sub>2</sub> of the Northern and Southern Sequences, may be distinguished on the basis of some detailed petrographic criteria as well as the compositional variability discussed in the Analysis of Pebble and Point Count Data.

Quartzite rock fragments in T<sub>1</sub> and T<sub>2</sub> samples from the Northern Sequence tend to be less spherical and the quartz grains in the quartzites finer grained than those in the Southern Sequence (see Figures 16 and 17). Individual quartz grains in the Southern Sequence sandstones tend to be more rounded and the only rounded quartz grains with overgrowths in optical continuity are found in Southern Sequence sandstones.

Rock fragments of sediments in sandstones from the Southern Sequence are mostly carbonate rock fragments and minor quartzarenites. Rock fragments of terrigenous sediments, both arenites and wackes, are the most common type of sedimentary rock fragments in Northern Sequence sandstones. Fine grained, wacke-textured fragments are more common in Northern Sequence than in the Southern Sequence. These wacke-textured fragments have hematite plus clay



Figure 16. Photomicrograph of a typical T<sub>1</sub> Northern Sequence sandstone, X35, plane light. Note the large sub-rounded, elongate phyllite clast on the left of the photo and the large quartzite clast on the right. The dark coating on these and other grains is opaque to translucent iron oxide. The smaller grains are mostly quartz grains and phyllite rock fragments.



Figure 17. Photomicrograph of a typical T<sub>1</sub> Southern Sequence sandstone, X35, crossed nicols. Note the four quartzite rock fragments outlined in black and how the quartz in the fragments varies from very fine grained to coarse grained. Opaque iron oxide is common in these rock fragments. Note the absence of phyllite rock fragments and the abundance of hematite plus clay minerals matrix and resulting immature texture.



minerals matrix and resemble  $T_1$  and  $T_2$  sandstones and siltstones.

Conglomerates and sandstones of  $T_3$  are distinguished from  $T_1$  and  $T_2$  by the presence of substantial proportions of igneous rock fragments in the conglomerates and chert plus feldspar plus igneous rock fragments in the sandstones (see Figure 19). Although igneous rock fragments do appear in uppermost  $T_2$  conglomerates and sandstones in the Northern Sequence they are present in very minor quantities. The most abundant type of  $T_3$  igneous rock fragments are fine grained and light colored (pink, grey, light reddish-brown) in hand specimen. Coarse grained igneous rock fragments and fine grained dark colored fragments are present only in minor quantities. In thin section the most common types of igneous rock fragments are fine grained and composed of chert, quartz, plagioclase, and opaques as described in detail above. Quartzite and limestone pebbles in  $T_3$  are similar in hand specimen and thin section to these pebbles in  $T_1$  and  $T_2$  conglomerates and sandstones of the Southern Sequence, although a few angular quartzite pebbles and grains with fine grained quartz, typical of the Northern Sequence, are present. Terrigenous rock fragments in  $T_3$  are reddish-brown siltstones and sandstones similar in hand specimen and petrographically to  $T_1$  and  $T_2$  siltstones and sandstones.

#### Petrography of $T_2$ Silty Micrite or Micrite Beds

Three thin sections of beds in  $T_2$  described in Chapter

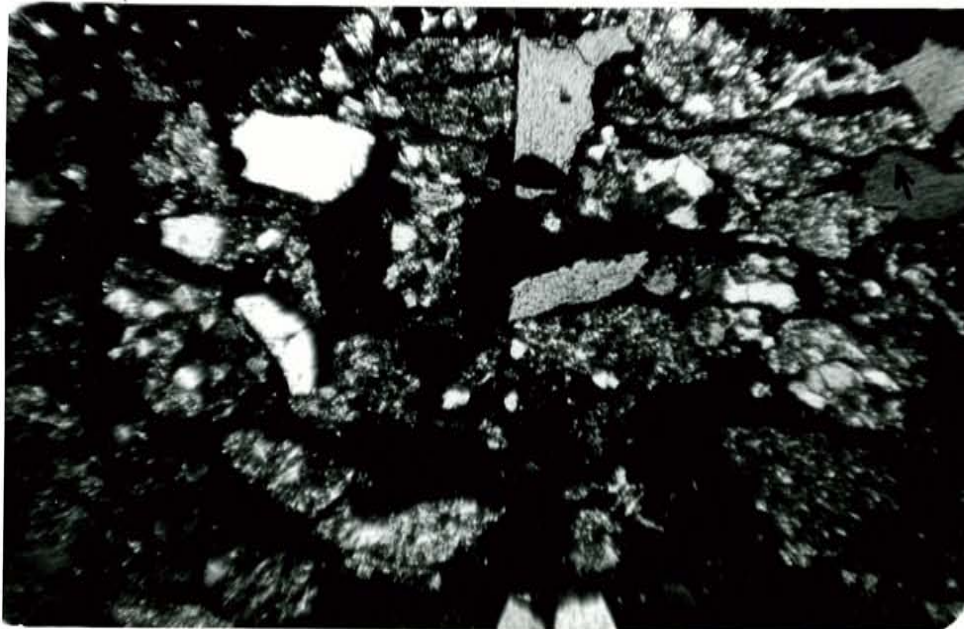


Figure 18. Photomicrograph of a typical T<sub>2</sub> sandstone, X35, cross nicols. This sample from the Northern Sequence has subequal amounts of phyllite, quartzite with fine grained quartz grains, and quartz. Note the immature texture due to the abundance of hematite plus clay minerals matrix and the poor rounding. Note how the quartz grain in the upper right hand corner is indenting the elongated metamorphic rock fragment (by arrow).

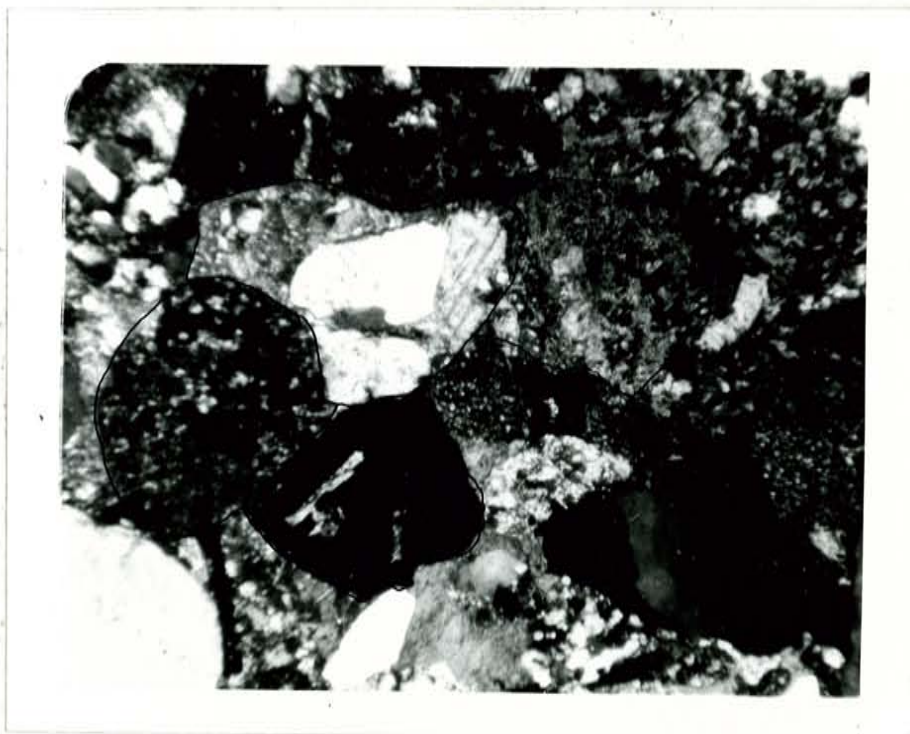


Figure 19. Photomicrograph of a typical T<sub>3</sub> sandstone, X35, cross nicols. The four encircled grains are igneous rock fragments composed of chert, quartz, opaque iron oxide and magnetite, and plagioclase. Note how grain boundaries are modified by post-depositional compaction. Surrounding the igneous rock fragments are grains of quartz, rock fragments of quartzite and phyllite, and hematite plus clay minerals matrix.



II as carbonate beds (see sections I and VI of the Northern Sequence) were studied. Two of these samples are partly re-crystallized silty micrites with the following characteristics: angular quartz grains comprise from 5 to 30 percent of the samples; reddish-brown hematite plus clay minerals matrix comprises up to 20 percent of both samples; the majority of these samples consists of grey microsparite or micrite; and internally they are in part homogeneous, and in part mottled or clotted with clumps of micrite surrounded by hematite plus clay minerals matrix or sparry calcite. The third sample was a poorly sorted, very fine grained, quartzarenite cemented by sparry calcite, with minor hematite plus clay minerals matrix. This sample displayed disrupted laminations and lenticular laminations defined by hematite plus clay minerals matrix.

As mentioned in the preceding chapter, in outcrop these T<sub>2</sub> carbonate or carbonate cemented sandstone beds are thin to medium bedded and nodular or homogeneous internally with occasional discontinuous wavy laminae commonly at the base of the bed.

The carbonate beds are found to be usually gradational with underlying horizontally laminated or burrowed reddish-brown siltstones, and overlain by reddish-brown siltstones or scoured above by conglomerates and/or sandstones. These stratigraphic characteristics as well as the petrographic characteristics described above suggest the carbonate beds are ancient fresh water limestone beds of the type described

by Pettijohn (1957) and Picard and High (1968).

### Petrography of Inferred Source Rocks

Samples of the lower Paleozoic metamorphic rocks, Hercynian extrusive rocks, and Stephanian sedimentary rocks, presently exposed to the east of T<sub>1</sub>, T<sub>2</sub>, and T<sub>3</sub> lithologies, were studied petrographically.

Field traverses in the lower Paleozoic rocks indicate that phyllites and quartzites with fine sand sized quartz grains are the dominant lithologies. Two samples of the phyllites and one of the quartzites were described.

In the field the phyllites have a wide variety of colors from dark reddish-brown, to green, to light gray. Petrographically they are composed of from 40 to 60 percent sericite, with minor muscovite, chlorite, silt sized angular quartz with undulatory extinction, opaques, and iron oxide. Iron oxide comprises up to 30 percent of one sample as a grain coating and imparts a dark reddish-brown color to the sample. Fractures are filled with silica and iron oxide. Both samples are schistose.

The quartzite sample is composed of 60 to 70 percent very fine sand sized, subequant, angular to subangular, slightly undulatory, single quartz grains, 5 to 10 percent sericite matrix, 0 to 5 percent opaque grains, and less than one percent hornblende. Opaque to dark brown iron oxide occurs as a fracture filling and comprises up to 30 percent of the sample.

Two samples of Stephanian terrigenous sediments were described. One sample is a coarse silt to very fine sand sized, chlorite cemented, quartzarenite, with very minor Albite twinned and Carlsbad-Albite twinned plagioclase feldspar, detrital muscovite, quartzite rock fragments, opaques, and heavy minerals (rutile). Iron oxide, concentrated around opaque grains, comprises up to 5 percent of the sample. The other Stephanian sample is a pebble-granule conglomerate with clasts mostly of subequant, subangular quartzites and a few tabular, subrounded phyllites with a detrital sandy matrix of quartz grains and minor sericite.

The only sample of a Hercynian rock is a sample of amygdaloidal basalt. The sample is porphyritic and is composed of 60 to 70 percent Albite twinned and Carlsbad-Albite twinned euhedral plagioclase grains up to 7 millimeters long. These euhedra are surrounded by a microcrystalline dark gray, translucent matrix which comprises 10 to 20 percent of the sample. The remainder of the sample is composed of 5 to 10 percent subequant, anhedral, opaque grains, less than 5 percent olivine, and 5 to 10 percent amygdule filling chlorite and sparry calcite. No detailed compositional determinations of the plagioclase grains were carried out in order to compare them with the plagioclase in  $T_1$ ,  $T_2$ , and  $T_3$  sandstones because fresh Carlsbad-Albite twinned grains are very rare in the sandstones.

## CHAPTER IV. PROVENANCE

## INTRODUCTION

Tixeront (1971) and Brown (1974) have shown from paleo-current studies that the transport direction for the T<sub>1</sub> to T<sub>4</sub> red beds was generally east to west. Also, data collected in this study in T<sub>2</sub> of Section V (see Plate A) indicate a mean azimuth for the flow direction of 257° or S77W. Data summarized in the previous chapter as well as textural data presented in this chapter suggest a nearby source area for T<sub>1</sub>, T<sub>2</sub>, and T<sub>3</sub> conglomerates and sandstones.

The field and petrographic data indicate a wide variety of source rocks for T<sub>1</sub>, T<sub>2</sub>, and T<sub>3</sub> detritus. In general, the order of abundance of these rocks is: quartzites, phyllites, limestones, porphyritic igneous rocks, phaneritic igneous rocks, vein quartz, and terrigenous sediments.

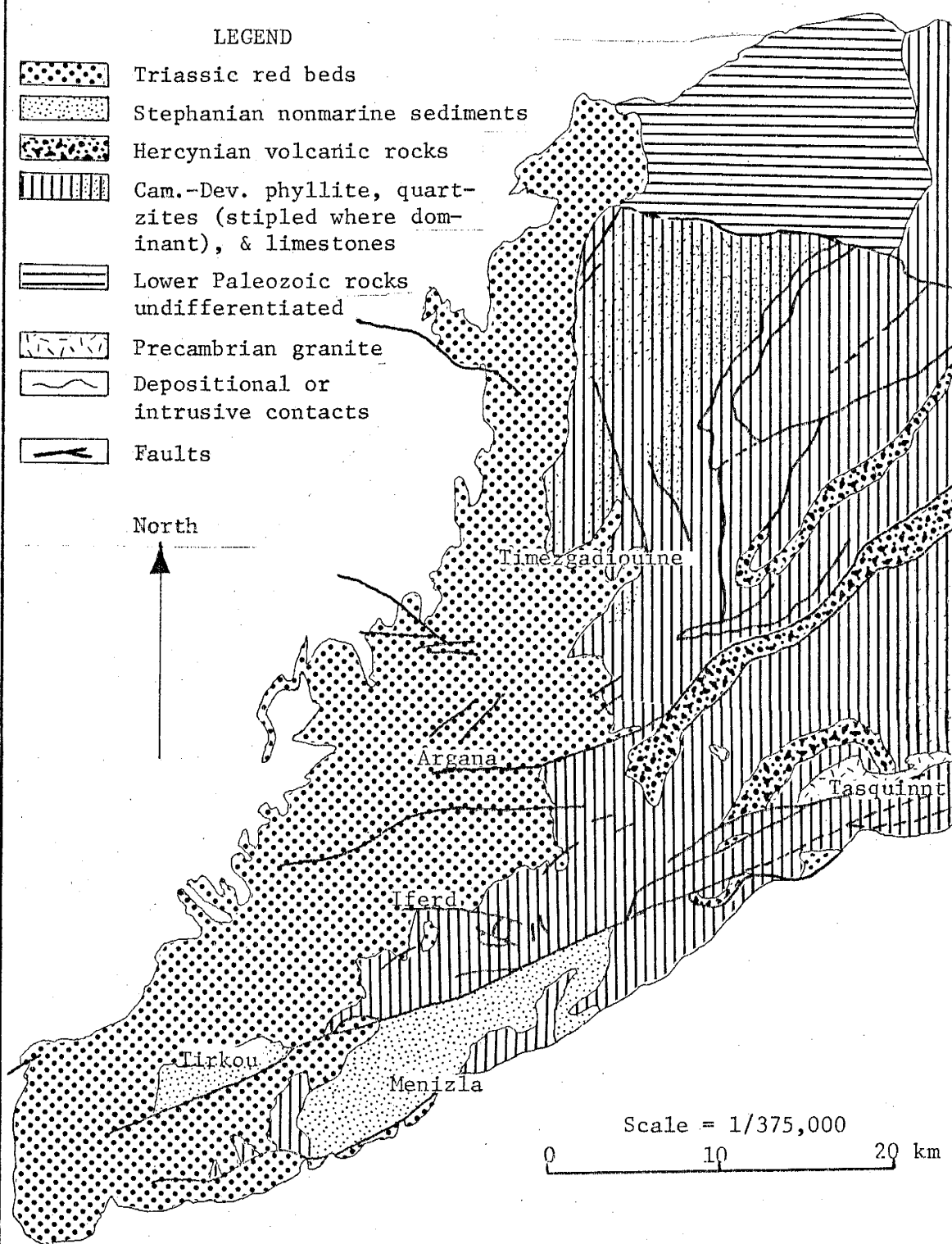
PROVENANCE FOR T<sub>1</sub> AND T<sub>2</sub> LITHOLOGIES

Pebble and point count data indicate that a low grade metamorphic source provides the majority of the detritus for T<sub>1</sub> and T<sub>2</sub> of the Northern Sequence. Point count data indicate that terrigenous sediments and coarse grained igneous rocks are minor source rock types. Cambrian, Ordovician, and Silurian rocks exposed directly east of T<sub>1</sub> and T<sub>2</sub> outcrops are low grade phyllites and quartzites with fine grained quartz grains, which petrographically resemble the phyllite and quartzite pebbles and rock fragments in T<sub>1</sub> and

T<sub>2</sub> conglomerates and sandstones of the Northern Sequence. A dominance of Ordovician quartzites to the east and north of sample 19, that is, north of Timezgadouine (see Figure 20), is reflected in the T<sub>1</sub> conglomerates and sandstones of that area, which have higher proportions of quartzite pebbles and quartz plus quartzite grains, than other T<sub>1</sub> Northern Sequence samples. Samples 1, 4, and 12, located near the base of T<sub>1</sub> at intervals along strike between Timezgadouine and Argana (see Figure 20), do not show any significant systematic geographic variation in the quartzite to phyllite ratio of the conglomerates or the quartz plus quartzite to phyllite plus chlorite and muscovite ratio of the sandstones. Traverses in the lower Paleozoic rocks to the east of these sample areas likewise do not show any geographic variations in the amounts of phyllite and quartzite, which are roughly equal in abundance.

Sandstone samples D, E, C, and F located at 200 meter intervals in T<sub>1</sub> within stratigraphic section I 3 kilometers southeast of Timezgadouine (see Figure 20), show an increase in the quartz plus quartzite to phyllite plus clay matrix ratio up section (see Figure 12). This can be explained in two ways. Either a more quartzite source area is continually being unroofed, or stratigraphically higher sediments in T<sub>1</sub> are deposited farther away from the source area with the result that less competent phyllite grains are destroyed in transport over a greater distance. The general homogeneity of the lower Paleozoic rocks and the fining upward

Figure 20. Geologic map of the Argana Valley and the inferred source areas



(adapted from Moroccan Geological Survey, Marrakech Sheet, 1/500,000)

nature of  $T_1$  suggest the latter explanation is probably correct. Samples 12, 25, and 13, located at 100 meter intervals along stratigraphic section II east of Argana (see Figure 20) do not show as systematic a variation in the ratio, however  $T_2$  samples 13 and 25 do have a higher value of the ratio than  $T_1$  sample 12 (see Figure 12).

The source for the pink colored granitic boulders and pebbles found locally in minor abundance at sample areas 1, 4, and 12 is questionable. In hand specimen these clasts do not resemble the light grey and white intrusive rocks of the Tichka Massif which was probably not unroofed at the time of  $T_1$  deposition (Tom Vogel, personal communication, 1974). A suggested source is the Precambrian granite body near Tasquinnt (see Figure 20), although samples of this granite were not taken to petrographically substantiate this as a source rock.

As indicated previously, the sedimentary rock fragments found in samples 1, 12, and 13 are reddish-brown sandstones, siltstones, or mudstones with hematite plus clay minerals matrix, which petrographically resemble  $T_1$  sandstones, siltstones, and mudstones. The fact that  $T_1$  once extended farther to the east of the present day erosional limit makes  $T_1$  a likely source for the sedimentary rock fragments in samples 1, 12, and 13.

Pebble and point count data for  $T_1$  and  $T_2$  of the Southern Sequence indicate different source rocks for these sediments than for Northern Sequence samples. Sections

measured near the fault boundary between the two sequences indicate no interbedding of conglomerates from  $T_1$  of the two sequences. However, there are a few interbeds of Southern Sequence conglomerates in  $T_2$  within stratigraphic section II east of Argana (see Figure 20) in the Northern Sequence. Traverses in the lower Paleozoic rocks to the east of the two sequences indicate no change in dominant lithology across the Fault of Argana. The following questions arise. If the lower Paleozoic rocks show no drastic change in lithology across the fault, why are tabular clasts of phyllite and tabular and angular rock fragments of quartzite present in the Northern Sequence, minor or absent in the Southern Sequence? Why do pebbles of limestone occur in the Southern Sequence and not in the Northern Sequence? Why are pebbles of sandstone more common in the Southern Sequence conglomerates than in the Northern Sequence conglomerates? Finally, what are the probable source rocks for the Southern Sequence?

Petrologic and faunal studies of the limestone pebbles indicate a Devonian age for these limestones. Previous work (Choubert, 1952, Plate 7) indicates that these Devonian limestones were only patchily deposited in the region of the Argana Valley. It is feasible therefore that these limestones were only present south of the Fault of Argana and thereby only served as a source rock for detritus of the Southern Sequence. Tables Ia and IIa indicate no systematic geographic or lithologic variability in the



proportion of limestone pebbles or grains in  $T_1$  and  $T_2$  of the Southern Sequence. As mentioned previously, field work indicates that limestone pebbles are present in some conglomerate beds and are minor or absent in other beds. This also suggests a patchy distribution of limestone in the source area.

A source for the subequant, subrounded, quartzite pebbles with fine to coarse grained quartz grains, the quartzarenite pebbles, and quartz pebble conglomerate fragments in the Southern Sequence does not appear to be the lower Paleozoic metamorphic rocks now exposed to the east of the sequence. Traverses in the Stephanian nonmarine sediments now exposed at Tirkou and northeast of Menizla (see Figure 20) show there the presence of conglomerates with angular to subrounded pebbles and boulders of quartzite. Furthermore, the quartzite conglomerates in these sediments are more abundant northeast of Menizla than to the west at Tirkou and pebble and point count data indicate a general decrease in the proportions of quartzite pebbles and quartz plus quartzite grains from east to west in the Southern Sequence. Statistical analysis of pebble count data indicates that samples 10, 11-a, and 21 come from populations with similar distributions of pebble compositions. The  $T_1$  conglomerates at sample 10 overlie the Stephanian sediments with angular unconformity.

These Stephanian sediments are proposed as a source area for the subrounded, subequant quartzite pebbles, the

quartzarenite pebbles, and the quartz pebble conglomerate fragments in  $T_1$  and  $T_2$  conglomerates and sandstones of the Southern Sequence. The original depositional limit of the Stephanian sediments is questionable, but the suggestion from the data above is that they were either not deposited or only very thin to the north of the Fault of Argana and thus were not a major source of detritus for the Northern Sequence.

### PROVENANCE FOR $T_3$ LITHOLOGIES

Conglomerates and sandstones of  $T_3$  exhibit the widest variety of constituents of  $T_1$ ,  $T_2$ , and  $T_3$  lithologies. Tectonic uplift, some minor folding, and a period of erosion precede  $T_3$  deposition locally. This tectonic activity results in the appearance of mostly angular porphyritic igneous rock fragments in  $T_3$  which distinguish it from  $T_1$  and  $T_2$ . Potassium-argon dates for three of these igneous rock fragments are:  $247 \pm 15$  m.y.,  $280 \pm 15$  m.y., and  $300 \pm 22$  m.y. (Harold Krueger, personal communication, 1974). These dates probably indicate that these pebbles come from Hercynian rocks, which are more abundant north of Argana than south (see Figure 20). Conglomerates of  $T_3$  reflect this distribution by an increase in the proportion of igneous rock fragments and vein quartz from south to north (see Table Ia). A local source is indicated by the angularity of the clasts. Sandstones in  $T_3$  do not have such a regular geographic variation in the proportion of chert

plus feldspar plus igneous rock fragments.

Quartzite pebbles in  $T_3$  conglomerates are subequant, and subround to round, and have fine to coarse grained quartz grains south of the Fault of Argana. To the north of the fault the proportion of quartzite decreases abruptly and tabular, subangular quartzite pebbles with fine grained quartz grains appear in minor abundance. These data suggest the quartzite pebbles in  $T_3$  are either (1) second cycle clasts derived from Stephanian conglomerates to the south of the Fault of Argana or first cycle clasts derived from lower Paleozoic rocks to the north of the fault or (2) they are derived from  $T_1$  and  $T_2$  conglomerates which reflect similar changes in dominant clast lithology. In the absence of detailed paleocurrent data for  $T_3$ , it is difficult to say where the subequant, subround to round quartzite pebbles with fine to coarse grained quartz grains found in  $T_3$  north of the Fault of Argana come from. The thickness and geometry of the unit suggest the source area is to the southeast, in which case the quartzite pebbles could be derived from either the Stephanian conglomerates or  $T_1$  and  $T_2$  of the Southern Sequence. Sandstones in  $T_3$  do not show any systematic geographic variations in the proportion of quartz plus quartzite grains.

The proportion of limestone pebbles in  $T_3$  conglomerates shows a general decrease from south to north (see Table Ia) similar to quartzite pebbles. In terms of provenance, a similar explanation is offered for the limestone pebbles

in  $T_3$  as for these pebbles in  $T_1$  and  $T_2$ , that is, they are derived from Devonian limestones whose original distribution was south of Argana. However,  $T_1$  and  $T_2$  conglomerates of the Southern Sequence are a possible source for the limestone clasts in  $T_3$ . Limestone grains are very minor in  $T_3$  sandstones.

Terrigenous sandstone and siltstone pebbles and rock fragments in  $T_3$  conglomerates and sandstones resemble Stephanian,  $T_1$ , and  $T_2$  lithologies. These constituents are minor in  $T_3$ . Pebbles of terrigenous sedimentary rocks in  $T_3$  conglomerates decrease in abundance from south to north possibly as a result of destruction in transport over greater distances, since the source of  $T_3$  is probably to the southeast.

Phyllite pebbles and rock fragments in  $T_3$  conglomerates and sandstones are derived from the lower Paleozoic phyllites, or phyllite clasts in  $T_1$  and  $T_2$  conglomerates. In general they decrease in abundance from south to north probably as a result of selective destruction in transport over greater distances.

## CHAPTER V. DEPOSITIONAL MODEL

## LATERAL AND VERTICAL CHANGES IN DEPOSITIONAL ENVIRONMENTS

In Chapter II environments of deposition are proposed for units  $T_1$ ,  $T_2$ , and  $T_3$  based on lithology and lithologic associations, thickness and geometry, and sedimentary structures and textures. The purpose of this section is to discuss the lateral and vertical variations in the environments of deposition and construct a model for the deposition of  $T_1$ ,  $T_2$ , and  $T_3$ .

Plate B is a summary of the lateral and vertical changes in environments of deposition in the study area. In the figure, measured sections have been hung from  $T_3$ , which, because of its low thickness, lateral continuity and stratigraphic position above an unconformity (see Plate B), is considered to represent a depositional event covering a short period of time. Field work indicates that the angular unconformity between  $T_2$  and  $T_3$  is greatest in the south and diminishes to the north. Therefore it is not certain whether  $T_2$  actually thins from north to south or whether the section is thinner in the south due to more erosion of  $T_2$  there. The Fault of Argana is shown in the figure not to indicate displacement, but rather to show the boundary between the Northern and Southern Sequences, and the abrupt change in thickness of  $T_1$  across the fault.

North of the fault,  $T_1$  is only 100 meters thick but south of the fault,  $T_1$  abruptly increases to 350 meters

thick. Although the environments of deposition of  $T_1$  are the same on either side of the fault, namely, braided stream channel fill deposits of alluvial fans, the Northern and Southern Sequences are compositionally distinct (see Chapter III) and no interbedding of these sequences occurs in  $T_1$ .

The data are insufficient to determine if the two deposits are discrete and not interfingering, or if they interfinger and the zone of interfingering is now faulted out. That  $T_1$  of the Northern Sequence is contemporaneous, at least in part, with  $T_1$  of the Southern Sequence is suggested by the fact that  $T_2$  is gradational below with  $T_1$  and that  $T_2$  of the Northern and Southern Sequences interfinger at the Fault of Argana. The abrupt increase in thickness of  $T_1$  south of the Fault of Argana suggests that some of the northern part of the Southern  $T_1$  Sequence has been faulted out. If this is the case, perhaps the faulted out horizons are interbeds of Northern and Southern  $T_1$  Sequences, and  $T_1$  deposits of both sequences are interfingering. Another possibility is that  $T_1$  of the Northern Sequence represents the deposits of one alluvial fan which was adjacent to, but not interfingering with, the Southern  $T_1$  Sequence alluvial fan. If this is the case, then some interfingering should be expected in the subsurface to the west as the two alluvial fans build out and coalesce.

Of interest is the fact that mudflows in  $T_1$  are much more abundant where  $T_1$  is thickest (see Plate B). The presence of mudflows here may be the result of fan-head

entrenchment resulting in an increase in the amount of fine grained sediment in streams on the central portions of the Northern Sequence alluvial fan.

In all sections except section III (see Appendix B),  $T_1$  is fining upward. This is accomplished by an upward decrease in average and largest clast size in the conglomerates and an increase in the number and thickness of finer grained lithologies. In section III however, the size of the largest clast increases significantly upward in the section but the average clast size changes very little. The largest clasts in this area are subequant to tabular, angular to subangular quartzite boulders. These data suggest shifting of drainage in the source area to erode local quartzite bodies rather than increased tectonic uplift in the source area which would cause a substantial increase in average as well as largest clast size.

In all sections except sections V and VI,  $T_2$  is also an overall fining upward sequence. The upward fining in  $T_2$  is represented not only by a decrease in the average and largest clast size in the conglomerates but also by a decrease in the abundance and thickness of the coarser lithologies (compare sections VII and VIII in Appendix B). Lateral continuity of channel fill deposits increases upward and the channel fills become finer grained and tabular in shape indicating an increase in stream sinuosity (Moody-Stuart, 1966) up section. In sections V and VI however, the upper 50 to 100 meters of  $T_2$  show an increase in the abundance of

the pebbly-coarse to medium sand fractions. In section VI the uppermost 50 meters of  $T_2$  is dominantly coarse to medium grained sandstones with increased feldspar content. This coarsening upward is probably due to tectonic uplift preceding  $T_3$  deposition.

Although pebble and point count data (see Tables I and II) indicate  $T_2$  sandstones and conglomerates of the Northern and Southern Sequences are distinct, field work indicates that limestone and well rounded quartzite pebbles occur in very minor abundance in  $T_2$  conglomerates and coarse sandstones in several beds from 140 to 170 meters and from 230 to 240 meters in section II, near the fault boundary between the two sequences. These types of clasts are common to  $T_2$  conglomerates and coarse sandstones of the Southern Sequence indicating  $T_2$  deposits of both sequences interfinger in this area.

Overlying  $T_2$  deposits of both sequences is  $T_3$ . Conglomerates of  $T_3$  become thinner and finer grained from south to north. The braided stream depositional environment for  $T_3$  does not change laterally. To the north, however,  $T_3$  channel fills are thinner and there is an increase in the abundance of sandstones and siltstones.

#### DEPOSITIONAL MODEL FOR $T_1$ THROUGH $T_3$ DEPOSITION

During deposition of  $T_1$  alluvial fans were deposited largely by braided streams draining easterly source areas (see Chapter V). The Northern and Southern  $T_1$  Sequences



represent the deposits of two distinct alluvial fans, one with an apex at Iferd, the Southern Sequence, the other with an apex near sample area 1, the Northern Sequence (see Plate A). If contemporaneous, the two fans may or may not have coalesced, or they may represent slightly different periods of time dependent on different times and locations of uplift to the east. Both fan deposits decrease in grain size upward, suggesting the source areas supplying the detritus are continually being worn down or that stratigraphically higher deposits represent deposition further from the source area as the basin widens. Mudflow deposits in the central upper part of the Northern Sequence alluvial fan (see Plate B) may be the result of fan-head entrenchment in that area. Later during deposition of  $T_1$ , braided stream or mudflow deposits interfinger laterally with meandering river-floodplain deposits characteristic of  $T_2$ .

Early during deposition of  $T_2$ , the meandering streams have lower sinuosity and channel deposits are about equal in abundance with floodplain deposits. Later, as stream sinuosity increases there is a corresponding decrease in grain size and increase in the abundance and thickness of floodplain deposits. Data suggest that during deposition of  $T_2$ , deposits of the Northern and Southern Sequences interfinger as streams increase in sinuosity and migrate over wider geographic areas.

Meandering river deposition is interrupted by a period of tectonic activity which in the south, near Iferd, involves

uplift, folding, and erosion of T<sub>2</sub> sediments, and in the north, uplift, tilting of T<sub>2</sub> sediments toward the west, and erosion. Following this tectonic activity and a period of erosion is the deposition of the braided stream deposits of T<sub>3</sub>, which were probably derived from a southeasterly source which included T<sub>1</sub> and T<sub>2</sub> lithologies as well as older rocks. Braided stream deposits of T<sub>3</sub> are conformable with overlying T<sub>4</sub> deposits (see Tixeront, 1971, and Brown, 1974, for descriptions of T<sub>4</sub>).

CHAPTER VI. AGE OF T<sub>1</sub>, T<sub>2</sub>, AND T<sub>3</sub>

Many authors (Choubert, 1952; de Koning, 1957; Duffaud et al., 1966; and Tixeront, 1971) have investigated the age of the basal units T<sub>1</sub>, T<sub>2</sub>, and T<sub>3</sub> of the Argana Valley. This is due to the general lack of fossils in these units on which to base either a definite Permian or Triassic age. Choubert (1952) points out that there is no evidence for assigning a Permian age to the units, and that all of the fossils (both vertebrate and plant) found up to that time in the stratigraphically higher T<sub>4</sub> through T<sub>8</sub> units indicate a Late Triassic (Keuper equivalent) age. De Koning (1957) also emphasizes a Triassic age for T<sub>1</sub>, T<sub>2</sub>, and T<sub>3</sub> citing the presence of a fossil plant Voltizia heterophylla Brogniart in T<sub>2</sub> which is considered a Triassic flora. In support of this he states (XVII International Geological Congress, v. 1, p. 396-407) that T<sub>1</sub> conglomerates overlie Stephanian deposits with angular unconformity. Nevertheless, Duffaud et al. (1966) indicate that T<sub>1</sub> and T<sub>2</sub> in the Argana Basin (their conglomerates of l'Assif N'Ait Driss and of Tiskey, and sandstones of Tourbiain) units are enclosed between two major unconformities and prefer to assign them a Permian age, and assign a Triassic age to T<sub>3</sub> (their conglomerate of Tanameurt).

Detailed work in this study shows that the angular unconformity between T<sub>2</sub> and T<sub>3</sub> is not a major one; rather it dies out from south to north, and T<sub>2</sub> and T<sub>3</sub> are conformable northward of a point about 3 kilometers southeast

of Timezgadouine (see Plate A). Tixeront (1971) argues in favor of a Triassic age assignment for  $T_1$ ,  $T_2$ , and  $T_3$  but conservatively refers to the units as Permo-Triassic in age.

Until this study, only Voltizia heterophylla plant fossils have been found which could be used to correlate the basal units of the Argana Valley with Triassic rocks of Europe; no fossils have been found to use to correlate these units with Triassic rocks of North America. In  $T_2$  (see section VIII, Appendix B), 4 kilometers southeast of Timezgadouine (see Plate A), trace fossils in the form of reptilian footprints were found by the author on top of a horizontally laminated siltstone bed covered with 1 millimeter of mudstone. These footprints have been identified by Donald Baird (personal communication, 1974) as Rhynchosauroides species, a small, herbivorous, lizard-like reptile. Baird (1957, 1962 and 1964), Baird and Take (1959), and Bock (1952) report similar footprints from Late Triassic rocks of New Jersey, Pennsylvania, Nova Scotia, and New Mexico. Other occurrences of these reptile footprints are in the Early Triassic Moenkopi Formation of Arizona and Utah (Peabody, 1948), the Triassic Chugwater Formation in Wyoming (Branson, 1947), the Late Triassic Muschelkalk Formation of the Netherlands (Faber, 1958), and the Triassic Keuper II of England (Maidwell, 1914).

On the basis of the occurrence of these footprints in rocks of well established Triassic age in North America, Europe, and England, the unit  $T_2$  of the Argana Valley should

also be considered to be Triassic in age. The contact between  $T_1$  and  $T_2$  is a gradational and interfingering contact and the environments of deposition of the units do not differ as a result of major tectonic events (see Chapter II. Environments of Deposition). Units of  $T_1$  are interpreted as alluvial fan deposits which have high sedimentation rates so that it would not require a long period of time to deposit the 1000 meters of  $T_1$  stratigraphically below  $T_2$ . Therefore, it is possible that all of  $T_1$  is also Triassic in age although its environment of deposition is not favorable for preservation of fossils, and none were found in the unit to substantiate a Triassic age.

A maximum age for  $T_3$  is provided by potassium-argon dating of a pebble of an igneous rock found in a  $T_3$  conglomerate bed. The age of the pebble was determined as  $247 \pm 15$  m.y. or Permian (Harold Krueger, personal communication, 1974). Because  $T_3$  is stratigraphically above  $T_2$ , where the fossils are found, it is also Triassic in age.

## CHAPTER VII. SUMMARY AND CONCLUSIONS

In the preceding chapters data are presented in order to solve the following problems concerning the basal red bed units of the Argana Valley, named and mapped by Tixeront (1971) as  $T_1$ ,  $T_2$ , and  $T_3$ : the age of the units; the environments of deposition of these units; the provenance for the units as it relates to the pre-Triassic surface on which they were deposited; the relationship between the two major  $T_1$  and  $T_2$  sequences distinguished by clast composition; the nature of the contact between  $T_3$  and underlying rocks and its bearing on the above problems. This thesis is part of a larger project whose objective is to compare, in the light of an Atlantic Rifting Model, the basal red beds of the Argana Valley with other red beds in Morocco and North America which have similar ages and paleotectonic settings. Speculations on these topics are presented in Appendices C and D.

ENVIRONMENTS OF DEPOSITION AND  
STRATIGRAPHIC MODEL FOR  $T_1$ ,  $T_2$ , AND  $T_3$ 

The units  $T_1$  through  $T_2$  record mostly overall fining upward alluvial and fluvial sequences. Although many previous workers (de Koning, 1957; Duffaud, 1957; Ambroggi, 1963; Tixeront, 1971) have indicated the continental fluvial nature of  $T_1$  and  $T_2$ , their depositional environments are more precisely defined in this study.

Normal block faulting (Kanes, et al., 1974) results

in the formation of mountains to the east of the Argana Valley during  $T_1$  and  $T_2$  deposition. The Northern and Southern  $T_1$  Sequences represent the deposits of two major alluvial fans in the center of the Valley which may or may not have coalesced. The Northern Sequence alluvial fan, with an apex near sample area 1, was derived largely from lower Paleozoic low grade quartzites and phyllites and represents the deposits of braided streams and subordinate mudflows. The Southern Sequence alluvial fan, with an apex near Iferd, was built by the same depositional processes and was derived from Stephanian nonmarine sediments, patchily distributed Devonian limestones, and minor lower Paleozoic low grade metamorphic rocks. Diminishing relief in the source area and/or concurrent faulting which continually moves the basin margin farther eastward may be responsible for the overall fining upward nature of  $T_1$ . As the alluvial fans built up and outward, their deposits interfingered with meandering river deposits characteristic of  $T_2$ .

The deposits of  $T_2$  have similar source areas as  $T_1$  lithologies, but  $T_1$  and any previously deposited  $T_2$  lithologies are also sources of detritus. With time,  $T_2$  streams become more highly sinuous and floodplain sediments become dominant over channel-fill deposits (see Figure 8). Although statistical analyses of pebble and point counted samples (see Chapter III) indicate that  $T_2$  conglomerates and sandstones differ significantly between the Northern and Southern Sequences, there is some interfingering of the

two sequences near the Fault of Argana (see Plate A and section II). As  $T_2$  streams become more sinuous, this inter-fingering is to be expected. A pulse of tectonic activity is probably responsible for a slight coarsening of  $T_2$  deposits in the upper 50 meters of  $T_2$  in sections V and VI (see Appendix B).

This tectonic activity increased in the south near Iferd (see Plate A) where  $T_2$  is folded into open folds, but north and east of Argana,  $T_2$  beds are only tilted westward, and are unaffected northeast of Timezgadouine. Following this tectonic activity, a period of erosion precedes deposition of  $T_3$ .

During tectonism a shift in the drainage pattern from streams draining westward to streams draining northwestward occurs. In the source area a new major source for the deposits of  $T_3$  is unroofed--Hercynian fine grained, felsic and mafic, extrusive and shallow intrusive igneous rocks. These rocks do not appear to be a source of detritus for  $T_4$  (Tixeront, 1971; Brown, 1974) suggesting they may have been covered by Triassic rocks after deposition of  $T_3$ . Devonian limestones, Stephanian nonmarine sediments, and  $T_1$  and  $T_2$  deposits are minor source rocks for  $T_3$  lithologies.









#### AGE OF $T_1$ , $T_2$ , AND $T_3$

The age of  $T_2$  is Triassic on the basis of the fossil plant Voltizia heterophylla (de Koning, 1957) and the trace fossil reptilian footprint of Rhynchosauroides found by



the writer and identified by Donald Baird (personal communication, 1974), which both occur in rocks of well established Triassic age elsewhere. The gradational contact between  $T_2$  and  $T_1$  indicates that  $T_1$  is Triassic, but there is a lack of fossil evidence to determine whether  $T_1$  is completely or partly Permian or Triassic in age. The age of  $T_3$  is Triassic due to its stratigraphic position above  $T_2$ . A maximum age for  $T_3$  conglomerates is  $247 \pm 15$  m.y. This age is provided by potassium-argon dating of a pink, porphyritic volcanic pebble from a  $T_3$  conglomerate bed (Harold Krueger, personal communication, 1974).

APPENDIX A  
CLASSIFICATION SYSTEMS

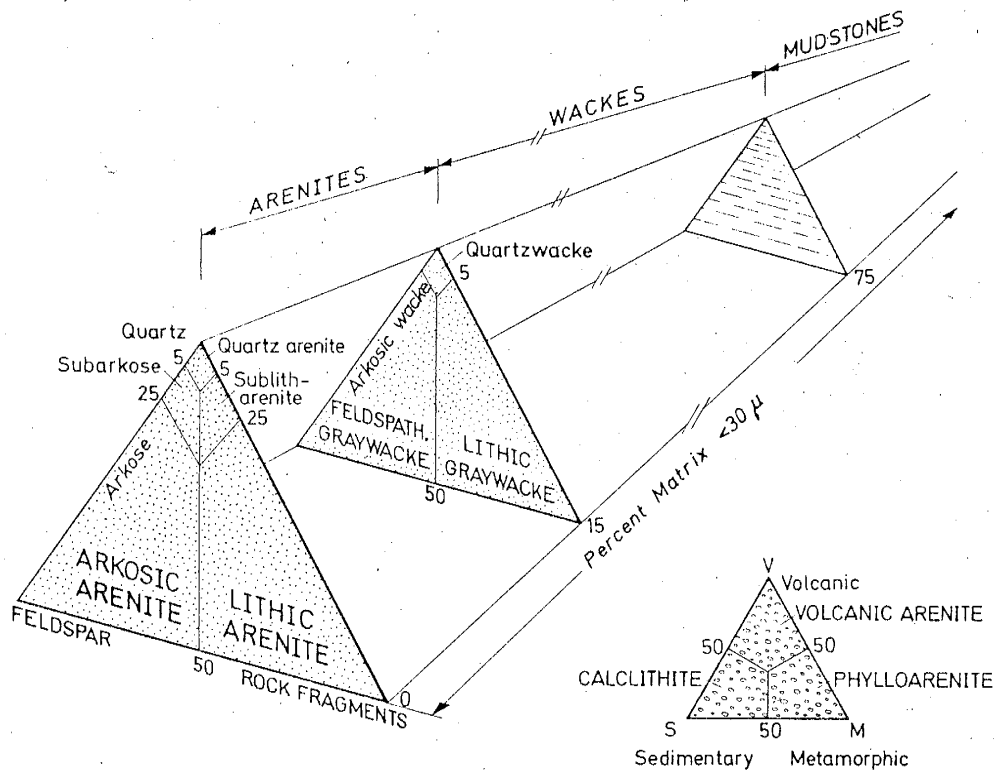
	OVER 2/3 LIME MUD MATRIX				SUBEQUAL SPAR AND LIME MUD	OVER 2/3 SPAR CEMENT		
	0-1%	1-10%	10-50%	OVER 50%		SORTING POOR	SORTING GOOD	ROUNDED AND ABRADED
Percent Allochems								
Representative Rock Terms	Micrite and Dismicrite	Fossiliferous Micrite	Sparse Biomicrite	Packed Biomicrite	Poorly Washed Biosparite	Unsorted Biosparite	Sorted Biosparite	Rounded Biosparite
								
1959 Terminology	Micrite and Dismicrite	Fossiliferous Micrite	Biomicrite		Biosparite			
Terrigenous Analogues	Claystone		Sandy Claystone	Clayey or immature Sandstone	Submature Sandstone	Mature Sandstone	Supermature Sandstone	

 Lime mud matrix       Sparry calcite cement

CARBONATE TEXTURAL SPECTRUM

Folk's classification of carbonate rocks.

Al. Classification scheme used in petrographic descriptions of limestone grains in T<sub>1</sub>, T<sub>2</sub>, and T<sub>3</sub> sandstones (from Folk, R.L., in Blatt, H., 1972, p. 474).



Classification of terrigenous sandstones (Modified from Dott, 1964, Fig. 3)

A2. Classification scheme used in hand specimen and petrographic descriptions of terrigenous sedimentary rock fragments in T<sub>1</sub>, T<sub>2</sub>, and T<sub>3</sub> sandstones and conglomerates (Dott, R.H., in Pettijohn, F.J., et. al., 1973).

## A3. Textural classification (Wentworth, C.K., 1922)

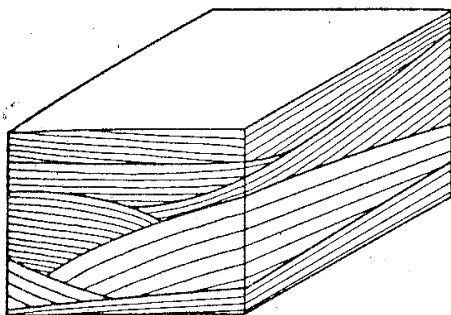
Size class	values	grain size in mm
boulder	<-7	> 256
cobble	-6 to -7	64 to 256
pebble	-2 to -6	4 to 64
granule	-1 to -2	2 to 4
very coarse sand	0 to -1	1 to 2
coarse sand	1 to 0	0.5 to 1
medium sand	2 to 1	0.25 to 0.5
fine sand	3 to 2	0.12 to 0.25
very fine sand	4 to 3	.062 to 0.12
coarse silt	5 to 4	.031 to .062
medium to very fine silt	8 to 5	.0039 to .031
clay	> 8	<.0039

## A4. Bed thickness classification (Ingram, R.L., 1954)

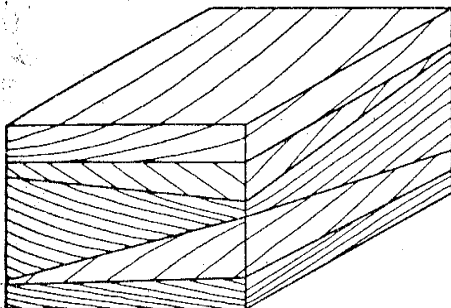
thickness class	bed thickness in centimeters
very thick-bedded	100 to 1000
thick-bedded	60 to 100
medium-bedded	10 to 60
thin-bedded	3 to 10
very thin-bedded	1 to 3
laminated	0.1 to 1

TABLE 4.—CLASSIFICATION OF CROSS-STRATIFIED UNITS

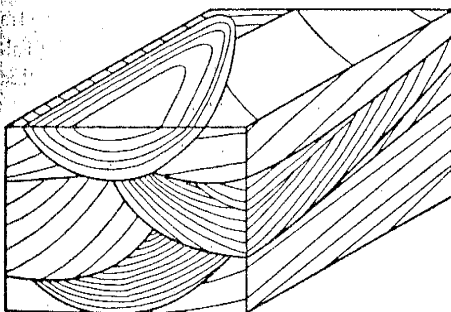
Basic Criterion	Subordinate Criteria			
	Shape of sets of cross-strata	Arching of cross-strata	Dip of cross-strata	Length of cross-strata
Character of lower boundary surface of set of cross-strata				
Nonerosional surfaces (simple cross-stratification)	Lenticular	Concave	High angle (> 20 degrees)	Small scale (< 1 foot)
Planar surfaces of erosion (planar cross-stratification)	Tabular	Straight		Medium scale (1 to 20 feet)
Curved surfaces of erosion (trough cross-stratification)	Wedge-shaped	Convex	Low angle (< 20 degrees)	Large scale (> 20 feet)

**SIMPLE CROSS-STRATIFICATION**

The lower bounding surfaces of sets are nonerosional surfaces

**PLANAR CROSS-STRATIFICATION**

The lower bounding surfaces of sets are planar surfaces of erosion

**TROUGH CROSS-STRATIFICATION**

The lower bounding surfaces of sets are curved surfaces of erosion

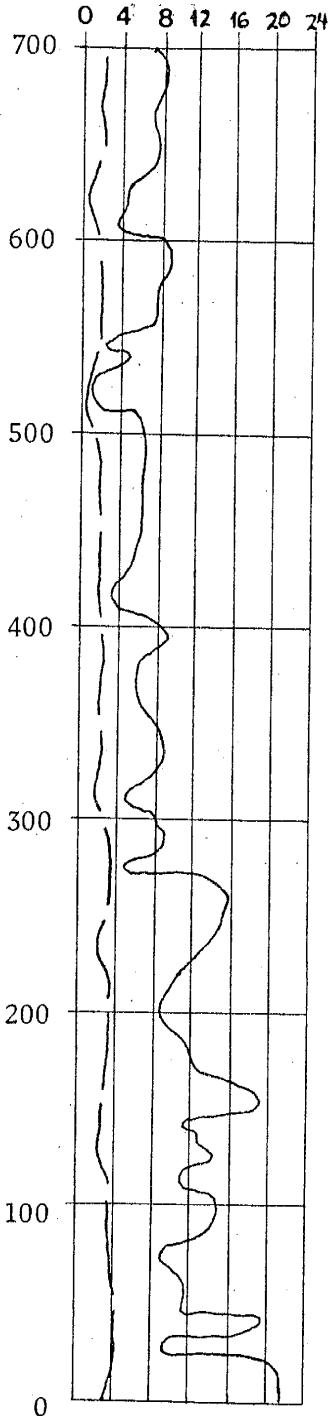
FIGURE 2.—BASIC ELEMENTS OF CLASSIFICATION OF CROSS-STRATIFICATION

A5. Crossbedding classification (McKee, E.D., and Weir, G.W., 1955)

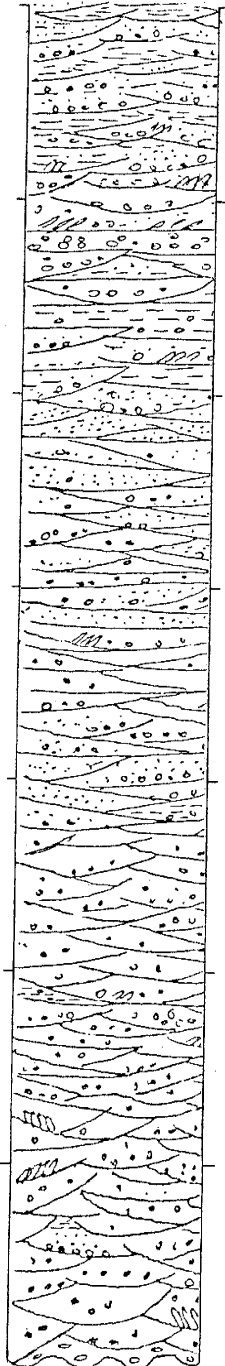
APPENDIX B  
MEASURED STRATIGRAPHIC SECTIONS

SECTION I (see Plate A for location)

Scale (in m) Average (—) & Largest (—) clast size (in cm)



Bedding



Description

0 to 700 meters:  
 cobble, at base, to granule, at top, conglomerate; poorly to moderately sorted; reddish-brown to lavender color with minor grey to tan reduced zones; clasts of phyllite, quartzite, granite, and vein quartz are subangular to angular and bladed or tabular; bedding (1/2 to 1 m thick) ill-defined and irregular, cut and fill common, low angle trough cross-bedding defined by grain size and orientation, abundant imbrications; normal and reverse graded bedding over several cms common; sandstone and siltstone beds rare; 1 m thick pebbly mudstones at 180 m and 296 m; 1 m thick coarse sandstone at 170 m; inter-bedded pebbly mudstones common from 650 to 700 m.

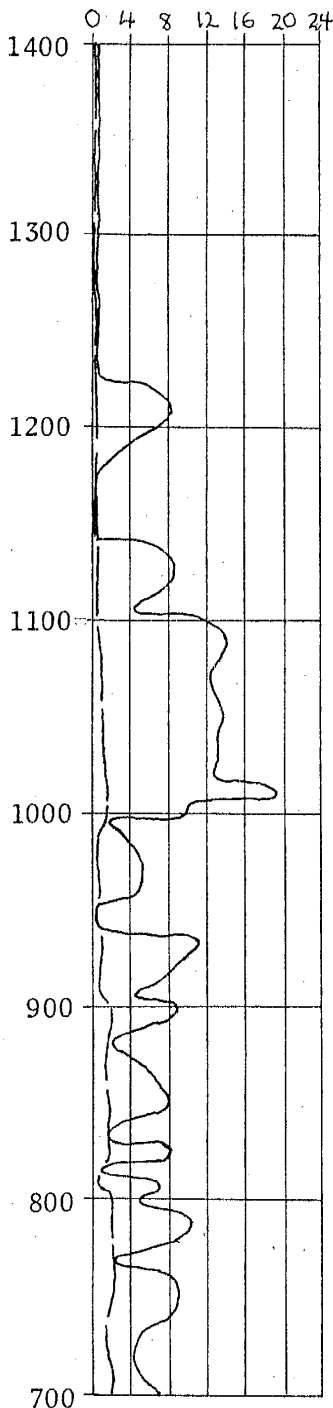
Strike N11E, Dip 15NW

Angular unconformity with lower Paleozoic metamorphic rocks



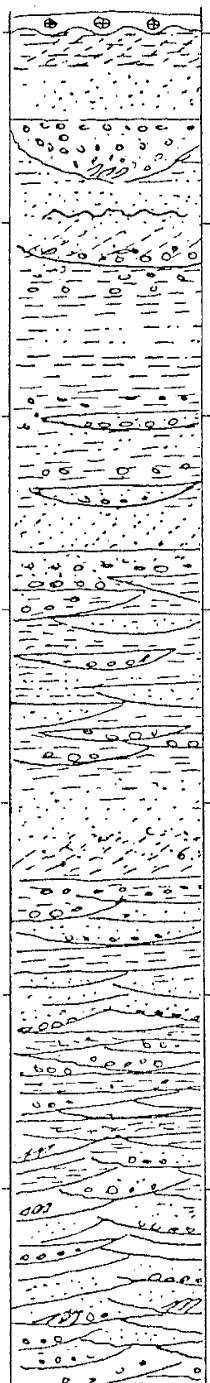
SECTION I (continued)

Scale (in m) Average (---) & Largest (—) clast size (in cm)



Bedding

Description



T<sub>3</sub> at 1405 m: Strike N38E, Dip 31NW; 2 m thick, cobble to granule conglomerate; clasts of igneous rocks, quartzite, phyllite, and vein quartz.

1100 to 1405 m: fining upward cycles (average 3 every 7 m) from coarse pebbly sandstone at base to interbedded fine to very fine sandstones at top; coarse pebbly to fine sandstones internally normal graded, trough crossbedded, planar crossbedded, or homogeneous; fine to very fine sandstones parallel laminated; Strike N48E, Dip 24NW.

900 to 1100 m: pebble conglomerate and interbedded coarse to fine sandstones; cut and fill common; beds 1/2 to 1 m thick; normal and reverse graded beds common in coarse to medium sandstones, fine sandstones parallel bedded.

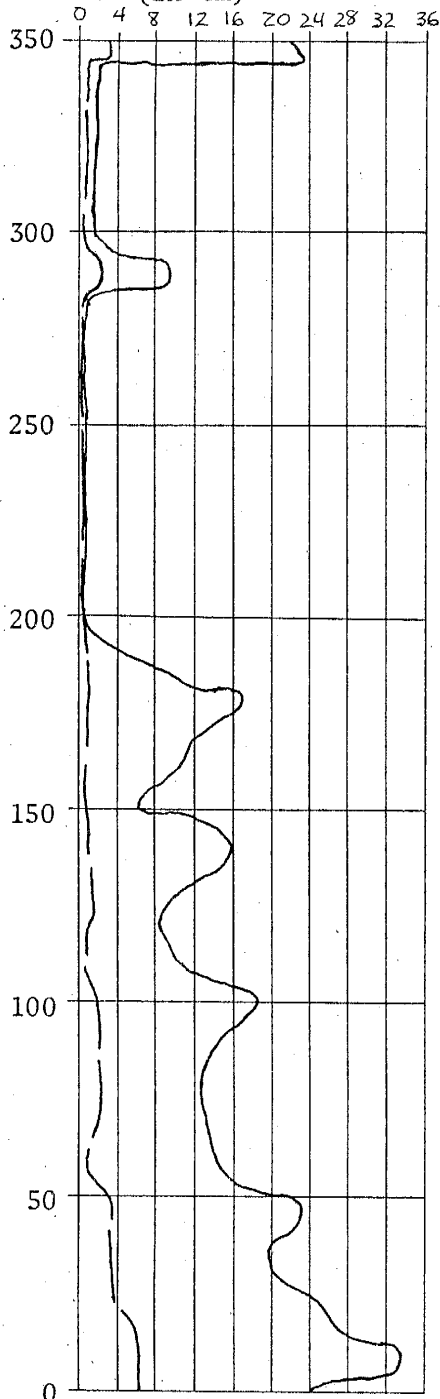
Strike N33E, Dip 40NW.

800 to 900 m: cobbly mudstones and interbedded conglomerates; shape of cobbly mudstone beds modified by scour surfaces; cut and fill common.

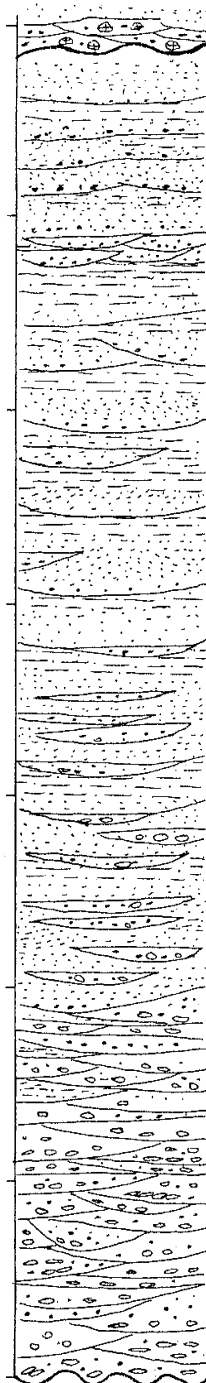
700 to 800 m: cobble to granule conglomerate with minor calcareous sandstone and siltstone interbeds continuous up to 8 m laterally.

## SECTION II (see Plate A for location)

Scale (in m) Average (—) & Largest (—) clast size (in cm)



Bedding



Description

340 to 350 m:  $T_3$  conglomerate; Strike N15W, Dip 19SW; cut and fill bedded (1/2 to 1 m thick) minor sandstone interbeds.

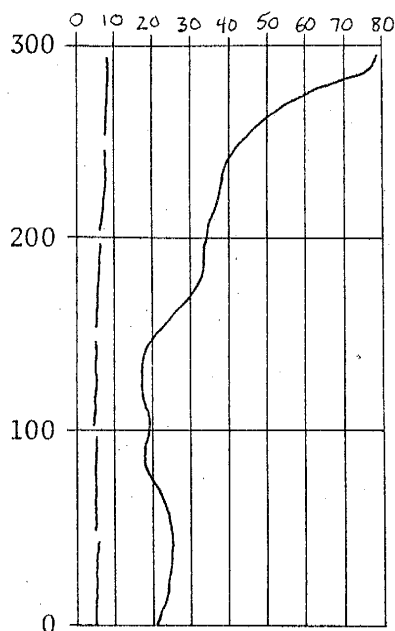
100- 340 m: fining upward cycles from coarse pebbly at base to very fine sandstone at top; see section VII & VIII for detailed description of sedimentary structures..

Strike N, Dip 17W

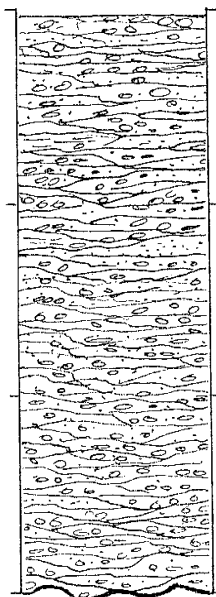
0 to 100 m: cobble at base to granule at top, conglomerate; clasts of phyllite, quartzite, granite, and vein quartz are subangular to angular and bladed or tabular; cut and fill bedding common, pebble imbrication common; interbedded sandstones common from 75 to 100 m; Strike N26E, Dip 18NW. Angular unconformity at base with lower Paleozoic metamorphic rocks.

## SECTION III (see Plate A for location)

Scale (in m)      Average (—) & Largest (—) clast size (in cm)



Bedding



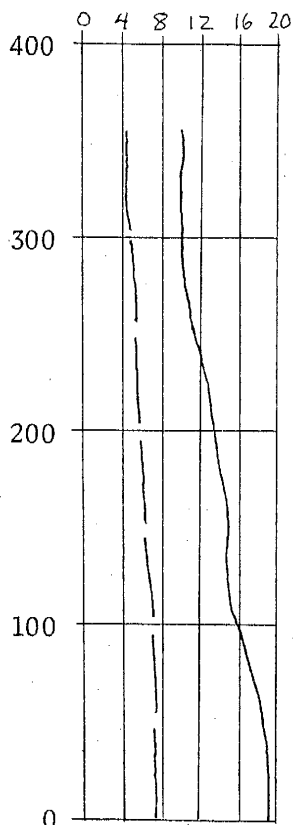
Description

Homogeneous cobble (at base) to boulder-cobble (at top) purplish conglomerate; bedding highly irregular to crudely lenticular, 1 to 2 m thick (thick to very thickly bedded); internally cut and fill bedded, highly imbricated, and occasionally irregularly trough crossbedded; interbedded pebbly mudstones and coarse to fine sandstones less than 1 m thick, and minor in abundance; pebble composition of conglomerate in Table I, sample 19.

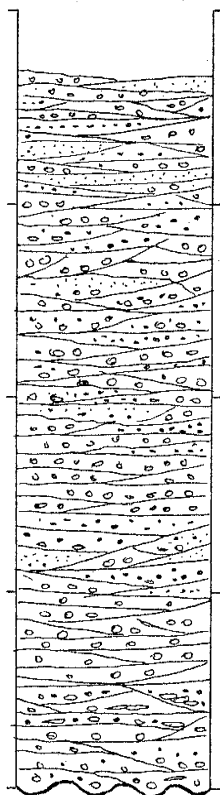
Angular unconformity with lower Paleozoic metamorphic rocks.

## SECTION IV (see Plate A for location)

Scale (in m) & Average (---) & Largest (—) clast size (in cm)



Bedding

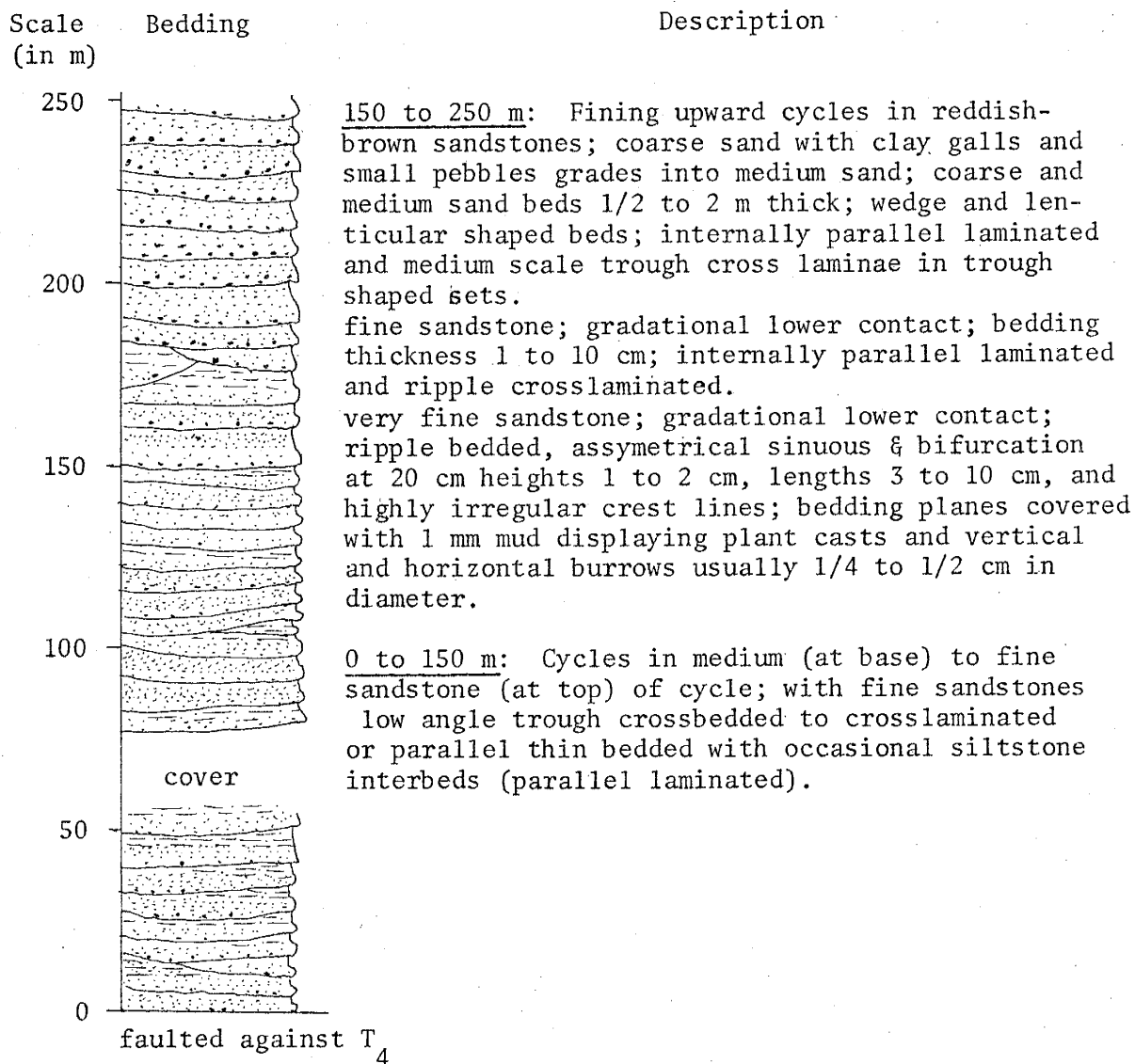


Description

300 to 350 m: conglomerate beds thinner (1/2 to 1 m thick); numerous coarse pebbly to medium sandstone interbeds usually gradational with conglomerate below; sandstones display horizontal laminations and low to high angle, concave upward, tangential base, cross laminae in trough shaped sets, laminae defined by alignment of larger pebbles and grains.

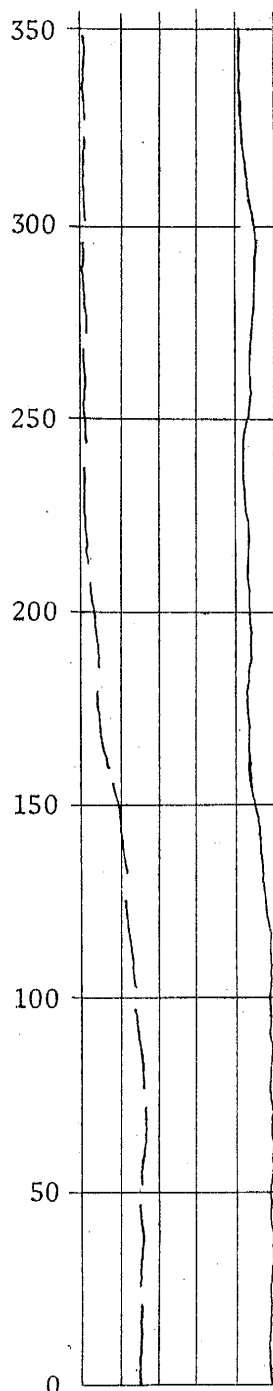
0 to 300 m: homogeneous conglomerate (1/2 to 2 m thick beds); cut and fill bedding common at base; at top beds are stacked with only local mild scour bases; beds continuous along dip 20 m, along strike 10 m; occasionally conglomerate grades upward into or is overlain sharply by poorly sorted coarse pebbly to fine grained sandstone beds whose shapes are modified by scour surfaces. Angular unconformity at base with lower Paleozoic metamorphic rocks.

## SECTION V (see Plate A for location)

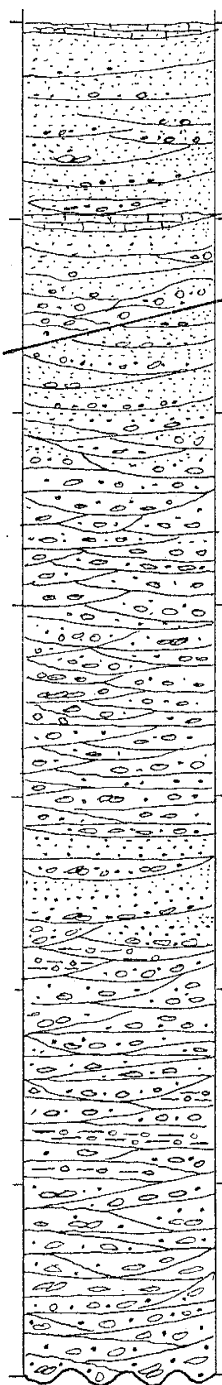


## SECTION VI (see Plate A for location)

Scale (in m) & Average (—) & Largest (—) clast size (in cm)



Bedding



Description

200 to 270 m: same as from 100 to 150 m except conglomerate beds are reduced in number, grain size, and thickness upward.

150 to 200 m: same as from 0 to 50 m except conglomerates are finer grained.

100 to 150 m: interbedded conglomerates and coarse to fine sandstones; conglomerates are as described below; sandstones are normally graded, homogeneous or large to medium scale, low to high angle, trough, or planar crossbedded, or parallel bedded.

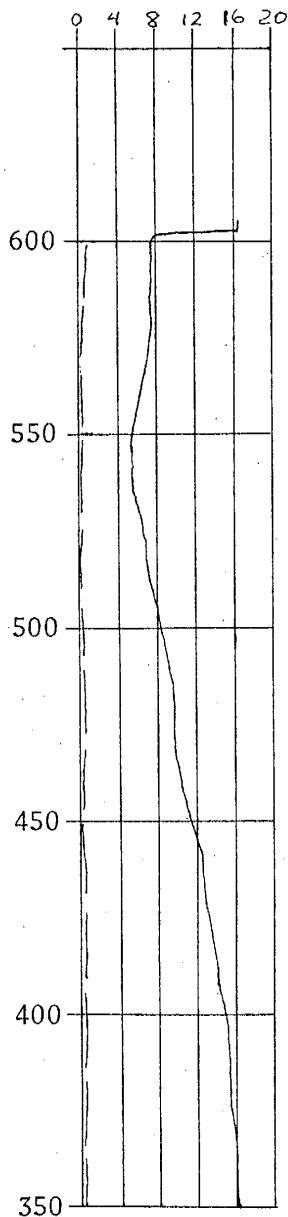
50 to 100 m: conglomerates as described above with interbeds of pebbly silt- or mudstone; internally pebbly mudstones are wacke-textured and the pebbles disoriented; shape of pebbly silt- or mudstone beds irregularly lenticular or modified by scour surfaces.

0 to 50 m: cobble to pebble conglomerate; beds 1/4 to 1 m thick; cut and fill bedding common; irregularly lenticular, laterally discontinuous beds; highly variable, rapid and irregular, lateral and vertical changes in grain size within a bed; pebble imbrications common; sandstone to siltstone interbeds rare.

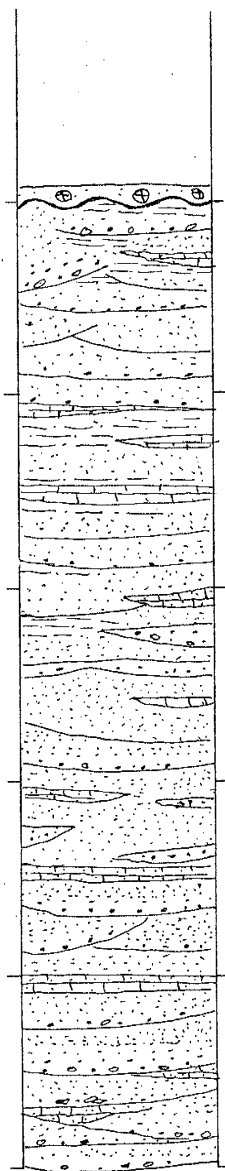
Angular unconformity with lower Paleozoic metamorphic rocks.

## SECTION VI (continued)

Scale (in m) & Average (---) & Largest (—) clast size (in cm)



Bedding



Description

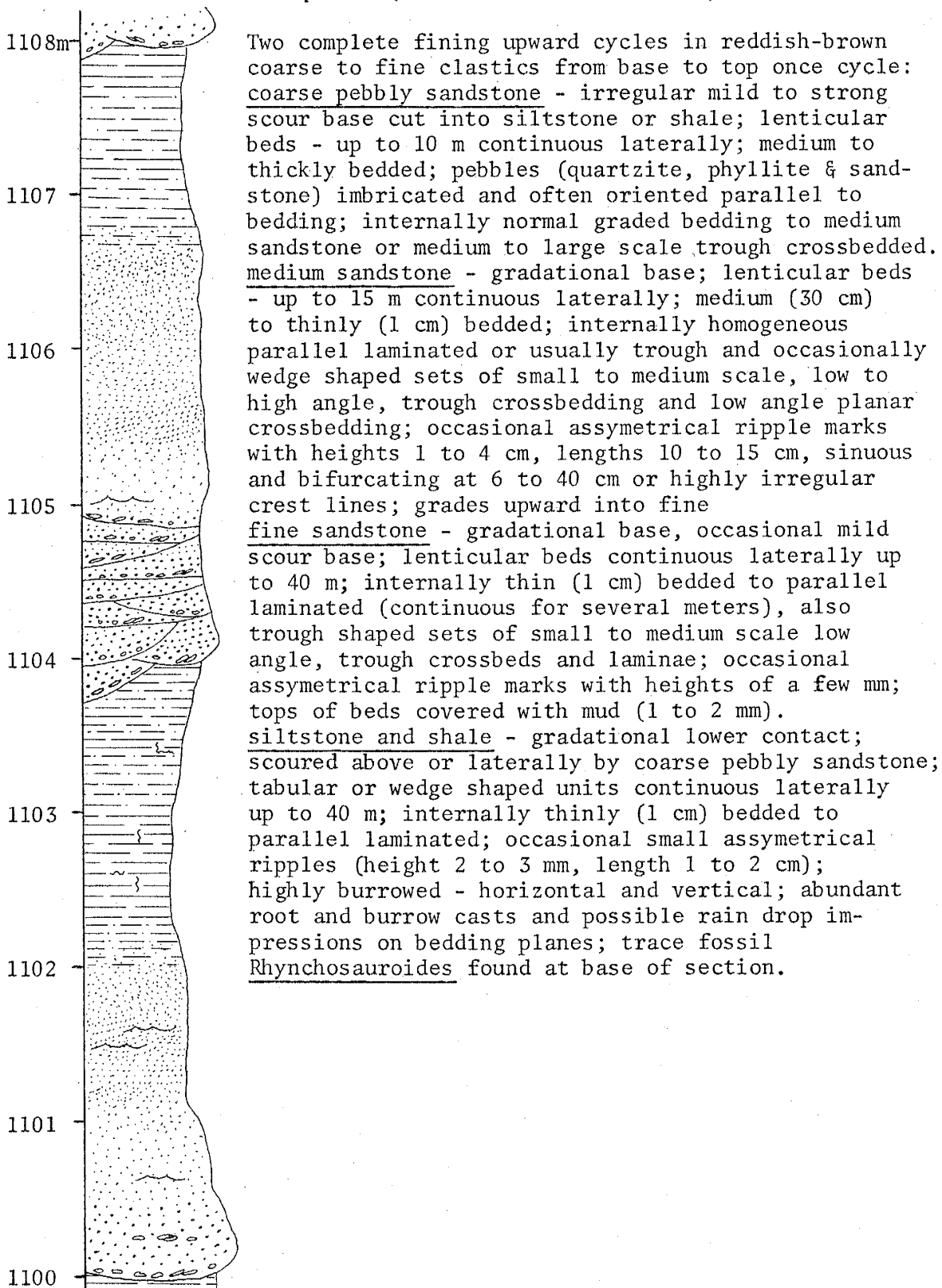
600 to 605 m:  $T_3$  conglomerates with minor sandstone interbeds; conglomerates are similar to the conglomerates from 0 to 50 m except they contain igneous and limestone rock fragments;  $T_3$ - $T_2$  contact is an angular unconformity.

550 to 600 m: same as from 270 to 500 m except cycles are in coarse to fine sandstones with few very fine sandstone, siltstone or mudstone interbeds; slight coarsening upward in this interval.

500 to 550 m: same as from 270 to 500 m except with numerous limestone interbeds, usually gradational below with very fine sandstones and siltstones; limestone beds 0 to 30 cm thick; laterally continuous up to 200 m with little change in thickness except where scoured out.


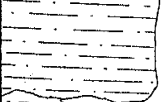




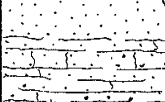


270 to 500 m: fining upward cycles from coarse pebbly sandstone (at base of cycle) to interbedded very fine sandstone and siltstone (at top of cycle; average of 3 cycles every 10 m; cycles are thicker at the top of the unit; similar sedimentary structures as in sections VII and VIII.

SECTION VII. Detailed Measured Section at 1100 m within Section I,  
Northern Sequence (see Plate A for location)



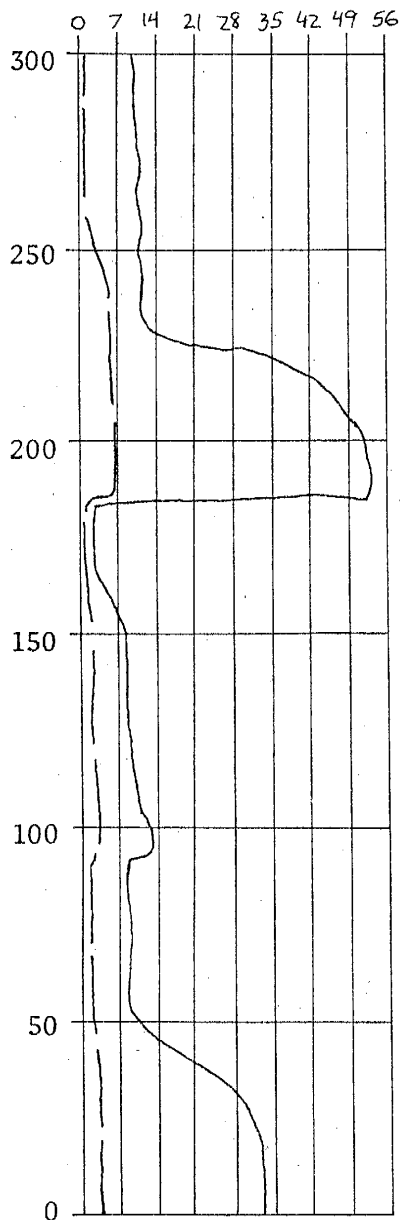


SECTION VIII. Detailed section of T<sub>2</sub> from 1350 M to 1358 M  
in Section I (see Plate A<sup>2</sup> for location)

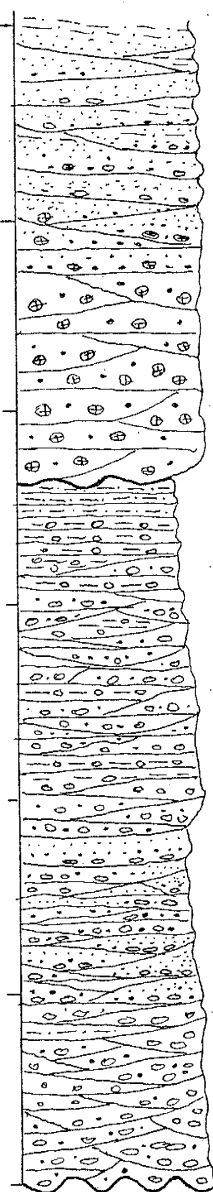
Scale (in m)	Bedding	Description
1358		Two fining upward cycles in reddish-brown sandstone from base to top:
1357		<u>coarse to medium sandstone</u> : lenticular beds 30 cm thick; medium scale, low to high angle, trough crossbedded; clay galls at base of crossbed sets; irregular moderate scour bases into siltstone or mudstone.
1356		<u>fine sandstone</u> : wedge shaped beds usually gradational with medium sandstone below; homogeneous, ripple crosslaminated internally or parallel laminated, or nodular due to increase in calcium carbonate cement.
1355		<u>siltstone and mudstone interbedded</u> : tabular beds, gradational base with fine sandstone; internally parallel laminated, ripple crosslaminated, or bioturbated; casts of horizontal and vertical burrows; scoured above by coarse to medium sandstones..
1354		
1353		
1352		
1351		
1350		

## SECTION IX. Basal Triassic Section at Tizi n' Test, Morocco

Scale (in m)      Average (---)  
& Largest (—) clast size  
(in cm)



Bedding



Description

238 to 300 m: fining upward cycles from coarse volcanic pebble sandstones with scour bases grading to medium sandstones, well crossbedded grading to parallel laminated and ripple crossbedded fine sand grading to parallel laminated siltstone and minor shale; average cycle thickness 2 m.

178 to 238 m: volcanic conglomerate; thickly to very thickly bedded (3 to 10 m); very poorly sorted with few imbricated pebbles.

165 to 178 m: parallel bedded shale and lenticular sandstone interbeds; laterally continuous for 100 m.

75 to 165 m: quartzitic conglomerate and interbedded pebbly mudstones; lenticular beds 1/2 to 1 m thick, laterally continuous up to 20 m; some normal graded bedding to coarse sandstone; thickness and number of pebbly mudstones increases up section.

0 to 75 m: reddish-brown phyllitic conglomerate; lower 50 m highly irregularly cut and fill bedded, beds 1 to 3 m thick, laterally continuous up to 3 m. Angular unconformity at base with lower Paleozoic metamorphic rocks.

## APPENDIX C

COMPARISON OF T<sub>1</sub>, T<sub>2</sub>, AND T<sub>3</sub> OF THE  
ARGANA VALLEY WITH THE BASAL TRIASSIC  
SECTION AT TIZI N' TEST, MOROCCO.

COMPARISON OF BASAL ARGANA VALLEY UNITS WITH  
THE TRIASSIC CONGLOMERATES AT TIZI N' TEST

For a detailed description of the measured section at Tizi n' Test see section IX in Appendix B. This stratigraphic section is divided into 4 main units based on environments of deposition and composition.

The lower two units are alluvial fan conglomerates composed of braided stream and mudflow deposits. This interpretation is based on the same criteria as the interpretations of Associations A and B in  $T_1$  of the Argana Valley. These units are derived dominantly from lower Paleozoic phyllites and quartzites, similar to the  $T_1$  conglomerates of the Northern Sequence in the Argana Valley. Quartzite pebbles increase in abundance upward in the section like  $T_1$  conglomerates of the Northern Sequence. Separating these alluvial fan conglomerates from an overlying conglomerate unit is a laterally continuous, 13 meter thick interval of parallel laminated, shales with minor lenticular sandstone interbeds interpreted as meandering stream floodplain deposits. Overlying this shale unit with slight angular unconformity is 140 meters of thick to very thickly bedded, very poorly sorted, boulder to cobble conglomerates, with clasts which resemble, both in hand specimen and petrographically, the volcanic clasts in  $T_3$  in the Argana Valley. These conglomerates are composed of debris flow deposits and minor interbedded braided stream deposits. This entire unit fines upward and grades

into meandering stream-floodplain deposits.

Thus, in terms of clast composition and, in part, depositional environments, the Triassic section at Tizi n' Test is very similar to the  $T_1$  through  $T_3$  section of the Argana Valley. The conglomerates at Tizi n' Test containing abundant clasts of volcanic rock fragments are probably a  $T_3$  equivalent as indicated by the clast composition. The  $T_2$  unit of the Argana Valley is probably represented at Tizi n' Test by the 13 meters of floodplain shales and minor interbedded channel sandstones, because it occurs immediately below the  $T_3$  equivalent conglomerates. The alluvial fan conglomerates underlying the 13 meter thick shale unit are probably Argana Valley  $T_1$  equivalents as indicated by environments of deposition and clast composition.

The conglomerates containing abundant boulders and cobbles of volcanic rock fragments at Tizi n' Test are much thicker than the  $T_3$  conglomerates in the Argana Valley. Paleocurrents in units gradational below with the  $T_3$  equivalent at Tizi n' Test indicate an easterly transport direction (Al Mattis, personal communication, 1974). These data indicate that the volcanic clasts are probably derived from Hercynian volcanic rocks associated with the emplacement of the Tischka Batholith which is much closer to the Tizi n' Test area. However, potassium-argon dating of 5 of the pebbles of volcanic rocks from the Tizi n' Test conglomerates yielded ages of  $83.2 \pm 4.0$  m.y.,  $91.4 \pm 4.4$  m.y.,  $96.8 \pm 6.9$  m.y.,  $129 \pm 6$  m.y., and  $189 \pm 13$  m.y. (Harold

Krueger, personal communication, 1974). These scattered dates may reflect the loss of argon during the Alpine event and the similarity, in hand specimen and thin section, between these clasts and clasts in  $T_3$  indicate they are also probably Hercynian in age.

In terms of paleotectonic setting the basal units of the Argana Valley and Tizi n' Test represent the initial basin fill deposits in grabens on either side of a north-south trending horst of Paleozoic rocks.

## APPENDIX D

COMPARISON OF  $T_1$ ,  $T_2$ , AND  $T_3$  OF THE ARGANA  
VALLEY WITH SIMILAR LITHOLOGIES IN THE NOVA SCOTIA,  
NEWARK-GETTYSBURG, AND CONNECTICUT BASINS IN NORTH AMERICA

COMPARISON OF THE BASAL ARGANA UNITS WITH SOME  
OF THE TRIASSIC BASIN-FILL DEPOSITS OF NORTH AMERICA

Figure 21 shows the Permian fit of Africa and North America constructed by Dietz and Holden (1970). In the figure the location of several Triassic basins in North America are shown as well as the Argana Valley. The fit suggests that the Argana Valley was closer to the Nova Scotia Basin, so that the Triassic rocks in the Argana Valley might resemble more closely those in the Nova Scotia Basin than those in the Newark-Gettysburg and Connecticut Basins. Table V compares  $T_1$  and  $T_2$  in the Argana Valley with the Wolfville and Blomidon Formations in the Nova Scotia Basin (Klein, 1962) and the Stockton Formation in the Newark-Gettysburg Basin (Glaesser, 1966). Data from Klein (1962) and Glaesser (1966) show that the composition of the coarse, basal detritus in the Nova Scotia and Newark-Gettysburg basins is determined by the composition of the preexisting rocks underlying the Triassic red beds. Data presented in this study indicates a similar provenance control of detrital composition in the Argana Valley and at Tizi n' Test. In the North American Grabens, granitic or gneissic source rocks are dominant toward the south, in the Newark-Gettysburg and Connecticut basins, but low grade metamorphic rocks are dominant toward the north, in the Nova Scotia Basin. In Morocco, a similar trend in the basement rock composition occurs, with the granitic basement of the West African Shield and Anti-Atlas Mountains to the south, but the low



Figure 21. Permian Fit of the Continents  
(adapted from Dietz and Holden, 1970)

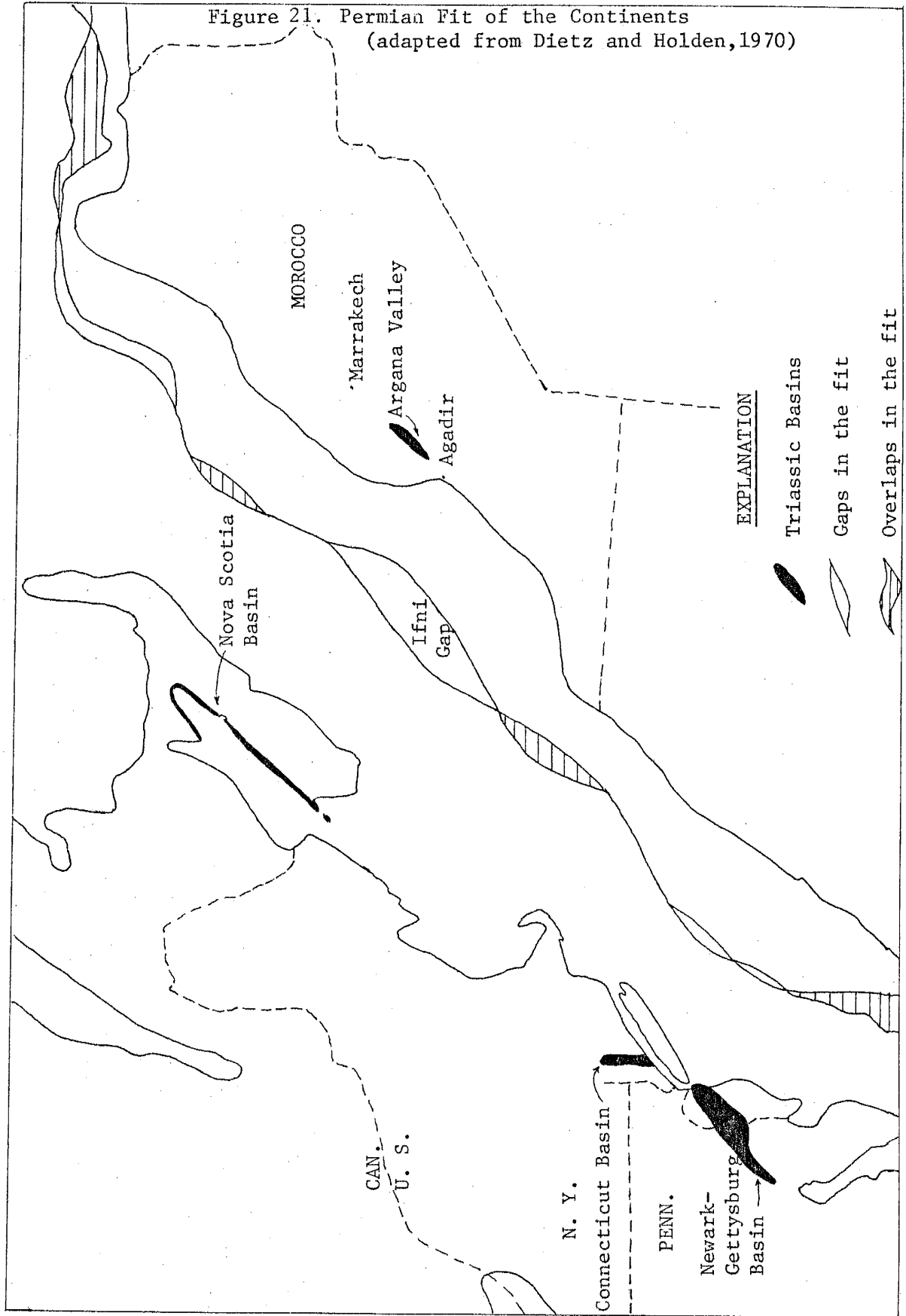


Table. V. Comparison of T<sub>1</sub> and T<sub>2</sub> of the Argana Valley with some Triassic Basin fill deposits of North America

	<u>Argana Valley</u> T <sub>1</sub> -T <sub>2</sub> units	<u>Nova Scotia Basin</u> (Klein, 1962) Wolfville and Blomidon Fms.	<u>Newark-Gettysburg Basin</u> (Glaesser, 1966) Stockton Fm.
Age	Problematical: Permo-Triassic or Triassic Fossils: <u>Voltizia heterophylla</u> , <u>Rhynchosauroides</u>	Late Triassic on basis of <u>Procolophonidae</u> , <u>Hetasauridae</u> , and <u>Rhynchosauroides</u>	Late Triassic on basis of varieties of siliified wood. Underlies conformably Lockatong Fm. containing <u>Rhynchosauroides</u>
Thickness and Geometry	750' - 4200' lenticular bodies continuous laterally up to 28 kilometers	225' - 3700' lenticular bodies continuous laterally more than 100 miles	0 - 5000' lenticular body continuous laterally more than 120 miles
Environments of Deposition	Braided stream deposits of alluvial fans gradational and interfingering with overlying meandering stream deposits	Alluvial fan deposits gradational and interfingering with overlying meandering stream deposits	High mechanical energy fluvial environment in part alluvial fan deposits gradational and interfingering with overlying lacustine Lackatong Formation
Clast composition of conglomerate fraction	dominant: lower grade metamorphic phyllite and quartzites minor: sedimentary rock fragments including sandstones, mudstones and limestones; granite, basalt, felsic volcanic rock fragments	dominant: low grade metamorphic rocks minor: granite, rhyolite sedimentary rock fragments	dominant: quartz and/or quartzite or quartz and/or quartzite plus sedimentary rock fragments minor: metamorphic rock fragments

Table V. Comparison of T<sub>1</sub> and T<sub>2</sub> of the Argana Valley with some Triassic Basin fill deposits of North America (continued)

	<u>Argana Valley</u> T <sub>1</sub> -T <sub>2</sub> units	<u>Nova Scotia Basin</u> (Klein, 1962) Wolfville and Blomidon Fms.	<u>Newark-Gettysburg Basin</u> (Glaesser, 1966) Stockston Fm.
Sandstone Compositions	orthoquartzites or low rank graywackes	wide variety--mostly ortho- quartzites, low rank graywackes	arkoses and orthoquartzites
Inferred source rock types	dominant: low grade metamorphic rocks (phyllites and meta- quartzites) minor: granitic, volcanic sedimentary rocks	dominant: low grade meta- morphic rocks minor: granitic, rhyolitic and sedimentary rocks	dominant: highly feldspathic gneissic and/or granitic rocks minor: sedimentary and low grade metamorphic rocks

grade metamorphic rocks of the High Atlas Mountains to the north, adjacent to the Argana Valley.

There is similarity in terms of vertical succession of lithologies, composition, and fauna, between the T<sub>1</sub>, T<sub>2</sub> and T<sub>3</sub> formations of the Argana Basin and the Wolfville, Blomidon, and Quaco Formations of Nova Scotia (Klein, 1962). In Nova Scotia, basal Triassic fanglomerates of the Wolfville Formation are derived from dominately low grade metamorphic rocks presently exposed to the east and southeast, and are gradational and interfingering with overlying meandering stream deposits of the Blomidon Formation. In both formations the trace fossil footprints of reptile Rhynchosauroides occur. Locally, the Wolfville Formation is unconformably overlain by conglomerates of the Quaco Formation which have clasts of dominately pre-Mississippian felsic volcanic, granitic, and metamorphic rocks. A similar sequence of lithologies is present in T<sub>1</sub>, T<sub>2</sub>, and T<sub>3</sub> of the Argana Basin.

From Table V, it is evident that the units are all very similar in terms of age, thickness and geometry, and environments of deposition. In terms of composition and provenance however, it is evident that the basal units of the Argana Valley are more like the Wolfville and Blomidon Formations than the Stockton Formation. These data lend support to the fit constructed by Dietz and Holden (1970).

## REFERENCES

- Allen, J. R. L., 1964, Studies in fluviatile sedimentation: six cyclothems from the Lower Old Red Sandstone, Anglo-Welsh Basin: *Sedimentology*, v. 3, p. 163-198.
- Ambroggi, R., 1963, Etude geologique du versant meridional du Haut Atlas occidental et de la plaine du Souss: Notes and Memoirs Service Geol. Maroc, no. 157, 332p.
- Baird, D., 1957, Triassic reptile footprint faunules from Milford, New Jersey: *Mus. Comparative Zoology Bull.*, v. 117, p. 447-529.
- Baird, D., 1962, Rhynchosaurs in the Late Triassic of Nova Scotia: *Geol. Soc. America Spec. Paper* 73, p. 107.
- Baird, D., 1964, Dockum (Late Triassic) reptile footprints from New Mexico: *Jour. Paleontology*, v. 38, p. 118-125.
- Baird, D., and Take, W. F., 1959, Triassic reptiles from Nova Scotia: *Geol. Soc. America Bull.*, v. 70, p. 1565-1566.
- Beatty, C. B., 1963, Origin of alluvial fans, White Mountains, California and Nevada: *Annual Assoc. American Geog.*, v. 53, p. 516-535.
- Blatt, H., Middleton, G., and Murray, B., 1972, Origin of sedimentary rocks: Englewood Cliffs, New Jersey, Prentice-Hall Inc., 634p.
- Blissenbach, E., 1965, Geology of alluvial fans in semi-arid regions: *Geol. Soc. America Bull.*, v. 65, p. 176-190.
- Bluck, B. J., 1967, Deposition of some Upper Old Red Sandstone conglomerates in the Clyde area: a study in the significance of bedding: *Scottish Jour. Geology*, v. 3, p. 139-167.
- Bock, W., 1952, Triassic reptilian tracks and trends of locomotive evolution: *Jour. Paleontology*, v. 26, p. 395-433.
- Branson, E. B., 1947, Triassic (Chugwater) footprints from Wyoming: *Jour. Paleontology*, v. 21, p. 588-590.
- Brown, R. H., Jr., 1974, The Argana Basin of Morocco; a Triassic model for early rifting: Master of Science Thesis, University of South Carolina, 54p.
- Bruck, P. M., Dedman, R. E., and Wilson, R. C. L., 1967, The New Red Sandstone of Bassay and Scalpay, Inner Hebrides: *Scottish Jour. Geology*, v. 3, p. 168-180.

- Bull, W. B., 1968, Alluvial fans: Jour. Geol. Ed., v. 16, p. 101-106.
- Bull, W. B., 1972, Recognition of alluvial fan deposits in the stratigraphic record (in) Recognition of ancient sedimentary environments, J. K. Rigby (ed): Soc. of Econ. Paleontologists and Mineralogists Spec. Pub. No. 16, p. 63-83.
- Bullard, E. C., Everett, J. E., and Smith, A. G., 1965, The fit of the continents around the Atlantic: Phil. Trans. Roy. Soc. London, A258, p. 41-51.
- Carver, R. E., 1971, Procedures in sedimentary petrology: New York, Wiley-Interscience, 653p.
- Chayes, F., 1971, Ratio correlation: Chicago, The University of Chicago Press, 99p.
- Choubert, G., 1952, Apercu structural (in) Geologie du Maroc: 19th Int. Geol. Cong., 3rd ser., no. 6, p. 117-139.
- Curray, J. R., 1956, The analysis of two-dimensional orientation data: Jour. Geology, v. 64, p. 117-131.
- Davis, W. M., 1938, Sheetfloods and streamfloods: Geol. Soc. America Bull., v. 49, p. 1337-1416.
- Dewey, J. F., and Bird, J. M., 1970, Mountain belts and the new global tectonics: Jour. Geophys. Research, v. 69, p. 1995-2002.
- Dietz, R. S., and Holden, J. C., 1970, The breakup of Pangaea (in) J. T. Wilson (ed), Continents adrift: San Francisco, W. H. Freeman and Company, p. 102-113.
- Doeglas, D. J., 1962, The structure and sedimentary deposits of braided rivers: Sedimentology, v. 1, p. 167-190.
- Duffaud, F., 1960, Contribution a l' etude stratigraphique du bassin secondaire du Haut Atlas occidental (Sud-Ouest Marocain): Bull. Soc. Geol. France, 7e ser., t. 2, no. 6, p. 728-734.
- Duffaud, F., Brun, M. M. L., and Plauchut, B., 1966, Les bassin du Sud-Ouest Marocain (in) Sedimentary basins of the African coast Part I, Atlantic Coast: Assoc. African Geol. Surveys, 303p.
- Faber, F. J., 1958, Fossiele voetstappen in de Muschelkalk van Winterswijk: Geologie en Mijnbouw (new series), 20 Jaarg., p. 317-321.

- Folk, R. L., 1974, Petrology of sedimentary rocks: Austin, Texas, Hemphill Publishing Co., 182p.
- Folk, R. L., and Ward, W. C., 1957, Brazos River Bar: a study in the significance of grain size parameters: Jour. Sedimentary Petrology, v. 27, p. 3-26.
- Friedman, G. M., 1958, Determination of sieve-size distribution from thin section data for sedimentary petrological studies: Jour. Geology, v. 60, p. 394-416.
- Ingram, R. L., 1954, Terminology for the thickness of stratification and parting units in sedimentary rocks: Geol. Soc. America Bull., v. 65, p. 937-938.
- Kanes, W. H., Saadi, M., Ehrlich, E., and Alem, A., 1973, Moroccan crustal response to Continental Drift: Science, v. 180, p. 950-952.
- Klein, G. de Vries, 1962, Triassic sedimentation, Maritime Provinces, Canada: Geol. Soc. America Bull., v. 73, p. 1127-1146.
- Koning, G. de, 1957, Geologie des Ida ou Zal (Maroc), stratigraphie, petrographie et tectonique de la partie SW du bloc occidental du Massif ancien du Haut Atlas: Eduardo Ijdo N. V. Leyde, v. 87, 210p.
- Krumbein, W. C., and Sloss, L. L., 1963, Stratigraphy and sedimentation: San Francisco, W. H. Freeman and Company, 660p.
- Mackie, W., 1899, The sands and sandstones of eastern Moray: Edinburgh Geol. Soc. Trans., v. 7, p. 148-172.
- Maidwell, F. T., 1914, Notes on footprints from the Keuper II: Liverpool Geol. Soc. Proc., v. 12, p. 53-71.
- Matthews, R. K., 1974, Dynamic stratigraphy: Englewood Cliffs, New Jersey, Prentice-Hall, Inc., 370p.
- McKee, E. D., and Weir, G. W., 1955, Terminology for stratification and cross stratification in sedimentary rocks: Geol. Soc. America Bull., v. 64, p. 381-390.
- Moody-Stuart, M., 1966, High- and low-sinuosity stream deposits with examples from the Devonian of Spitzbergen: Jour. Sedimentary Petrology, v. 36, p. 1102-1117.
- Peabody, F. E., 1948, Reptile and amphibian trackways from the Lower Triassic Moenkopi formation of Arizona and Utah: Univ. Cal. Pub. Dept. Geol. Sci. Bull., v. 27, p. 295-468.

- Pettijohn, F. J., 1957, Sedimentary rocks: New York, Harper and Row, Publishers, 718p.
- Pettijohn, F. J., and Potter, P. E., 1964, Atlas and glossary of primary sedimentary structures: New York, Springer, 370p.
- Pettijohn, F. J., Potter, P. E., and Siever, R., 1973, Sand and Sandstone: New York, Springer-Verlag, 618p.
- Picard, M. D., and High, L. R., Jr., 1968, Criteria for recognizing lacustrine rocks (in) Recognition of Ancient Sedimentary Environments, J. K. Rigby (ed): Soc. of Econ. Paleontologists and Mineralogists Spec. Pub. No. 16, p. 108-145.
- Powers, M. C., 1953, A new roundness scale for sedimentary particles: Jour. Sedimentary Petrology, v. 23, p. 117-119.
- Schenk, P. E., 1971, Southeastern Atlantic Canada, Northeastern Africa, and Continental Drift: Canadian Jour. Earth Sci., v. 8, p. 1218-1251.
- Scott, D. H., 1962, Studies in fossil botany: New York, Hafner Publishing Co., p. 380.
- Sharp, R. P., and Nobles, L. M., 1953, Mudflow of 1941 at Wrightwood, Southern California: Geol. Soc. America Bull., v. 64, p. 547-560.
- Smith, N. D., 1970, The braided stream depositional environment: comparison of the Platte River with some Silurian clastic rocks, North-central Appalachians: Geol. Soc. America Bull., v. 81, p. 2993-3014.
- Steel, R. J., 1974, New red sandstone floodplain and piedmont sedimentation in the Hebridean province, Scotland: Jour. Sedimentary Petrology, v. 44, p. 336-357.
- Suttner, L. J., 1969, Stratigraphic and petrographic analysis of Upper Jurassic-Lower Cretaceous Morrison and Kootenai formations, Southwest Montana: Am. Assoc. Petroleum Geologists Bull., v. 53, p. 1391-1410.
- Tixeront, M., 1971, Lithostratigraphic et mineralisations cupriferes et uraniferes stratiformes syngenetique et famileres des formations detritiques Permo-Triassic du Couloir d' Argana (Haut-Atlas Occidental, Maroc) et possibilites de reserches: Services d' Etudes des Gites Mineraux rapport no. 921, 37p.



- Van Houten, F. B., Brown, R. H., Jr., and Mattis, A., 1974, Nonmarine Permo-Triassic sedimentary rocks, Morocco: Am. Assoc. Petroleum Geologists, Ann. Mtg. Abstracts, v. 1, p. 92.
- Wentworth, C. K., 1922, A scale of grade and class terms for clastic sediments: Jour. Geol., v. 38, p. 377-392.
- Williams, P. F., and Rust, B. R., 1969, The sedimentology of a braided river: Jour. Sedimentary Petrology, v. 39, p. 649-679.
- Zingg, T., 1935, Beitrag zur Schotteranalyse: Schweiz. Min. u. Pet. Mitt., Bd. 15, p. 39-140.

This thesis is accepted on behalf of the faculty of the  
Institute by the following committee:

John R. McMillan

C. J. Pudding

Allen J. Getzler

\_\_\_\_\_

\_\_\_\_\_

Date July 3, 1975

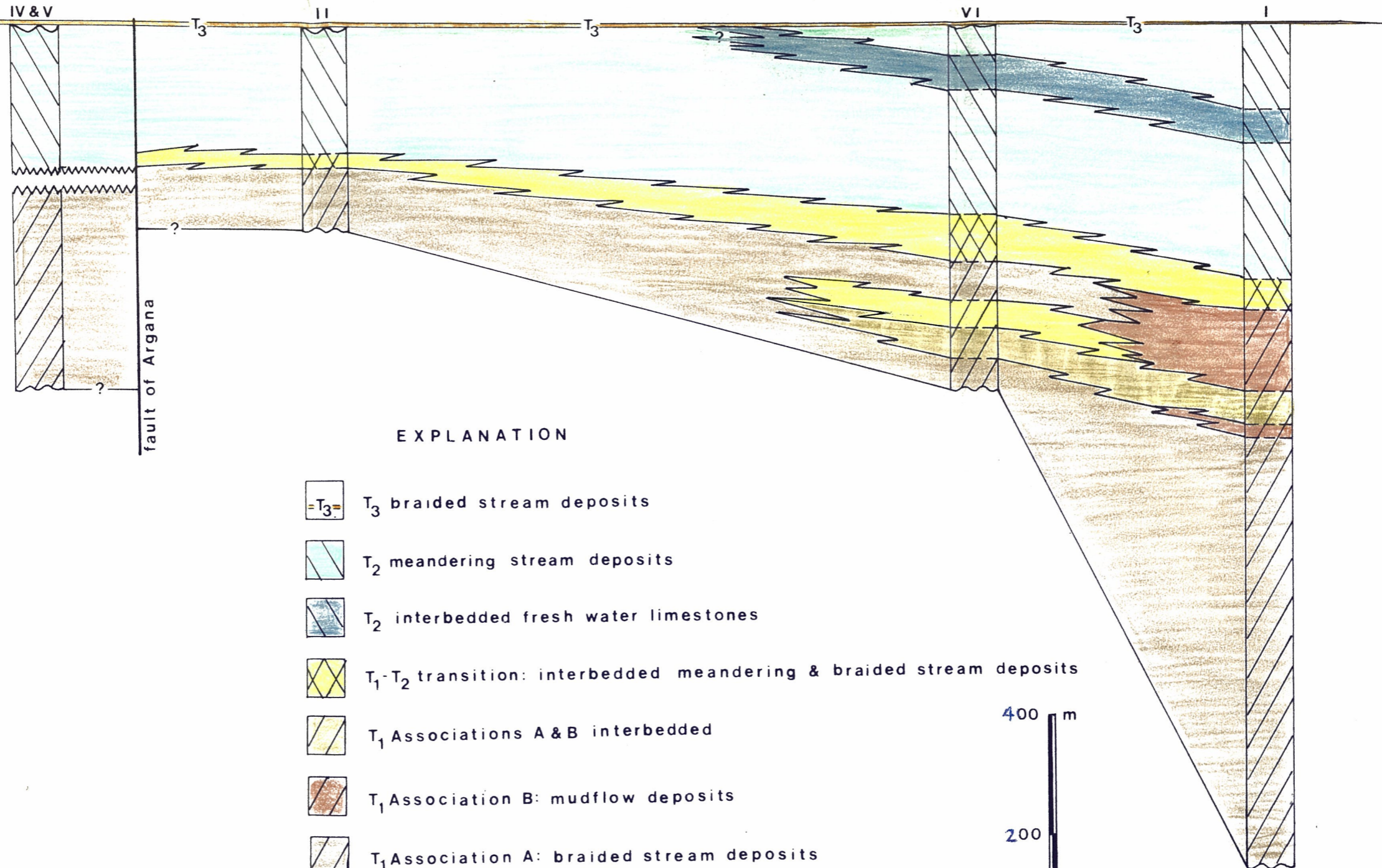
# PLATE B

## LATERAL & VERTICAL CHANGES IN ENVIRONMENTS OF DEPOSITION

SOUTH

NORTH

section no. IV & V



### EXPLANATION

- $T_3$  braided stream deposits
- $T_2$  meandering stream deposits
- $T_2$  interbedded fresh water limestones
- $T_1$ - $T_2$  transition: interbedded meandering & braided stream deposits
- $T_1$  Associations A & B interbedded
- $T_1$  Association B: mudflow deposits
- $T_1$  Association A: braided stream deposits

